
Masters Theses

Student Theses and Dissertations

Spring 2016

3D seismic structural and stratigraphic interpretation of the TUI-3D field, Taranaki Basin, New Zealand

Gorkem Yagci

Follow this and additional works at: https://scholarsmine.mst.edu/masters_theses



Part of the [Geology Commons](#), [Geophysics and Seismology Commons](#), and the [Other Engineering Commons](#)

Department:

Recommended Citation

Yagci, Gorkem, "3D seismic structural and stratigraphic interpretation of the TUI-3D field, Taranaki Basin, New Zealand" (2016). *Masters Theses*. 7529.

https://scholarsmine.mst.edu/masters_theses/7529

This thesis is brought to you by Scholars' Mine, a service of the Missouri S&T Library and Learning Resources. This work is protected by U. S. Copyright Law. Unauthorized use including reproduction for redistribution requires the permission of the copyright holder. For more information, please contact scholarsmine@mst.edu.

3D SEISMIC STRUCTURAL AND STRATIGRAPHIC INTERPRETATION
OF THE TUI-3D FIELD, TARANAKI BASIN, NEW ZEALAND

by

GORKEM YAGCI

A THESIS

Presented to the Faculty of the Graduate School of the
MISSOURI UNIVERSITY OF SCIENCE AND TECHNOLOGY

In Partial Fulfillment of the Requirements for the Degree

MASTER OF SCIENCE IN GEOLOGY AND GEOPHYSICS

2016

Approved by

Kelly H. Liu, Advisor

Stephen S. Gao

Wan Yang

© 2016
Gorkem Yagci
All Rights Reserved

ABSTRACT

Identifying seismic structures and stratigraphy are important for exploration of hydrocarbons. The purpose of this study is to discover seismic structural and stratigraphic features and to utilize the results for interpreting depositional environments. A 3D seismic dataset from the Tui-3D Field, the Taranaki Basin, New Zealand with well data were used to visualize structures, to detect stratigraphic features, to identify main lithology, to understand depositional environment, and to describe seismic facies and reflection patterns of the target horizons. The major formations are in the Kapuni Group.

Seismic structural interpretation indicates thirty-two minor faults, which may play an important role in oil migration from the Farewell “F” Sand to the Kaimiro “D” Sand, and many anticlines for possible oil traps. Depth maps show that the dipping of the Kapuni Group is toward the north. Seismic stratigraphic interpretation reveals features such as lineaments, gullies, and channels, which provide an understanding of evolution of the formations. The Kahu channel was identified in the Farewell “F” Sand, which may be a potential trap for oil accumulation. Gullies, which were discovered within the Giant Foresets Formation, are NW-SE oriented, straight to low sinuous, U-shaped, roughly parallel to each other, up to 12 km long, 10-50 m deep, and 20-500 m wide. NW-SE oriented and high to moderate sinuous channel complexes were found in the Moki “A” Sand. Lineament features and a canyon, which is NW-SE oriented, straight to low sinuous, approximately 2 km wide, 260 m deep, and 10 km long, were detected in the shallower part of the area. Petrophysical analysis demonstrates high porosity range from 10% to 25%, and high permeability up to ~322 md for the Kapuni Group.

ACKNOWLEDGMENTS

I would like to express my sincere gratitude to my advisor, Dr. Kelly Liu, for her guidance, patience, and assistance during my studies. I would also like to thank my committee members, Dr. Stephen Gao and Dr. Wan Yang, for their great suggestions, informative critiques, and comments, which helped me finalize this study.

I am very grateful to my sponsors, the Turkish Petroleum Corporation (TPAO) and the Turkish Ministry of National Education, for giving me this opportunity to pursue my graduate studies in the geology and geophysics program at the Missouri University of Science and Technology.

I would like to acknowledge New Zealand Petroleum and Minerals (NZP&M) for making the 2015 Petroleum Exploration Data Pack public. I also want to thank Aamer Alhakeem for sharing the data source and helpful ideas.

I would like to thank Amy Ketterer, the technical editor for the Office of Graduate Studies, for her English assistance on my thesis.

My deepest thanks to my mother, Sevim Yagci, and my wife, Fulya Gizem Yagci, for supporting me and believing in me in bad and good times. Without their love, I would not have come this far. Special thanks to Dr. Andrew Cassidy for his endless support. Last but not least, I am thankful to Suzan Oztoplu and Yalcin Oztoplu for their support and motivation.

DEDICATION

Dedicated to my father, Hasan Tahsin Yagci.
You will be in my heart and mind for the rest of my life.

TABLE OF CONTENTS

	Page
ABSTRACT.....	iii
ACKNOWLEDGMENTS	iv
DEDICATION.....	v
LIST OF ILLUSTRATIONS.....	x
LIST OF TABLES	xiv
NOMENCLATURE	xv
 SECTION	
1. INTRODUCTION.....	1
1.1. AREA OF STUDY	1
1.2. EXPLORATION HISTORY	4
1.3. OBJECTIVES.....	7
2. REGIONAL GEOLOGY	8
2.1. GEOLOGICAL SETTING AND TECTONIC HISTORY	8
2.2. GEOLOGICAL STRATIGRAPHY	12
2.2.1. North Cape Formation.....	12
2.2.2. Kapuni "D" Sandstone Formation.....	12
2.2.3. Kapuni "E" Shale Formation	14
2.2.4. Kapuni "F" Sandstone Formation.....	14
2.2.5. Giant Foresets Formation	16
2.2.6. Moki "A" Sandstone Formation	16
2.2.7. Tikorangi Limestone Formation.....	17

2.2.8. Basement	17
2.3. PETROLEUM SYSTEM.....	17
2.3.1. Source.....	18
2.3.2. Migration	19
2.3.3. Reservoir	19
2.3.4. Seal.....	19
2.3.5. Trap.....	19
2.3.6. Timing	21
3. DATA.....	22
3.1. TUI-3D SEISMIC DATA.....	22
3.1.1. Polarity Check	22
3.1.2. Well Data.....	25
3.1.3. Artifacts of the 3D Data	29
4. STRUCTURAL INTERPRETATION.....	31
4.1. PROCEDURE.....	31
4.2. SYNTHETIC GENERATION AND MATCHING	34
4.3. FAULT INTERPRETATION.....	36
4.4. HORIZON INTERPRETATION.....	40
4.5. STRUCTURAL MAPPING	44
4.5.1. Time Structural Map	44
4.5.2. Depth Map by Average Velocity.....	49
4.5.3. Time-Depth Conversion.....	63
4.5.4. Isopach Map	64

4.5.4.1. Interval velocity map	64
4.5.4.2. Isopach map	70
5. SEISMIC STRATIGRAPHIC ANALYSIS	74
5.1. SEISMIC ATTRIBUTES	74
5.1.1. Local Flatness	74
5.1.2. Chaos	74
5.1.3. Sweetness	75
5.2. STRATIGRAPHIC FEATURES	76
5.2.1. Gullies in Giant Foresets Formation.	76
5.2.2. A Channel in Farewell “F” Sand	82
5.2.3. Channels in Moki “A” Sandstone Formation	85
5.2.4. A Canyon and Lineaments in Shallow Formation	89
5.3. SEISMIC STRATIGRAPHY	93
6. WELL LOGGING AND PETROPHYSICAL ANALYSES	102
6.1. WELL-TO-WELL LOG CORRELATION	102
6.2. PETROPHYSICAL ANALYSES	102
6.2.1. Net/Gross Ratio (NGR)	104
6.2.2. Porosity (ϕ)	106
6.2.3. Water Saturation (S_w)	107
6.2.4. Permeability (k)	108
6.2.5. Hydrocarbon Meters (HPV)	108
6.2.6. Volume of Shale (V_{sh})	109
6.3. CROSSPLOTS	111

7. CONCLUSIONS	114
7.1. STRUCTURAL INTERPRETATION	114
7.2. STRATIGRAPHIC INTERPRETATION	114
7.3. PETROPHYSICAL ANALYSES	115
7.4. RECOMMENDATIONS	116
BIBLIOGRAPHY	117
VITA	123

LIST OF ILLUSTRATIONS

Figure	Page
1.1. Location of the Tui-3D Field	2
1.2. Location of the Taranaki Basin showing structures and oil and gas fields.....	3
1.3. Location map of the wells.....	5
1.4. Schematic of the Tui-3D Field development	6
2.1. Location of the Taranaki Basin.....	9
2.2. The basement structure map of the Taranaki Basin.....	11
2.3. Illustration of stratigraphy for the offshore Taranaki Basin	13
2.4. Generalized stratigraphy for the Taranaki Basin	15
2.5. Location of the wells in the Tui-3D Field.....	18
2.6. Events chart for Taranaki petroleum systems.....	20
2.7. Possible oil migration pathways for the Tui-3D Field.....	21
3.1. Basemap of the Tui-3D field.....	23
3.2. Crossline 1626 showing deep smiles	29
3.3. Time slice at 2.28 s shown acquisition footprint	30
4.1. Uninterpreted Inline 3856 illustrating a general view of the seismic data	32
4.2. Time slice representing channels within the Moki “A” Sandstone Formation.....	33
4.3. Synthetic generation and matching for Well Tui-1.....	35
4.4. Time structure map of the Farewell “E” Shale with identified minor faults	37
4.5. Time structure map of the Farewell “F” Sand with identified minor faults	38
4.6. 3D cube shown thirty-two identified faults and five horizons.....	39
4.7. Inline 3813 shown synthetic seismogram with the horizons	42

4.8. Vertical seismic section of Crossline 1447 showing the five horizons	43
4.9. Time structure map of the Basetik (Oligocene) Horizon.....	45
4.10. Time structure map of the Kaimiro “D” Sand Horizon	46
4.11. Time structure map of the Farewell “E” Shale Horizon	47
4.12. Time structure map of the Farewell “F” Sand Horizon	48
4.13. Time structure map of the basement Horizon.....	49
4.14. Illustration of average velocity generation	50
4.15. Average velocity map of the Basetik (Oligocene) Horizon.....	52
4.16. Average velocity map of the Kaimiro “D” Sand Horizon	53
4.17. Average velocity map of the Farewell “E” Shale Horizon	54
4.18. Average velocity map of the Farewell “F” Sand Horizon	55
4.19. Average velocity map of the basement Horizon.....	56
4.20. Depth map of the Basetik (Oligocene) Horizon	58
4.21. Depth map of the Kaimiro “D” Sand Horizon.....	59
4.22. Depth map of the Farewell “E” Shale Horizon.....	60
4.23. Depth map of the Farewell “F” Sand Horizon.....	61
4.24. Depth map of the basement Horizon	62
4.25. 3D depth view of four horizons	63
4.26. Vertical seismic section of Inline 3813 in depth.....	64
4.27. Illustration displaying calculation of the interval velocity	65
4.28. Interval velocity map of the Kaimiro “D” Sand	67
4.29. Interval velocity map of the Farewell “E” Shale	68
4.30. Interval velocity map of the Farewell “F” Sand	69

4.31. Isopach map of the Kaimiro “D” Sand	71
4.32. Isopach map of the Farewell “E” Shale	72
4.33. Isopach map of the Farewell “F” Sand	73
5.1. Surface displaying sweetness attribute	75
5.2. Vertical seismic section of Inline 3895 showing Horizon A	77
5.3. Vertical seismic section of Crossline 1556 showing Horizon A	78
5.4. Horizon slice of chaos attribute of Horizon A showing gullies.....	79
5.5. Horizon slice of local flatness attribute of Horizon A showing gullies.....	80
5.6. Gullies in Horizon A shown in a 3D view.....	81
5.7. Sweetness attribute of horizon slice showing top of the Farewell “F” Sand.....	83
5.8. Arbitrary Line showing the targeted horizons and Kahu channel	84
5.9. Channels in the Moki "A" Sand.....	86
5.10. Vertical seismic section of Inline 3827 showing different channels	87
5.11. Chaos slice showing channels in the Moki "A" Sand.....	88
5.12. Inline and time slice showing channels in the Moki "A" Sand.....	89
5.13. Inline 4207 showing a canyon	90
5.14. Time slice at 0.792 s showing a canyon	91
5.15. Inline 3595 showing sea-floor and two lineament features	92
5.16. Sand sample that may cause the lineament features	92
5.17. Time slice at 0.312 s showing two lineaments	93
5.18. Crossline 1438 showing Oligocene unconformity.....	94
5.19. Clinoform surfaces showing prograding patterns in the Giant Foresets.....	95
5.20. Seismic reflection termination patterns	96

5.21. Inline 3806 illustrating reflection unit for the channel's infill.....	99
5.22. Inline 4247 showing reflection unit for the channel's infill	99
5.23. Time slice at 2.044 s showing three channels.....	100
5.24. Time slice at 0.752 s illustrating channels.....	101
6.1. Well logging correlation of four wells along the study area.....	103
6.2. VSH, PHIE, PHISW, and PHISXO logs for Well Amokura-1	110
6.3. VSH, PHIE, PHISW, and PHISXO logs for Well Taranui-1	111
6.4. Density-neutron crossplot for the Kaimiro "D" Sand in Well Taranui-1	112
6.5. Density-neutron crossplot for the Farewell "E" Shale in Well Taranui-1	113
6.6. Density-neutron crossplot for the Farewell "F" Sand in Well Taranui-1	113

LIST OF TABLES

Table	Page
3.1. SEGY file text header of the Tui-3D seismic data.....	24
3.2. Acquisition parameters for the Tui-3D Field.....	25
3.3. Log chart for each of the wells	26
3.4. Well type and symbol in the Tui-3D Field	27
3.5. Summary of lithostratigraphy of well Amokura-1	28
4.1. Interpreted seismic horizons	41
5.1. The five different seismic facies identified in the study area	98
6.1. Kaimiro “D” Sand’s calculated properties for each well.....	104
6.2. Farewell “E” Shale’s calculated properties for each well.....	105
6.3. Farewell “F” Sand’s calculated properties for each well.....	105
6.4. Kapuni Group’s calculated properties for each well.....	106

NOMENCLATURE

Symbol	Description
AI	Acoustic Impedance
3D	Three dimensional
Xline	Crossline
CDP	Common Depth Point
in ³	Cubic inch
SEG	Society of Exploration Geophysicists
BS	Bit Size
CALI	Caliper
DENS	Density
DRHO	Bulk Density Correction
DTC	Delta-T Compressional
DTS	Delta-T Shear
GR	Gamma Ray
Fm	Formation
NEUT	Neutron
RC	Reflection Coefficient
PEF	Photoelectric Factor
RESD	Deep Resistivity
RESM	Medium Resistivity
RESS	Shallow Resistivity

SP	Spontaneous Potential
TD	Time-depth
TEMP	Cartridge Temperature
TENS	Cable Tension
AHBRT	Along Hole Below Rotary Table
TVSS	True Vertical Depth Sub Sea Level
m	Meter
mmbbl	Million Barrels
bbl/d	Barrels Per Day
bopd	Barrels of Oil Per Day
m ³	Cubic Meter
bcf	Billion Cubic Feet
mdbl	Thousand Barrels
Hpv	Hydrocarbon Meters
Kh	Permeability Meters
Km	Mean Permeability
Ngr	Net/Gross Ratio
Pha	Average Porosity
Phih	Porosity Meters
Swa	Average Saturation
md	Millidarcy
P90	90 Percent Engineering Probability

1. INTRODUCTION

1.1. AREA OF STUDY

The Tui-3D Field (aka Tui Area Oil Fields) is located on the southwest coast of the North Island of New Zealand (Figure 1.1). It covers approximately 352 km² offshore of the south of the Taranaki Basin (Veritas DGC, 2003). There are three oil accumulations in the Tui-3D Field, which includes Tui, Amokura, and Pateke oil fields (NZP&M, 2014). Those oil fields were the first independent oil project in the offshore region of the Taranaki Basin. Production started shortly after their discovery (about 4.5 years) and the last investment (20 months).

The Taranaki Basin encompasses roughly 330,000 km². It is the only basin that is producing oil and gas in New Zealand. The basin is bounded by the Reinga Basin in the north and Patea-Tongaporutu High in the east. Some fields, which are Maui, Tui, Maari, Kupe, Kapuni, and Kaimiro, are producing oil and gas in the Taranaki Basin (Figure 1.2) (NZP&M, 2014). The Tui-3D Field is situated on the Western Platform, which is a steady region compare to the Northern Graben and the Cape Egmont Fault zone (Figure 1.2).

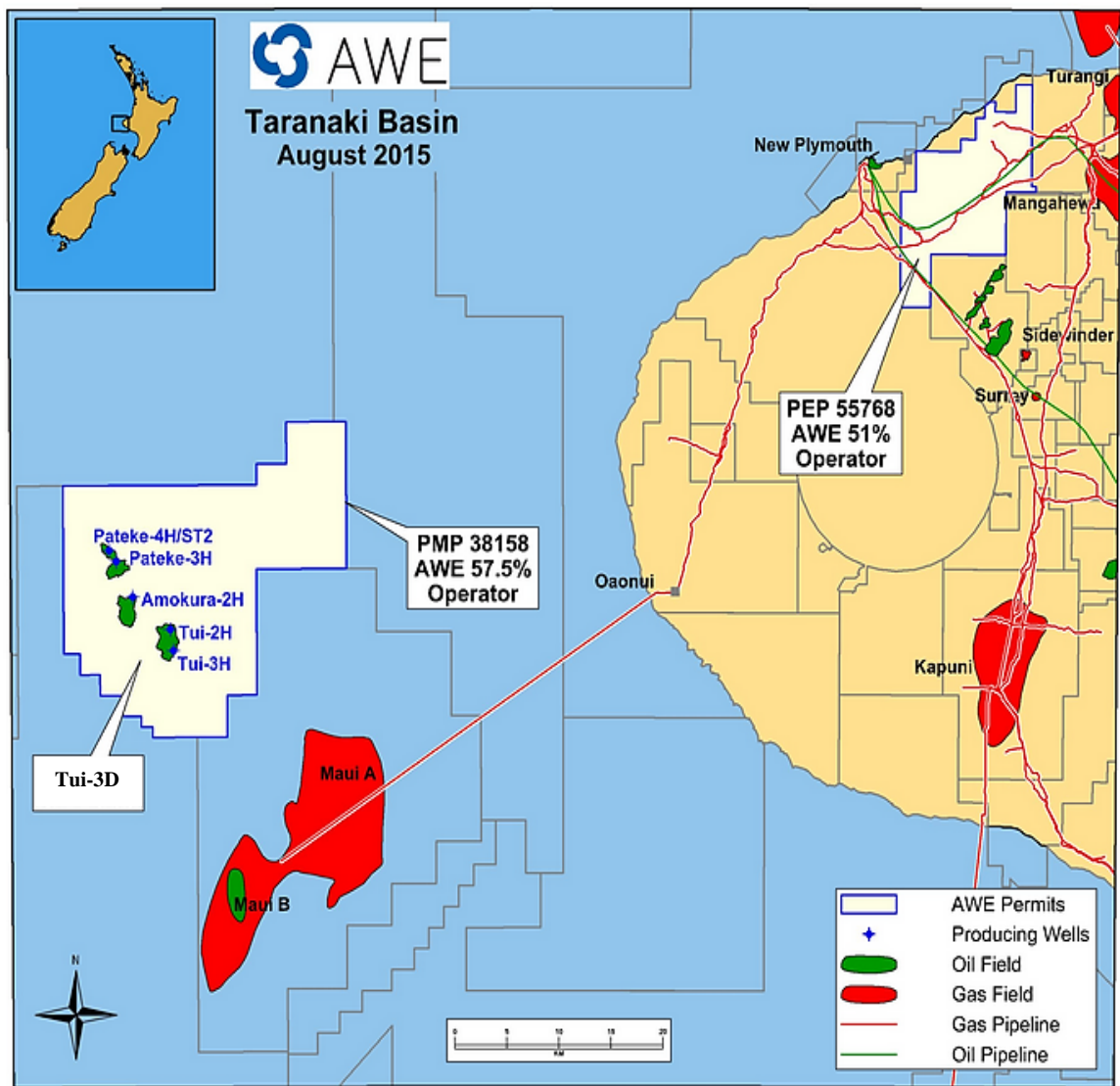


Figure 1.1. Location of the Tui-3D Field (Modified from Our Projects | AWE Limited, 2016).

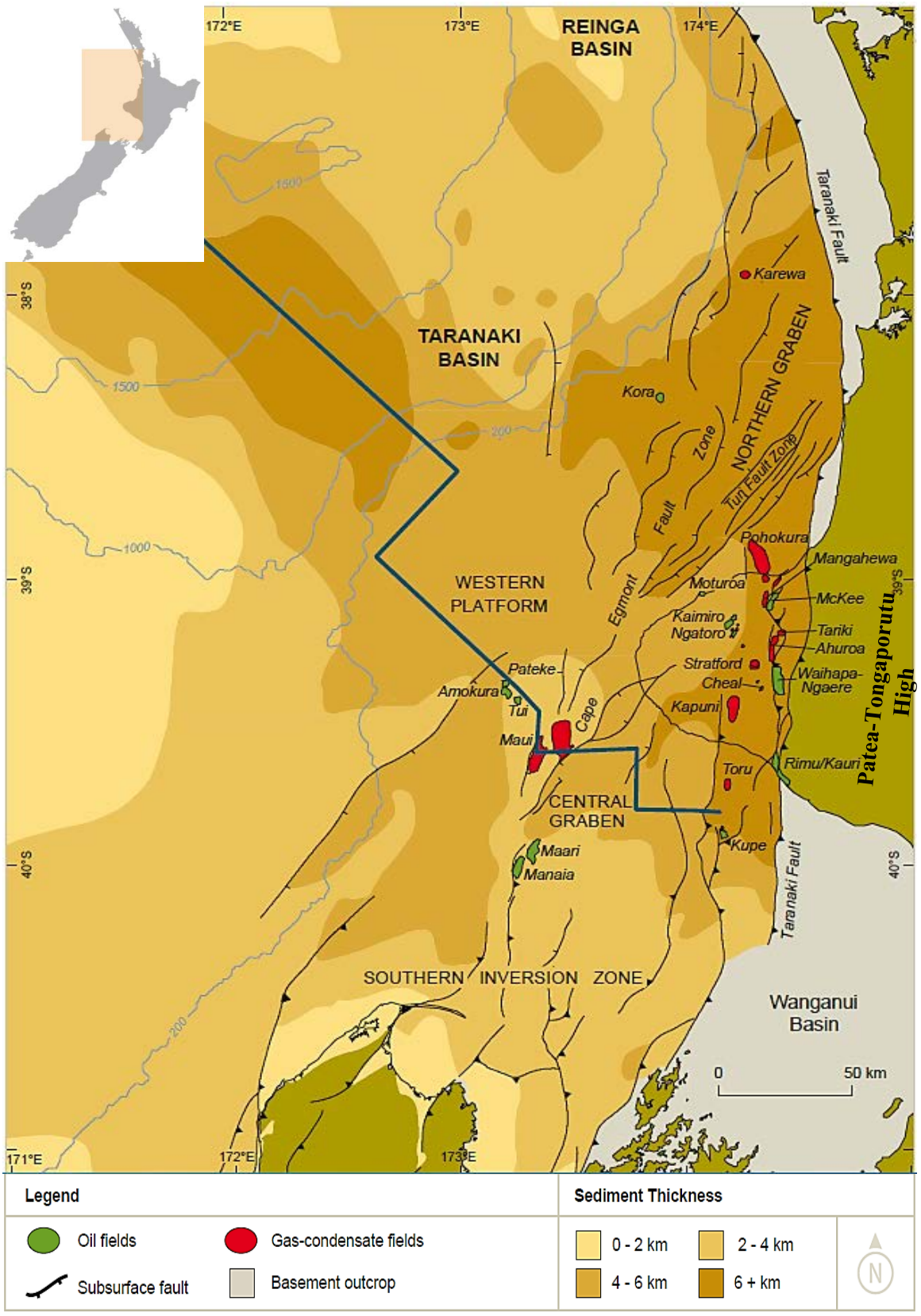


Figure 1.2. Location of the Taranaki Basin showing structures, oil and gas fields, and sediment thickness (Modified from NZP&M, 2014).

1.2. EXPLORATION HISTORY

The area, mostly including PEP-38460 permit field (Figure 2.2), was discovered and operated by Shell with 2D seismic data in the late 1970s and the early 1980s. Well Kiwa-1 was drilled in 1981 (Figure 1.3). Although the well is situated on a block with a broad, low relief, and velocity dependent 4-way dip closure, Kiwa-1 does not have hydrocarbon (Stroud et al., 2004).

In 1996 and 1998, two seismic surveys were conducted. Well Hochsetter-1 was the first well to be considered as a prospect (Figure 1.3). However, no hydrocarbon was shown after the well was drilled although it had good quality of reservoirs (AWE, 2012).

The permit was extended for 5 years in September, 2001. The well Tui-1 (Figure 1.3) was the second well drilled by New Zealand Overseas Petroleum (NZOP) in November, 2002. Hydrocarbon was found as the first discovery of oil with 10 m of oil accumulation at 3663.5 m depth in Tui-1. Additionally, two more reservoirs were discovered when a 3D seismic survey, over an area of 350 km², was acquired over the Tui Field. These reservoirs are located roughly at 3670 m depth, in wells Amokura-1, Pateke-1, and Pateke-2, which were drilled in 2004 (Figure 1.3). Kiwi-1 and Pukeko-1 were drilled as exploration wells but failed (AWE, 2012).

Australian Worldwide Exploration Limited (AWE) bought NZOP and became the permit's operator in February, 2006. The Petroleum Mining Permit (PMP) 38158 for the Tui Field was awarded in November, 2005. The first exploration well, Tieke-1, was drilled in November, 2006. Four oil producing wells, Tui-2H, Tui 3H, Amokura 2H, and Pateke 3H, were drilled by the middle of 2007. Taranui-1 was drilled in August / September, 2007, as the second exploration well (AWE, 2012).

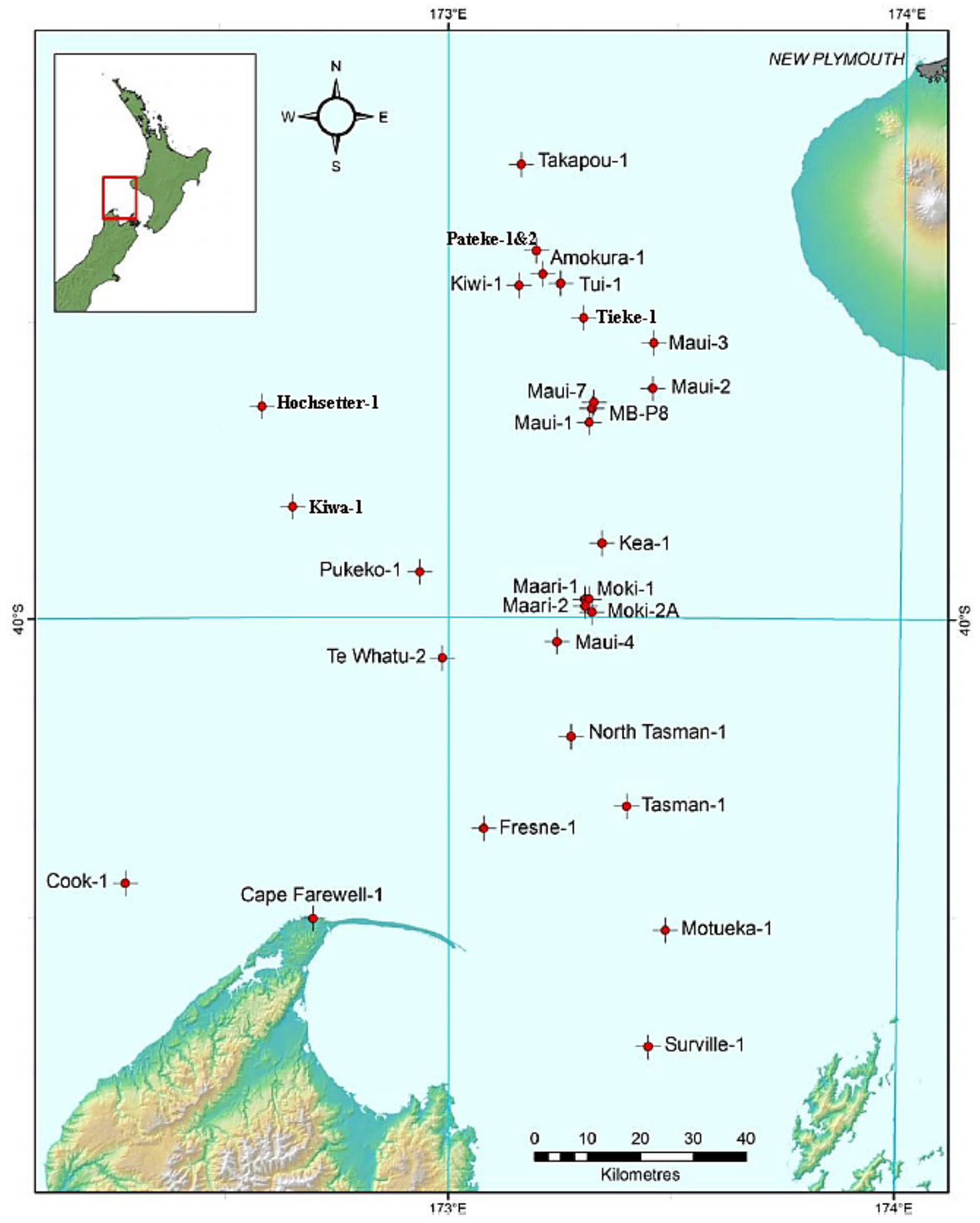


Figure 1.3. Location map of the wells (Modified from Roncaglia et al., 2013).

The Tui-3D area was estimated to have 37.6 mmbbl (million barrels) of recoverable oil. In January, 2013, the Tui-3D Field's gross cumulative production was 14.96 bcf (billion cubic feet) of gas and 35.5 mbbl (thousand barrels) of oil. The rest of the reserves (P90) were estimated as producing 3.5 mmbbl oil on January 1st, 2013. There are four horizontal wells in the Tui-3D Field that connect to FPSO Umuroa (Figure 1.4) (NZP&M, 2014).

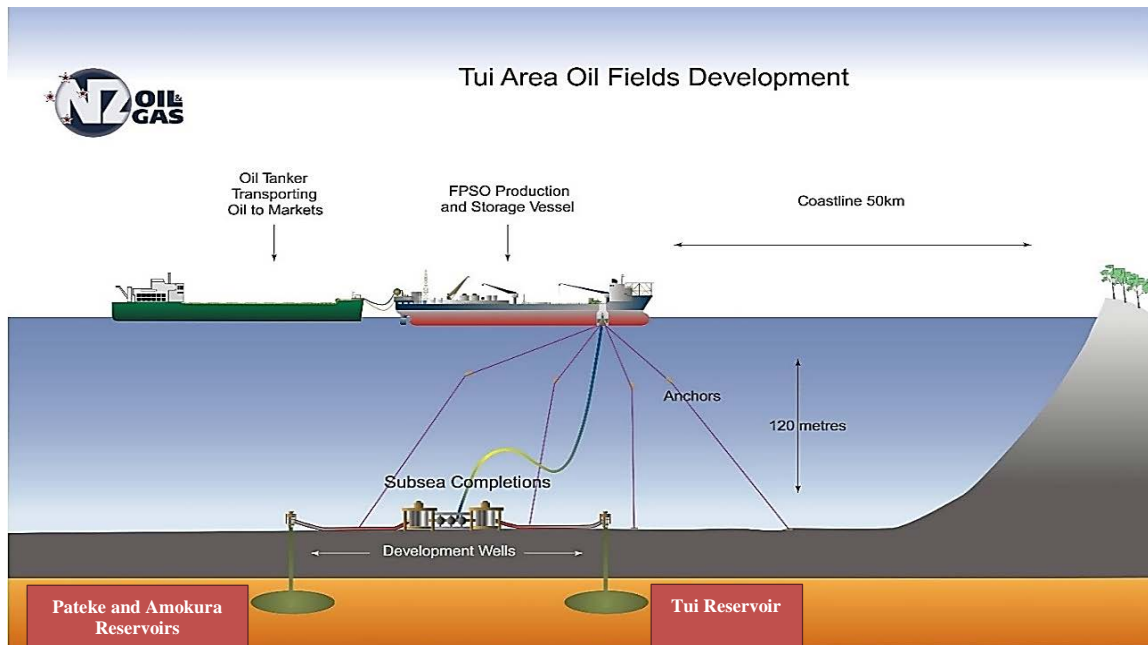


Figure 1.4. Schematic of the Tui-3D Field development (Modified from NZ Oil & Gas – Tui Area Oil Fields, 2016).

1.3. OBJECTIVES

The purpose of this study was to characterize structural settings and depositional environments of the Tui-3D Field using the available well log, well data, and seismic data. First, an interpretation of thirty-two minor faults and five horizons was conducted to provide an understanding of the structural and geologic features. Several types of maps, such as time structure, velocity, isopach, and depth, were generated. Several anticlines, which are potential traps, and dipping of each target horizons were displayed. In addition, a well logging correlation was created using four wells to observe distribution for subsurface of the target horizons over the study area.

In order to understand the depositional environment of target horizons, some geologic features such as lineaments, gullies, unconformities, seismic facies, reflection patterns, and channel infill geometries were identified. Seismic attributes such as chaos, sweetness, and local flatness were generated to better display stratigraphic features such as channels and gullies on time and horizon slices. In addition, a petrophysical analysis was conducted to examine properties of each target formation including effective porosity, permeability, volume of shale, water saturation, and average porosity. Finally, crossplots were generated to estimate lithology of each target formation.

2. REGIONAL GEOLOGY

2.1. GEOLOGICAL SETTING AND TECTONIC HISTORY

The Taranaki Basin is located on the west side of North Island, New Zealand (Palmer, 1985) and it is situated above the subduction zone where the Pacific Plate is subducting beneath the Australian Plate (Figure 2.1). The Western Platform and the Eastern Mobile Belt (formerly known as Taranaki Graben) are two main structural components of the basin (Pilaar & Wakefield, 1978; Knox, 1982) (Figure 2.2). The Western Platform, which is more than 100 km wide, underlies the deep water in the central and external unit of the continental shelf in the west. A large, easy to understand structure and 2,000-5,000 meters of sedimentary layer characterize this area (Palmer, 1985). The Eastern Mobile Belt is very well structured and regulated by Late Cretaceous-Eocene faults.

The Taranaki Basin is a very diverse structure (Figure 2.2) (NZP&M, 2013). Most of the structures are related to basement fault-block activity and basement-involved in the west and south parts of the basin. Although all parts of the Eastern Mobile Belt have been influenced by the movements of the complex compressional/wrench, these late movements have not highly influenced the Western Platform covering the Tui-3D Field. Thus, the seal unit should be preserved and existing accumulations should be conserved (Mills, 2000). In addition, most of the old half-grabens are kept where Oligocene to Pliocene sediments buried them in the Western Platform (King & Thrasher, 1996).

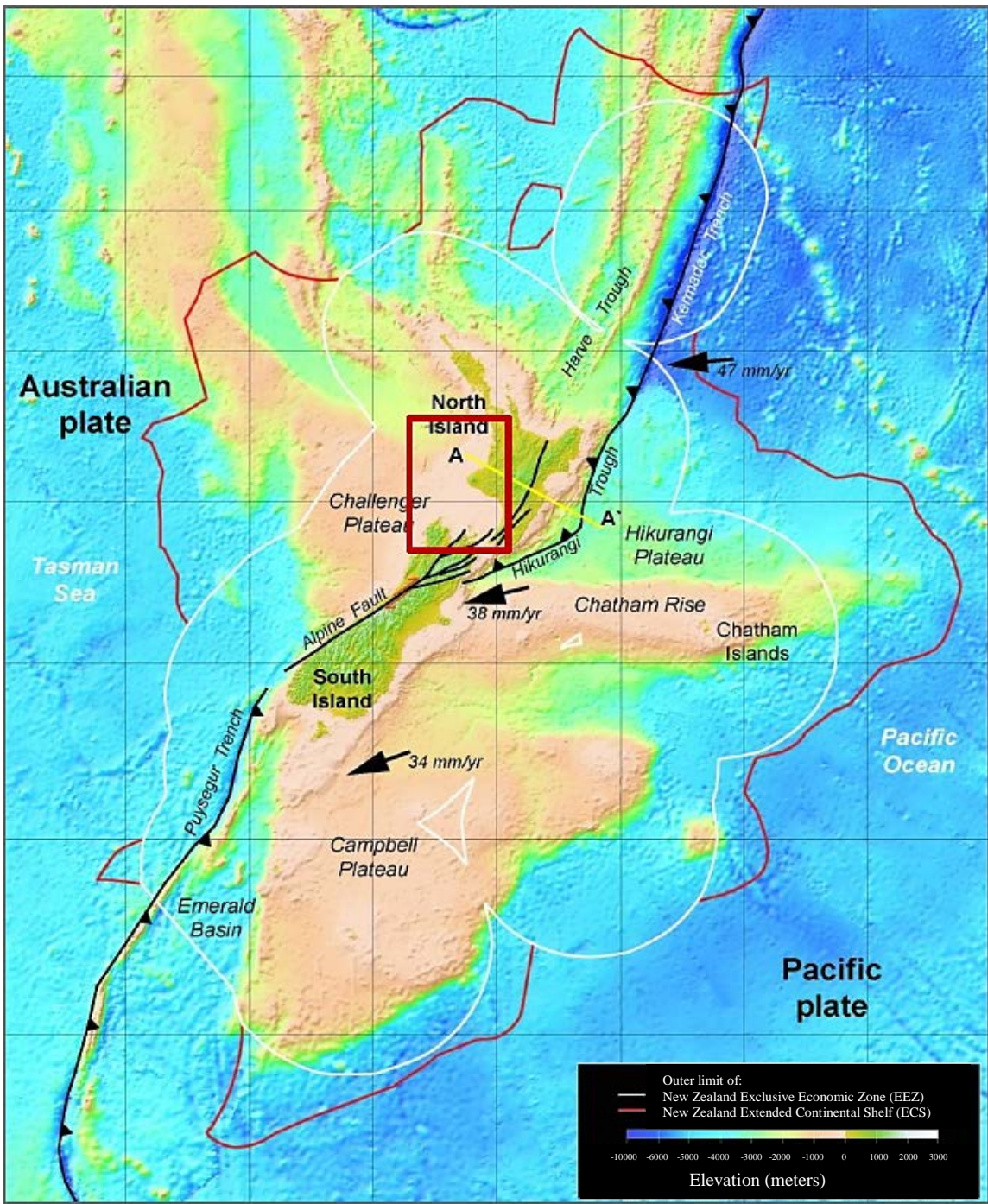


Figure 2.1. Location of the Taranaki Basin. The Pacific Plate is subducting beneath the Australian Plate, and the Taranaki Basin is located above this subduction zone as shown with a red rectangle (Modified from Stroger et al., 2012).

In the Late Cretaceous, extensional tectonics related to the separation of eastern Gondwana formed the Taranaki Basin (Laird, 1981; Browne & Field, 1988; Bradshaw, 1989). Many half-grabens, which were active up to the end of Paleocene in both North and South Island of New Zealand, were developed at that moment, and they positioned north–south and northeast-southwest (Walley, 1991). The south of the Taranaki Basin hosted terrestrial accumulation in Paleocene (King & Robinson, 1988). Subsidence continued gradually throughout Eocene (King & Thrasher, 1996). Towards the end of the Eocene period a transgression occurred (Walley, 1991). This field became full of marine circumstances toward northwest. There was a very quick subsidence of a foredeep that was mostly seen in the eastern side of the Taranaki Peninsula because a new compressional tectonic movement began in New Zealand in Oligocene (King, 1990). A foreland basin evolved at that moment, but it had formed by the time of the early Miocene, and compressional structures were developed in the basin.

An insignificant area of the basin was formed from the late Miocene by back-arc volcanoclastic substance. Compression diminished towards the end of Miocene (Mills, 2000). In the Pleistocene period, an extension around the plate boundaries affected the east of the Taranaki Basin and this event was occurred behind an active back-arc (Taylor & Karner, 1983). This occasion stimulated the subsidence of Northern and Central Grabens. The Cape Egmont Fault Zone (Figure 1.2) was the western border fault of the Eastern Mobile Belt (Figure 2.2) (Muir et al., 2000). When the Cape Egmont Fault Zone activated, Northern Grabens started to develop in the late Miocene. The Western Platform was not affected significantly by the extension of the plates and the earlier compressional phase.

The Tui-3D Field is located on the Western Platform in the Taranaki Basin. It is bounded by the high of the Challenger Rise on the west and the Eastern Mobile Belt on the east (Figure 2.2). In this area, there are three basement high trends, i.e. the Maui High, the Kiwa High, and the Hochstetter High (Mills, 2000).

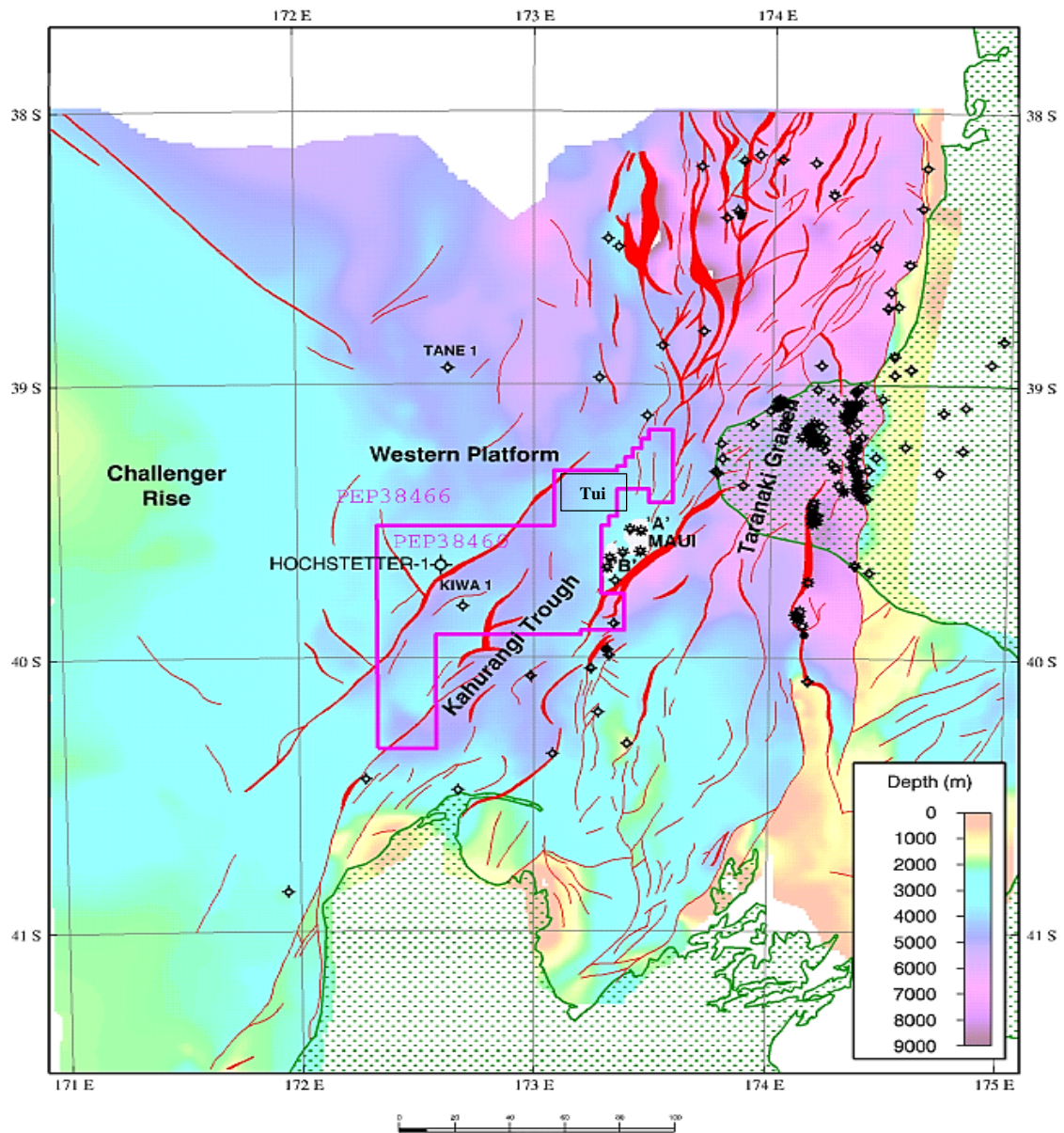


Figure 2.2. The basement structure map of the Taranaki Basin. The Eastern Mobile Belt (aka Taranaki Graben) and the Western Platform are two main structural elements (Modified from Mills, 2000).

2.2. GEOLOGICAL STRATIGRAPHY

The Taranaki Basin consists of complicated and highly variable sediments because of its mobile history (Mills, 2000). However, the main depositional environments become increasingly marine or deeper water to the northwest.

Many potential reservoirs exist in the Taranaki Basin. Over ten different stratigraphic units have oil and/or gas (NZP&M, 2014). They are all clastic except Oligocene Tikorangi Limestone. Paleocene-Eocene Kapuni Group sandstones, coastal facies, have an excellent quality of reservoirs (King & Thrasher, 1996).

In this research, the Kapuni Group, which consists of the Kaimiro Formation (Kapuni “D” Sandstone) and Farewell Formation (Kapuni “E” Shale and Kapuni “F” Sandstone) was studied in detail (Figure 2.3). In addition, some appealing geological features of the North Cape Formation, basement, Moki “A” Sandstone Formation, the Giant Foresets Formation, and the Tikorangi Limestone Formation (Basetik) were investigated through this study (Figure 2.4).

2.2.1. North Cape Formation. The formation is the top part of the Pakawau Group, and it mostly consists of sandstone, siltstone, and conglomerate with small coal joints (King & Thrasher, 1996). It is recommended by Higgs et al. (2004) that the unit be named North Cape Formation instead of the Rakopi Formation in the Tui-3D Field because it lacks the coaly component. The North Cape Formation is a shallow marine, paralic, and terrestrial environment which is Late Cretaceous in age (Suggate, 1956).

2.2.2. Kapuni “D” Sandstone Formation (Kaimiro “D” Sand). The Kapuni Group contains marginal marine and terrestrial units, which range from Paleocene to Eocene in age (King & Thrasher, 1996). Due to the migration of facies belts to the east of

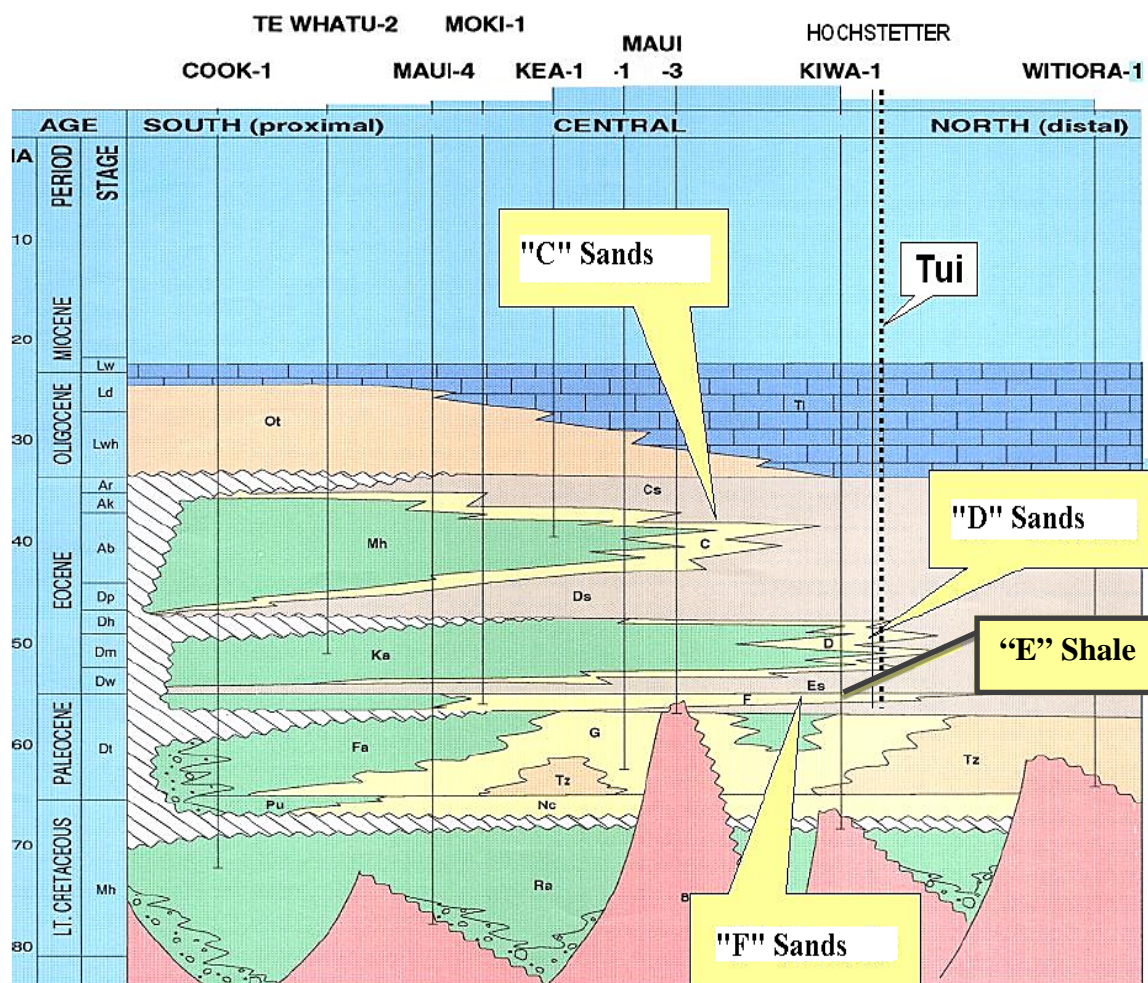


Figure 2.3. Illustration of stratigraphy for the offshore Taranaki Basin (Modified from Stroud, 2004).

the Tui Field by the mid-Eocene, there is no Kapuni “C” sand formation (Mangahewa Formation), the upper part of the Kapuni Group, in the Tui-3D Field (Matthews et al., 1998). The Kapuni “D” Sandstone (Kaimiro Formation) is a paralic facies (King & Thrasher, 1996; Matthews et al., 1998).

The Kapuni “D” Sandstone (Kaimiro Formation) consists of two kinds of sandstones within Early to Mid-Eocene. The first one has a grain size ranging from medium to coarse, moderately to well sorted, and contains quartz-dominated sandstones.

The second type is dark yellow brown to brownish grey, fine to medium grained, and contains intermittently argillaceous sandstones (Palmer, 1985).

The depositional environment of the Kaimiro Formation is low energy, marginal marine to lagoonal, and it is largely deposited as shoreline and coastal plain (Higgs et al., 2012).

2.2.3. Kapuni “E” Shale Formation (Farewell “E” Shale). The Kapuni “E” Shale is not only a part of the Turi Formation but is also interfingering with the Kapuni Group formations. The lower part of “E” is interpreted as the Tane Member of the Turi Formation. The uppermost part of the member is assumed to be an intra-Paleocene sequence border (King & Thrasher, 1996).

The “E” shale shows shelfal sedimentation with comparatively small clastic input. Hidden sedimentary cycles prove that there were little differences in sea level or the amount of sediment during the time of deposition for the “E” shale. Palynologic analysis illustrates that sediments are Early Eocene to Paleocene in age, although foraminifera shows nearshore to inner shelf paleoenvironments (Stroud et al., 2004).

According to core data, the upper part of the formation is deposited in shallow marine shelf (transgressive). The “E” shale was described as an offshore shale deposit from FMI logs by Schlumberger, even if most of the unit has a very fine sandstone.

2.2.4. Kapuni “F” Sandstone Formation (Farewell “F” Sand). The Kapuni “F” Sandstone is the upper part of the Farewell Formation, which is an essential formation of the Kapuni Group (King & Thrasher, 1996). The Farewell Formation is the lower part of the Kapuni Group in the Tui-3D Field, and it lies unconformably over the North Cape Formation.

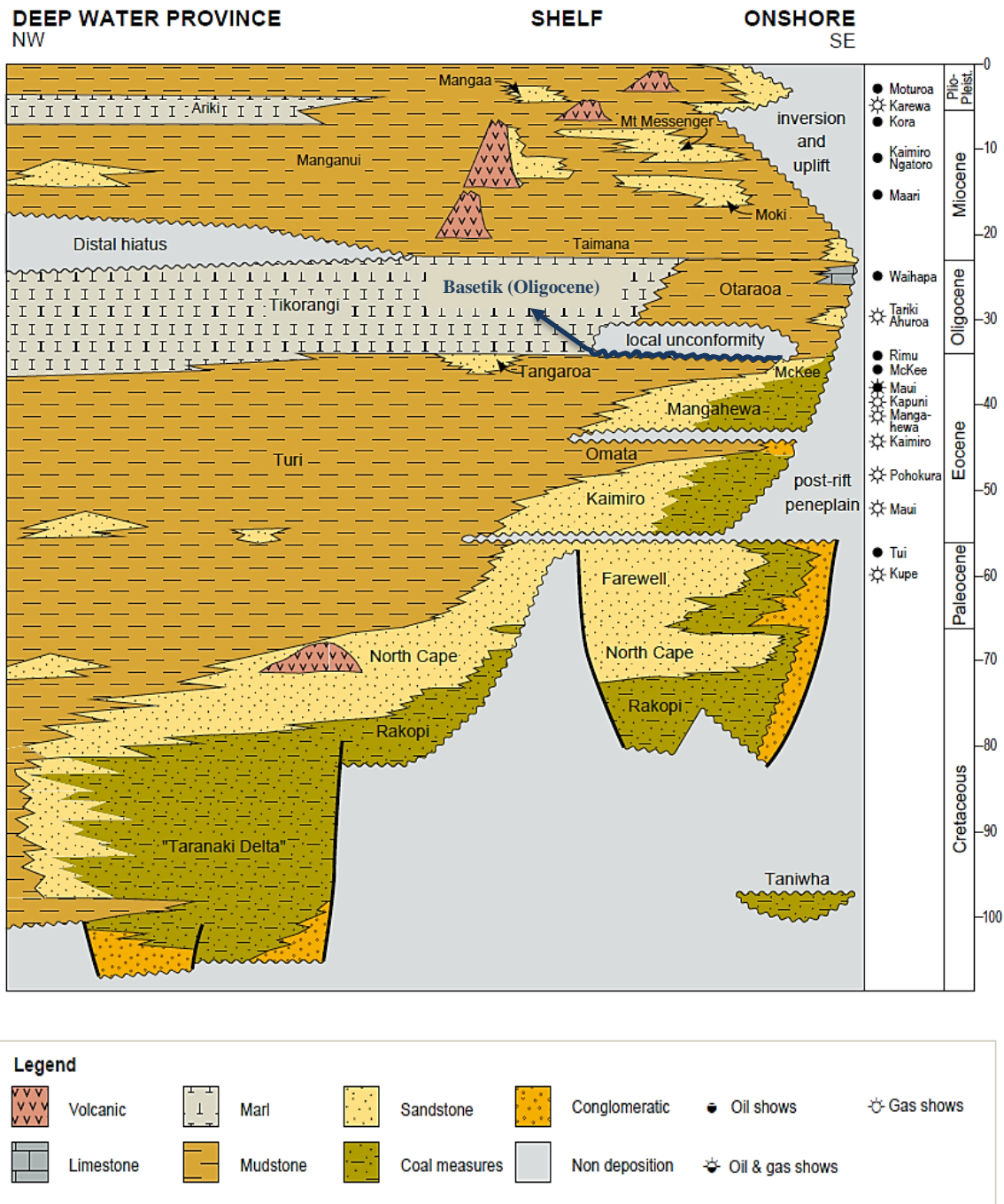


Figure 2.4. Generalized stratigraphy for the Taranaki Basin (Modified from NZP&M, 2014).

The Farewell Formation consists of siltstone and interbedded fine to coarse-grained sandstones. The lower “F” sand is primarily comprised of siltstones, which are brown-grey and grey, fine to coarse grained, loose, and interbedded sandstones.

North to northwest oriented draining fluvial system, which was grown in a valley regulated by the faults, deposited the sandstones that are Paleocene-Early Eocene in age. Palynological reports illustrate that the Paleocene section accumulated in a very near, heterolithic shelf with bottom circumstances ranging from completely oxic to anoxic (Strogen et al., 2010).

2.2.5. Giant Foresets Formation. The Giant Foresets Formation created the entire Plio-Pleistocene sequence on the Western Platform (King & Thrasher, 1996). The “Pliocene” and “Recent” parts show younger sequences within the Giant Foresets Formation. The north Taranaki Basin has the same units within the formation (Soenandar, 1992; Hansen & Kamp, 2002).

Great amounts of shell fragments characterized the sandy siltstone to mudstone units in the Giant Foresets Formation. The Giant Foresets Formation was deposited in a slope to shelfal environment and is Pliocene to Pleistocene in age (Pilaar & Wakefield, 1978). The Early Pliocene formation in the Tui-Amokura Field ranks laterally to a conformable offlapping unit (Matthews, 2002).

2.2.6. Moki “A” Sandstone Formation. The Moki Formation is comprised of fine to very fine grained and argillaceous sandstones and sandy units with interbedded mudstone and siltstone and limestone stringers (Lock, 1985).

The Moki Formation covers the Mid-Miocene sandstone sequence, which is seen over the Taranaki Basin. The Moki “A” Sandstones are the upper part of the Moki

Formation in the Tui-3D Field. The Moki “A” Sandstones were accumulated as seen in base-of-slope turbidites (Engbers, 2002). NW-SE meandering channels were found in different locations and times in the Maui 3D seismic survey along the Moki “A” accumulation (Bussell, 1994).

2.2.7. Tikorangi Limestone Formation. The Tikorangi Limestone Formation is a calcareous sequence seen all over the Taranaki Basin. This sequence shows a time of tectonic calmness from Oligocene to earliest Miocene ages (King & Thrasher, 1996). According to Stroud et al. (2004), the upper part of the formation is Early Miocene in age with lower bathyal paleoenvironments (1,000-2,000 m water depth), and the lower part of the formation is Oligocene in age with environments ranging from the mid shelf (50-100 m depth) to the outer shelf (100-400 m water depth).

2.2.8. Basement. The basement consists of Early Cretaceous granitoids of the Separation Point Suite or Paleozoic granitoids of the Median Tectonic Zone Suite on the Western Platform of the Taranaki Basin (Mortimer et al., 1997).

2.3. PETROLEUM SYSTEM

The wells of Amokura-1, Pateke-2, and Tui-1 (Figure 2.5) proved and broadened the Rakopi – North Cape (source), Kapuni “F” (carrier bed and reservoir), and Kapuni “E” (seal) petroleum system in the Tui-3D Field (NZOP, 2004).

Figure 2.6 shows petroleum system elements in the Taranaki Basin. This petroleum system section was based on New Zealand Overseas Petroleum Ltd. (NZOP) report, 2004.

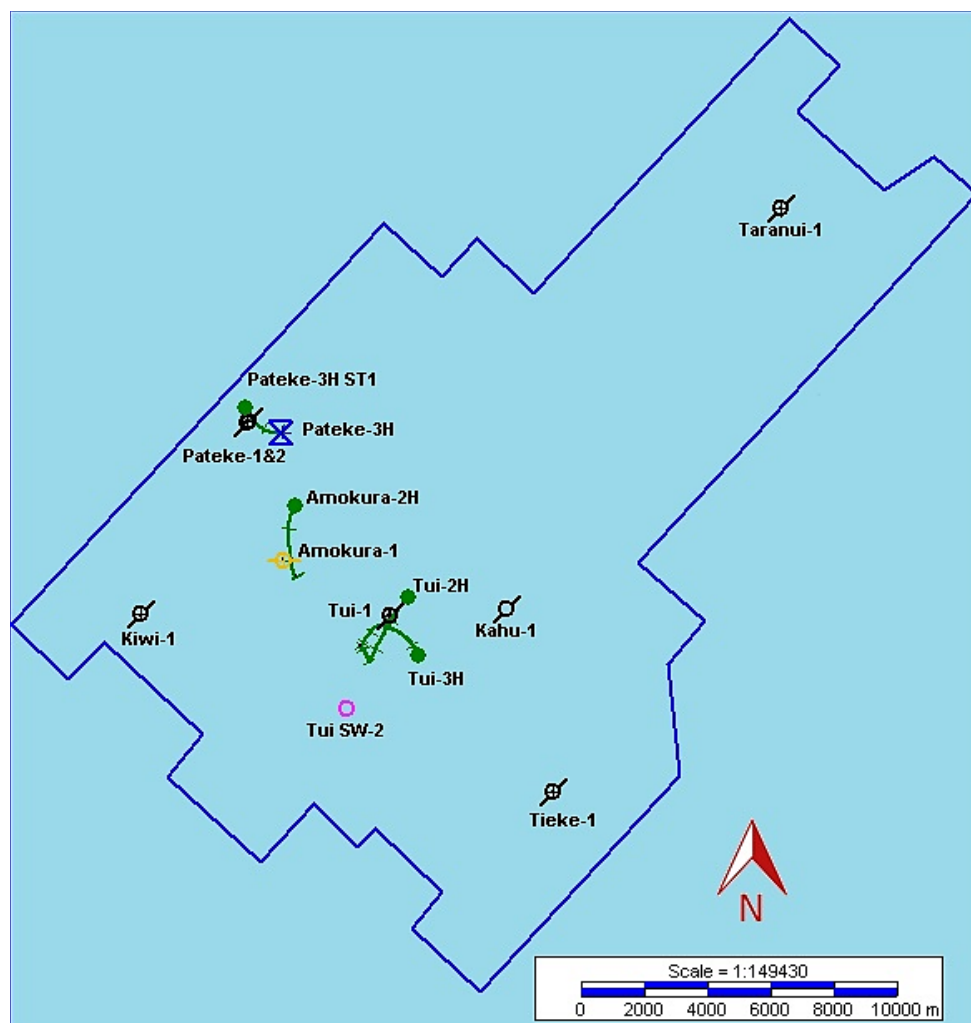


Figure 2.5. Location of the wells in the Tui-3D Field (for well symbols and types, refer to Table 3.3).

2.3.1. Source. Rakopi-North Cape coals and organic rich mudstones from the Kahurangi subbasin (west and northwest of Amokura-1, Pateke-2, and Tui-1 wells) are the source rocks. Oil has been produced and expelled in the last 5-10 million years (Killops & Sykes, 2003; Funnel et al., 2001). On the other hand, there could be some limited charge from the north and east (NZOP, 2004).

2.3.2. Migration. The base of the Paleocene Kapuni “F” Sandstones, paralic and coastal complex, is connected to the Cretaceous Rakopi-North Cape source unit in the Kahurangi trough, west and northwest of the wells (Amokura-1, Pateke-2, and Tui-1). The oil that is generated and expelled from the kitchen field passes into the base of the Kapuni “F” Sandstone and migrates up to the basement high at Maui. The oil also migrates towards the higher part of the Kapuni “F” Sandstone section in the Tui-3D Field (NZOP, 2004) (Figure 2.7). Usually, there is inadequate Kapuni “E” Shale (seal) in depositional environments of the paralic and coastal complex. If basement faulting continues through the Kapuni “E” Shale, oil could migrate vertically through the Kapuni “D” Sandstone (NZOP, 2004).

2.3.3. Reservoir. After migration within the sequence, oil accumulation occurs in the top of the Kapuni “F” paralic and coastal complex sandstones. The reservoir quality is very good in three oil wells. First, in the Tui-1 well, the Kapuni “F” reservoir has a permeability of 400 millidarcies in 36 meters of gross sand and a porosity of 18% with 10 m column of oil. Second, the Pateke-2 well has a porosity of 21% and roughly 27 meters of gross sand with a 12 m oil column in the uppermost member. Finally, the Amokura-1 well has a porosity of 18% and a permeability of 1.870 millidarcies in 37.5 meters of gross sand with a 12 m oil column in the top member (NZOP, 2004).

2.3.4. Seal. The oil fields of Amokura-1, Pateke-2, and Tui-1 are roughly 180 meters thick and have an excellent top seal of the Kapuni “E” Shale. Faulting does not affect the top seal within this area (NZOP, 2004).

2.3.5. Trap. As mentioned above, the Kapuni “F” Sandstone plays two roles in the petroleum system, i.e. oil migration through the unit and oil accumulation at the upper

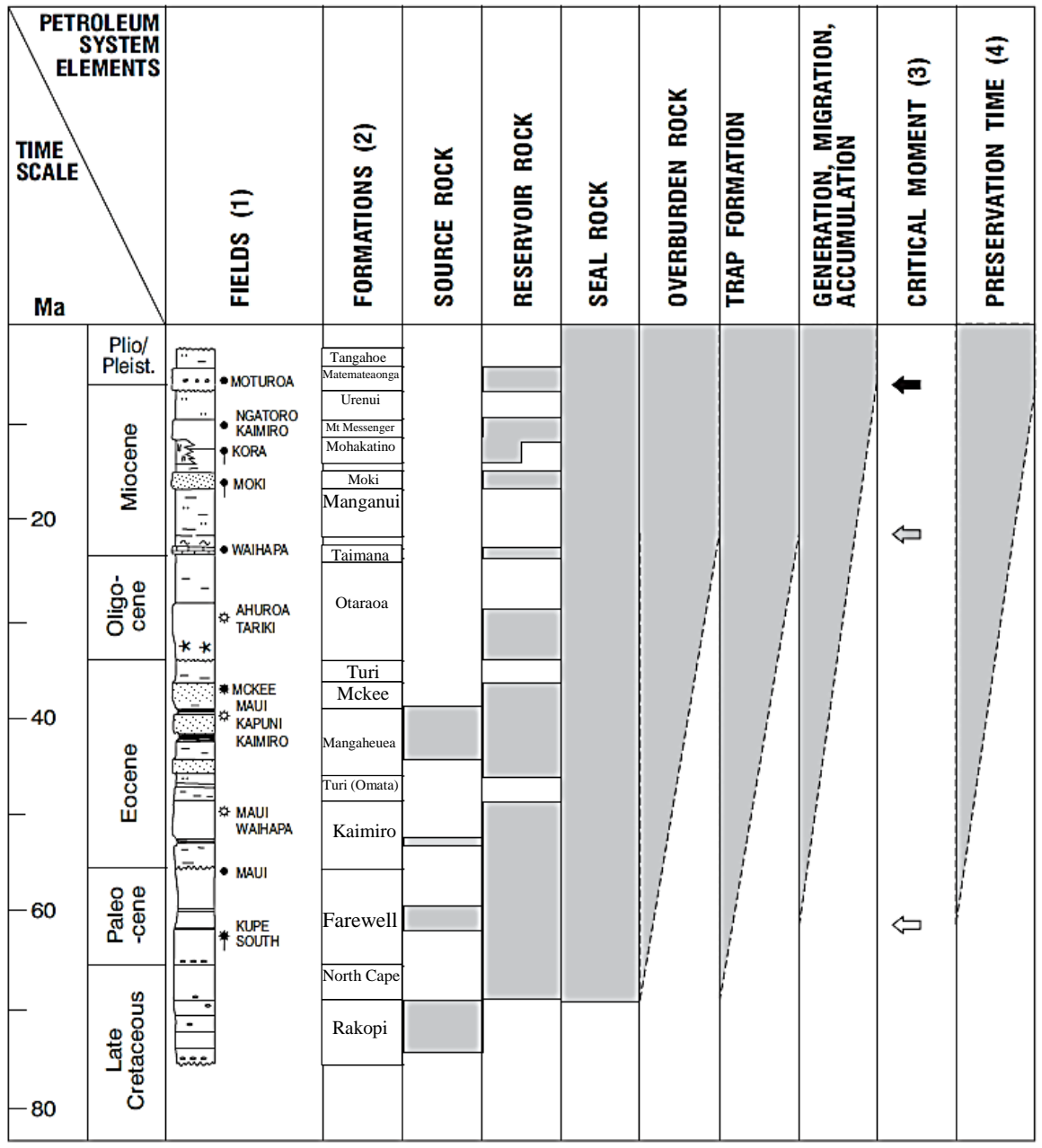


Figure 2.6. Event chart for the Taranaki petroleum systems showing relative timing of requisite elements (shading) (Modified from King & Thrasher, 1996).

part of the unit. Traps are local 4-way dip closures in the west and northwest dip of the Kapuni “F” Sandstone (Tui-1, Amokura-1, and Pateke-2) (NZOP, 2004).

2.3.6. Timing. The oil migration from the Kahurangi subbasin is Pliocene in age and active today. Thus, if there is any present or Pliocene structure within the Kapuni “F” reservoir through a migration direction from the source, it could be filling with oil and a prospective Kapuni “F” oil pool (NZOP, 2004). Before oil migration started, the Tui, Amokura, and Pateke structures were already in the area.

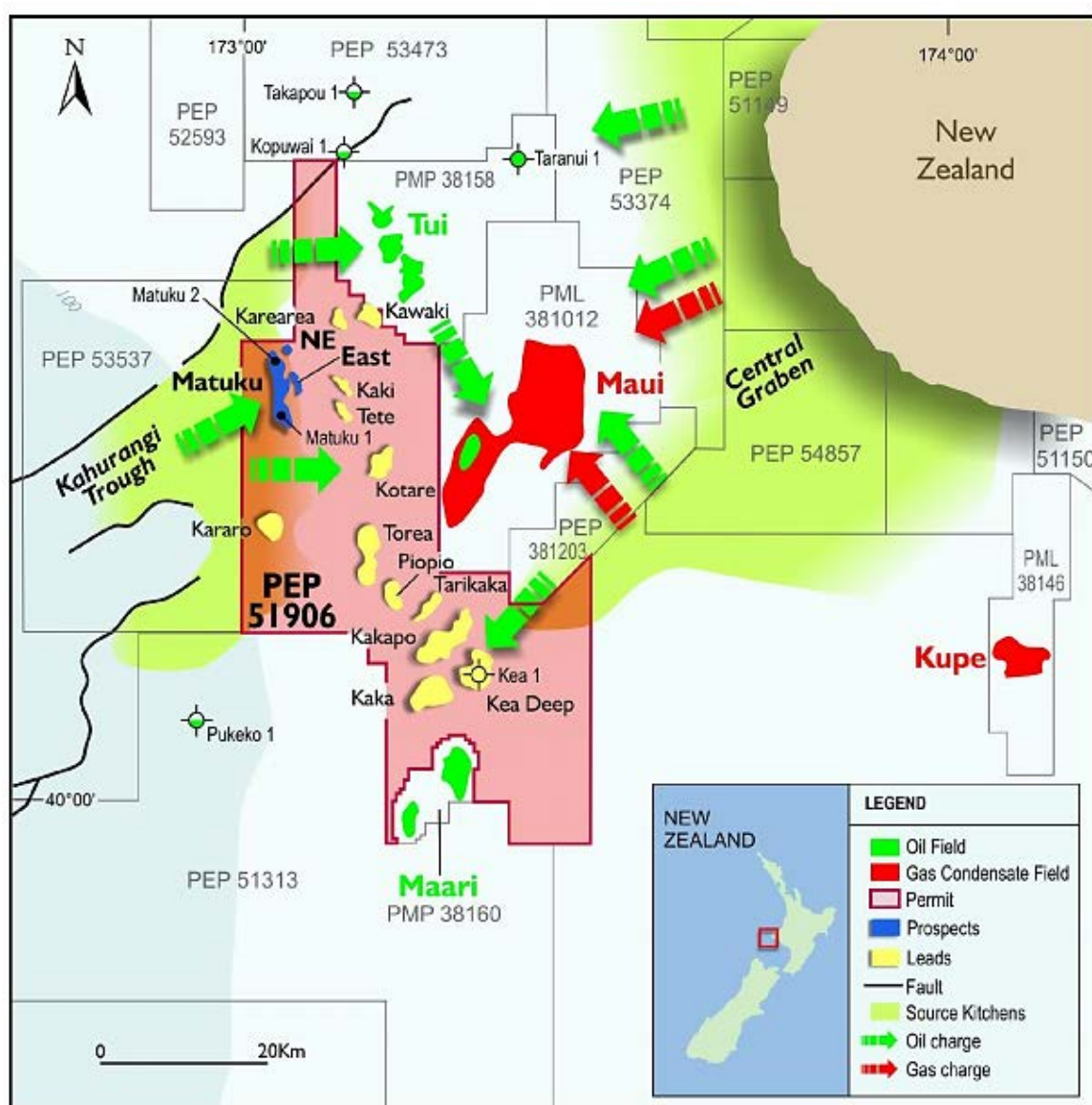


Figure 2.7. Possible oil migration pathways for the Tui-3D Field (Octanex, 2013).

3. DATA

3.1. TUI-3D SEISMIC DATA

The 3D marine seismic survey data, which were used in the study, were provided by New Zealand Overseas Petroleum Limited (NZOP) in the Tui-3D Field (PEP38460). The survey started on March 25, 2003 and was completed on May 10, 2003. The total 3D survey area is 352.195 km² (Figure 3.1), and the study area has 1500 inlines and 2474 crosslines with 12.5 m bin spacing (Veritas DGC, 2003).

In total, 12130 sail line kilometers were acquired. The survey area was located roughly 20 km southwest of New Plymouth, North Island. The average water depth was 130 m for the entire survey field. The 3D seismic survey was processed by Veritas DGC Australia Pty. Ltd (2003). The Tui-3D seismic SEG Y file text header is displayed in Table 3.1 and the acquisition parameters can be found in Table 3.2.

3.1.1. Polarity Check. Conventional SEG polarity was preserved through the survey for both acquisition and processing. All channels had the same polarity. If there was an increase in acoustic impedance, it was shown as a white trough and registered on tape as a negative number (Veritas DGC, 2003). However, since the phase shift was applied to the data by 180 ° using Petrel 2014, all data are shown as an American polarity throughout this study. The reason that the phase shift was applied is because the synthetic seismogram matches better with the seismic traces when the American polarity was used.

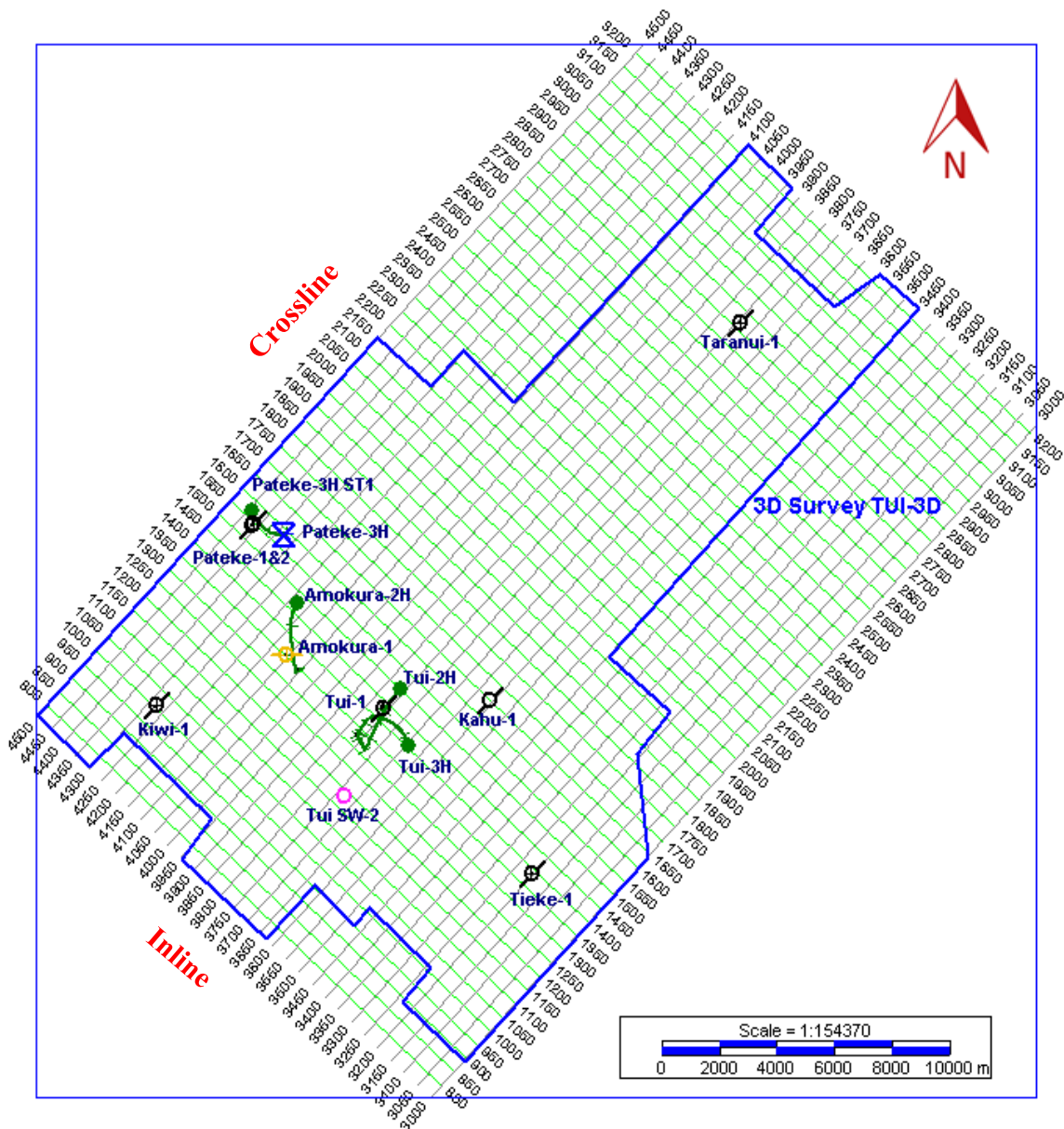


Figure 3.1. Basemap of the Tui-3D Field (for well symbols and types, refer to Table 3.3).

Table 3.1. SEGY file text header of the Tui-3D seismic data.

Area	Taranaki_Basin- TUI3D-PR2830 Migration
Survey	TUI-3D
Inline	3000 - 4500
Crossline	756 - 3230
CDP	30000756 - 45003230
Sample Rate	4000
Record Length	6000
Class	3D Seismic
Points Used For	Inline 3000 Xline 895 1624080-5623117
Survey Definition	Inline 3000 Xline 1636 1630397-5629892 Inline 4500 Xline 1636 1616685-5642679
Trace Header Byte Locations	
Inline	Bytes 13-16
Xline	Bytes 17-20
Projection	NZTM
Datum	NZGD2000

Table 3.2. Acquisition parameters for the Tui-3D Field (Veritas DGC, 2003).

PARAMETER	VALUE
SP Interval	18.75 meters flip/flop
3D Nominal Fold	48
Streamer Lengths	3600 meters (dual streamers)
Group Interval	12.5 meters
Near Offset	116 meters
Number of Traces	576 (288 per streamer)
Record Length	6144 milliseconds
Sampling Rate	2 milliseconds
Recording Instrument	(Not applied to data)
Data Tape Format	SEGD 8058
Energy Sources	Airgun 3200 in ³ (dual sources)
Streamer Depth	7 meters
Source Depth	9 meters
Streamer Separation	150 meters
Source Separation	75 meters

3.1.2. Well Data. The dataset included a 3D seismic survey, 14 wells, well logs, formation tops, and checkshots. Most of the wells have a diversity of logs such as caliper, density, sonic, gamma ray, neutron, resistivity, and SP logs except Well Pateke-1 and Well Pateke-3H, which have no logs (Table 3.3). Some of the wells were horizontal and deviated while others were vertical. Table 3.4 displays well type and symbol in the Tui-3D Field and Table 3.5 shows a lithology of Well Amokura-1 as an example.

Table 3.3. Log chart for each of the wells.

Amokura-1	BS	CALI	DENS	DRHO	DTC	DTS	GR	NEUT	PEF	RESD	RESM	RESS	SP	TEMP	TENS
Amokura-2H	BS						GR								TENS
Kahu-1		CALI	DENS	DRHO	DTC		GR	NEUT	PEF	RESD	RESM	RESS	SP		TENS
Kiwi-1	BS		DENS	DRHO			GR	NEUT	PEF	RESD	RESM	RESS		TEMP	
Pateke-2	BS		DENS	DRHO			GR	NEUT	PEF	RESD	RESM	RESS		TEMP	TENS
Pateke-3H ST1	BS	CALI	DENS	DRHO			GR	NEUT	PEF	RESD	RESM	RESS		TEMP	
Taranui-1	BS	CALI	DENS	DRHO	DTC	DTS	GR	NEUT	PEF	RESD	RESM	RESS	SP		
Tieke-1	BS	CALI	DENS	DRHO			GR	NEUT	PEF					TEMP	TENS
Tui SW-2		CALI	DENS	DRHO	DTC		GR	NEUT	PEF	RESD	RESM	RESS	SP		TENS
Tui-1	BS	CALI	DENS	DRHO	DTC	DTS	GR	NEUT	PEF	RESD	RESM	RESS	SP	TEMP	TENS
Tui-2H	BS	CALI					GR			RESD	RESM	RESS			TENS
Tui-3H	BS						GR			RESD	RESM	RESS			
Pateke-3H	NO	LOGS													
Pateke-1	NO	LOGS													

BS-Bit size; CALI-Caliper; DENS-Density; DRHO-Bulk density correction; DTC-Delta-T Compressional; DTS-Delta-T Shear; GR-Gamma Ray; NEUT-Neutron; PEF-Photoelectric factor; RESD-Deep Resistivity; RESM-Medium Resistivity; RESS-Shallow Resistivity; SP-Spontaneous Potential; TEMP-Cartridge Temperature; TENS-Cable Tension.

Table 3.4. Well type and symbol in the Tui-3D Field.



Well Name	Well Type	Well Symbol	Max. Depth (m)	Water Depth (m)
Amokura-1	Deviated	Suspended 	3995	121.9
Amokura-2H	Horizontal	Oil well 	5776	122.3
Kahu-1	Vertical	Abandoned 	3835	121
Kiwi-1	Deviated	Abandoned 	4238	124.7
Pateke-2	Deviated	Abandoned 	3861	124
Pateke-3H ST1	Horizontal	Oil well 	4895	123.3
Taranui-1	Deviated	Abandoned 	3915	121.2
Tieke-1	Deviated	Abandoned 	3578.8	119.38
Tui SW-2	Vertical	Location only 	3740	121.6
Tui-1	Deviated	Abandoned 	3902	122.7
Tui-2H	Horizontal	Oil well 	5950	121.6
Tui-3H	Horizontal	Oil well 	5384	121.8
Pateke-3H	Deviated	Active 	4895	123.3
Pateke-1	Vertical	Abandoned 	2256	124

Table 3.5. Summary of lithostratigraphy of well Amokura-1 (Stroud et al., 2004).

<i>Formation</i>	<i>Age</i>	<i>Formation top AHBRT (m)</i>	<i>Formation top TVSS (m)</i>	<i>Thickness (m)</i>	<i>Lithology</i>
Unnamed	Recent	148 (sea-floor)	123	272	Muds, silts
Unnamed	Pliocene	420	395	670	Mudstone siltstone
Giant Foresets	Pliocene - Miocene	1,187	1,162	673	Mudstone sandstone
Manganui (upper)	Miocene	1,860	1,835	593.5	Claystone
Moki "A" Sandstone	Miocene	2,453.5	2,428	150.5	Sandstone with claystone
Manganui (mid)	Miocene	2,604	2,579	83	Claystone
Moki "B" Sandstone	Miocene	2,687	2,662	110.5	Sandstone with claystone
Manganui (lower)	Miocene	2,797.5	2,772.5	147.5	Claystone
Tikorangi Limestone	Oligocene	2,945	2,920	81	Argillaceous limestone
Turi "Ash" unit	Eocene	3,026	3,001	23	Siltstone and claystone
Turi	Eocene	3,049	3,024	282	Glauconitic siltstone and claystone
Kapuni "D" Sand	Eocene	3,331	3,306	166	Silty sandstone, quartz sand
Kapuni "E" Shale	Eocene– Paleocene	3,497	3,472	177	Siltstone and claystone
Kapuni "F" Sand	Paleocene	3,674	3,649	12	Quartz sandstone
Kapuni "F" Sand	Paleocene	3,674	3,649	260	Quartz sandstone
North Cape	Cretaceous	3,934	3,909	44	Siltstone
Basement	Mesozoic	3,978	3,953	17+	Granitoid

3.1.3. Artifacts of the 3D Data. According to previous study (PR2830), the target in the Tui-3D was between 2 and 3 seconds. In general, the quality of the data was high (Veritas DGC, 2003).

Some acquisition and processing artifacts were diagnosed throughout the 3D data. Smiles (Figure 3.2), which are processing artifacts, and a footprint (Figure 3.3), which is a seismic acquisition artifact, were identified in the Tui-3D seismic data. These artifacts did not affect the interpretation of the target horizons.

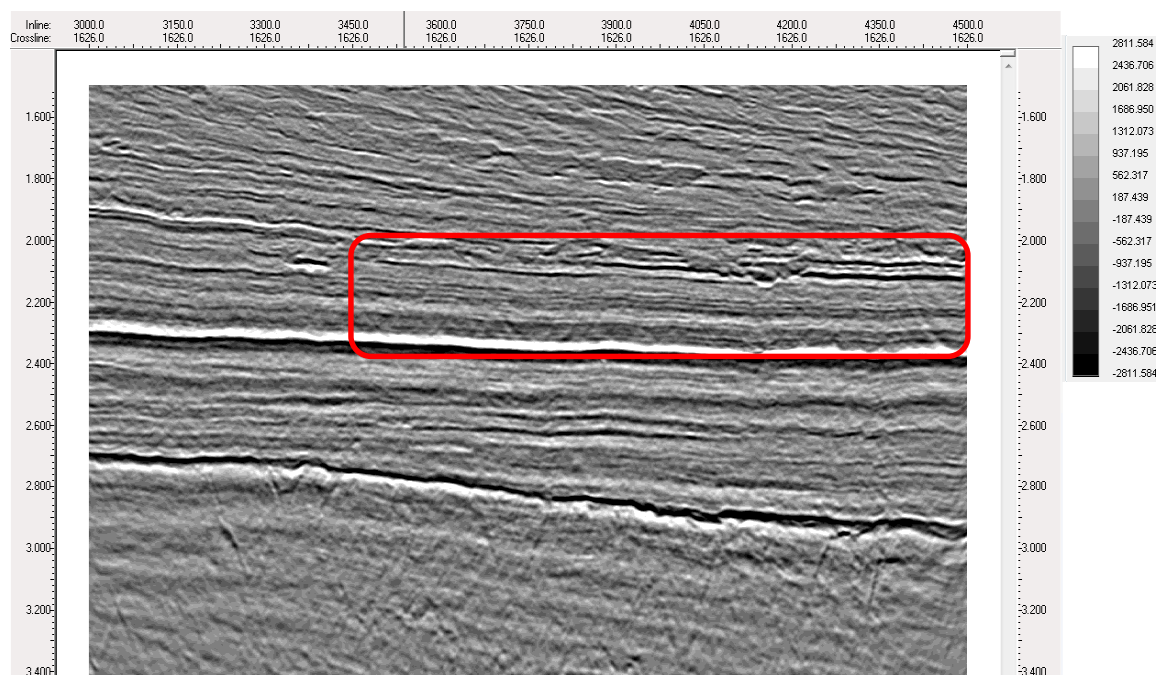


Figure 3.2. Crossline 1626 shown deep smiles indicated with red rectangular. These artifacts are generated by over migration around 2.3 s above high amplitude layer due to assigned high velocities.

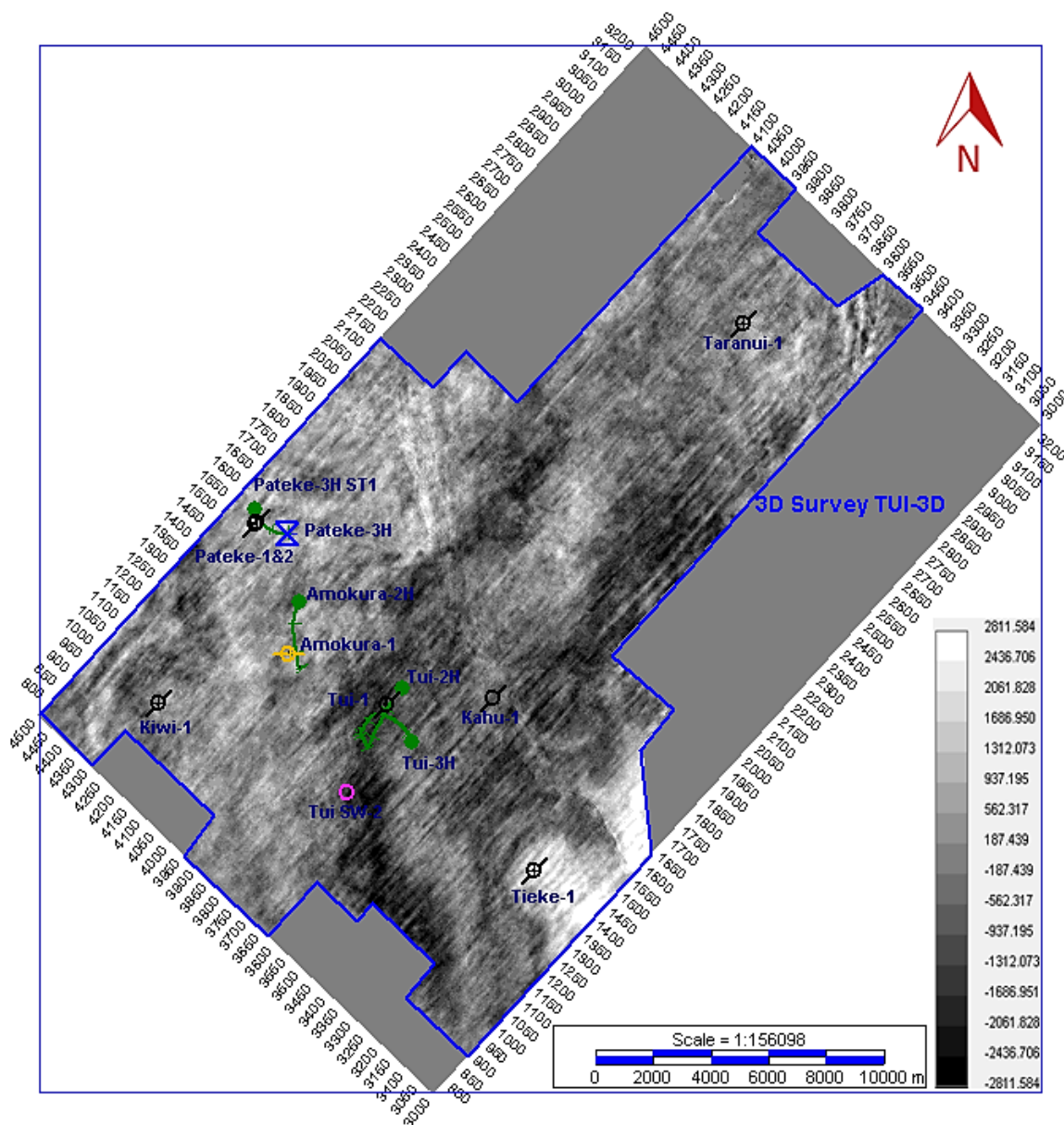


Figure 3.3. Time slice at 2.28 s shown acquisition footprint shown as amplitude stripes. They are observed in the target horizons and shallow events.

4. STRUCTURAL INTERPRETATION

The Kingdom Software 2015 was utilized for both geophysical and geological interpretations such as seismic-to-well tie, fault and horizon picking, and stratigraphic and structural interpretations. In addition, Petrel 2014 was used for attribute calculations, such as chaos, sweetness, and local flatness.

4.1. PROCEDURE

The structural and seismic stratigraphy of the Tui-3D area in the Taranaki Basin were interpreted using 3D seismic data correlating with well logs. Both Kingdom 2015 and Petrel 2014 were used to interpret faults and horizons and generate some attributes to gain knowledge of the structure and stratigraphic features of the study area. Maps, such as average and interval velocity, isopach, and time structure, were generated.

The vertical and horizontal seismic sections were carefully evaluated to understand a general view of the structural and stratigraphic features of the target horizons (Figures 4.1 and 4.2). In this research, the procedure of interpretation is as follows: 1) the 3D data was imported to the Kingdom and the Petrel software; 2) the polarity and phase of the data were determined; 3) a synthetic seismogram was generated and matched with the seismic trace; 4) minor faults were identified since no major faults were found in the study area; 5) horizon interpretation was conducted using matched synthetic seismogram for Well Tui-1; 6) time structure, average velocity, depth, interval velocity, isochron, and isopach maps were generated for structure and stratigraphic analysis; 7) time-depth conversion was performed to better understand geologic features;

8) seismic attribute volumes such as chaos, sweetness, and local flatness were constructed using Petrel 2014 and imported back to the Kingdom Suite for further analyses; and 9) well log and petrophysical analyses were performed to interpret the depositional environment of the target horizons.

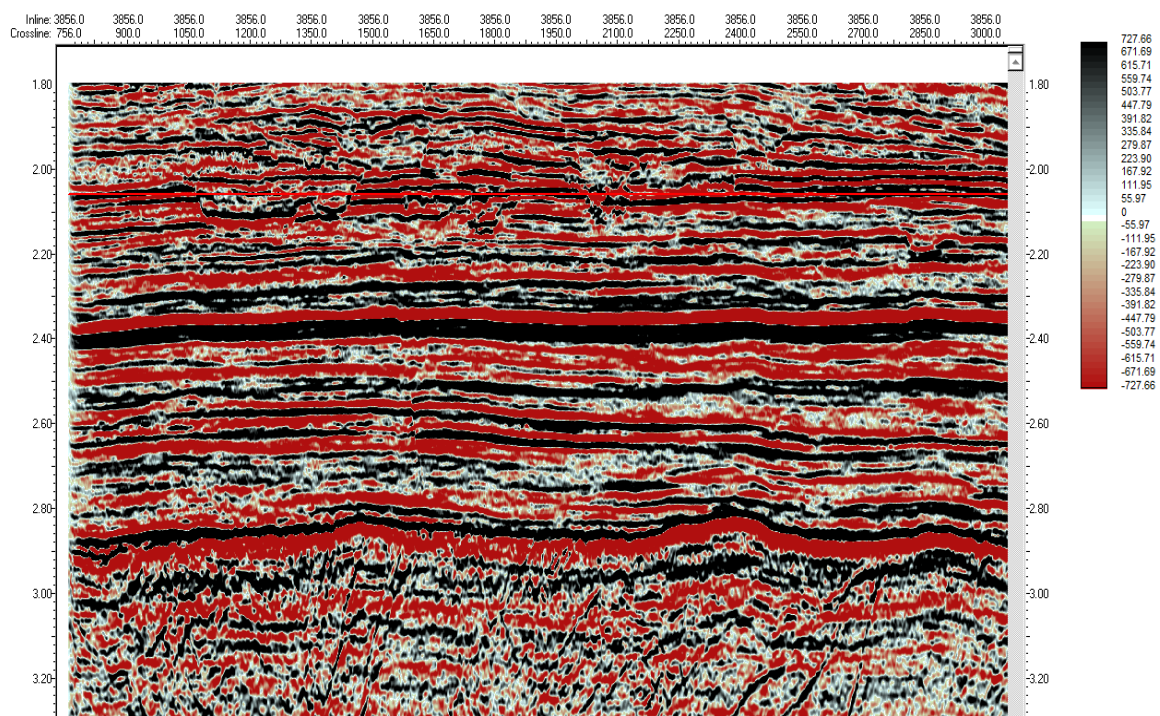


Figure 4.1. Uninterpreted Inline 3856 illustrating a general view of the seismic data. The color bar shows the amplitude values. The target horizons are between 2 to 3 seconds (28.6 km long section).

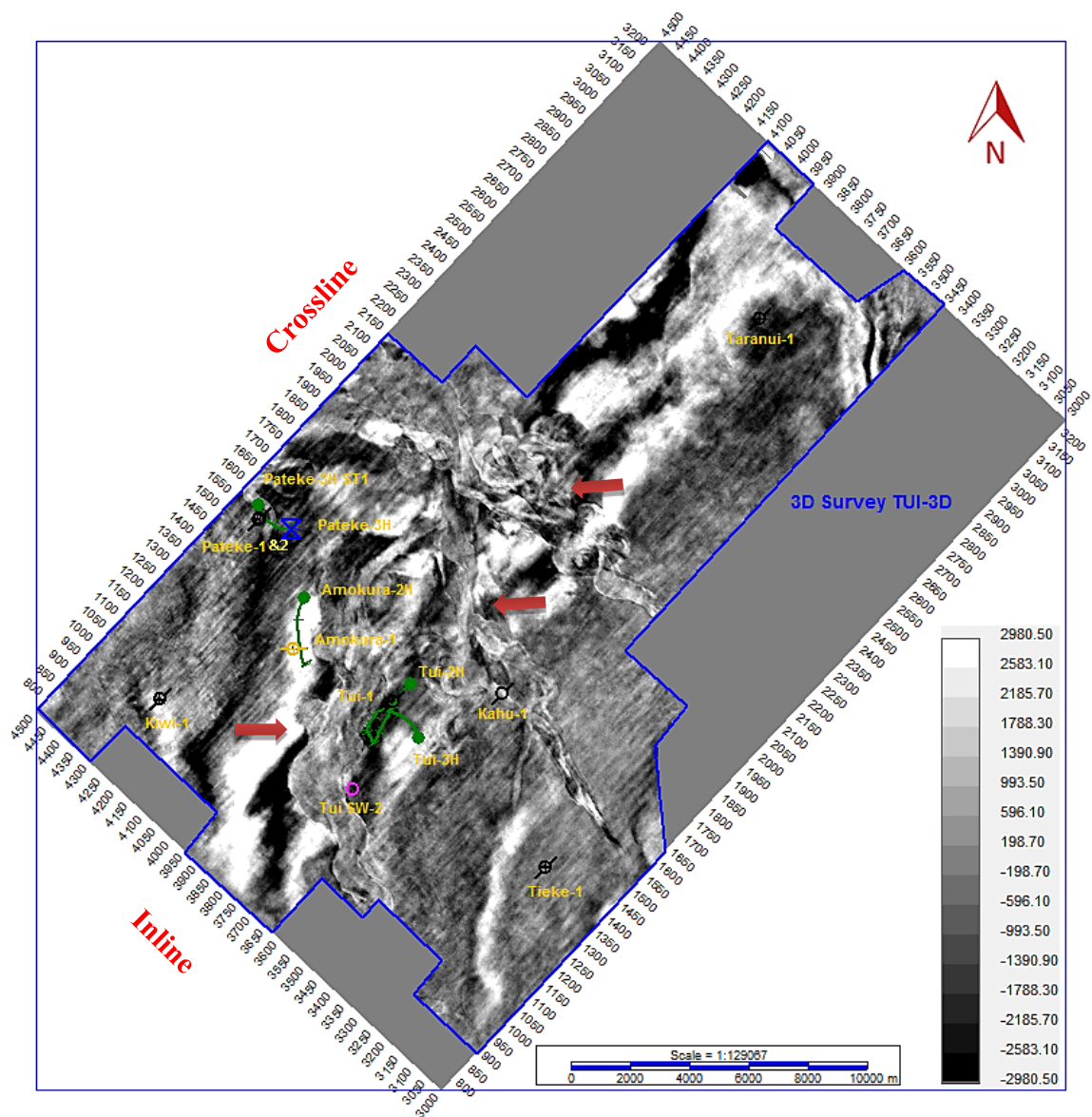


Figure 4.2. Time slice 2.06 s shown a general view of channel complexes within the Moki “A” Sandstone Formation.

4.2. SYNTHETIC GENERATION AND MATCHING

Synthetic seismogram is generated and to match the seismic trace with well logs to pick horizons correctly for target formation tops. To generate a synthetic seismogram, a Time-Depth (TD) chart, velocity and density logs, Reflection Coefficient (RC), and a wavelet are required. Density and velocity logs are crucial components to calculate Acoustic Impedance (AI), which can be calculated from sonic, density, or resistivity logs using Gardner's and Faust's correlations.

In this study, near-vertical Well Tui-1 was used for synthetic generation and matching. A TD chart was obtained from the check shot data of the well. A Gamma Ray log was used as the reference log and the DTC log was used as the Sonic log. A synthetic trace was generated by convolving the extracted wavelet and the reflection coefficient values and matching them with the real seismic trace as shown in Figure 4.3.

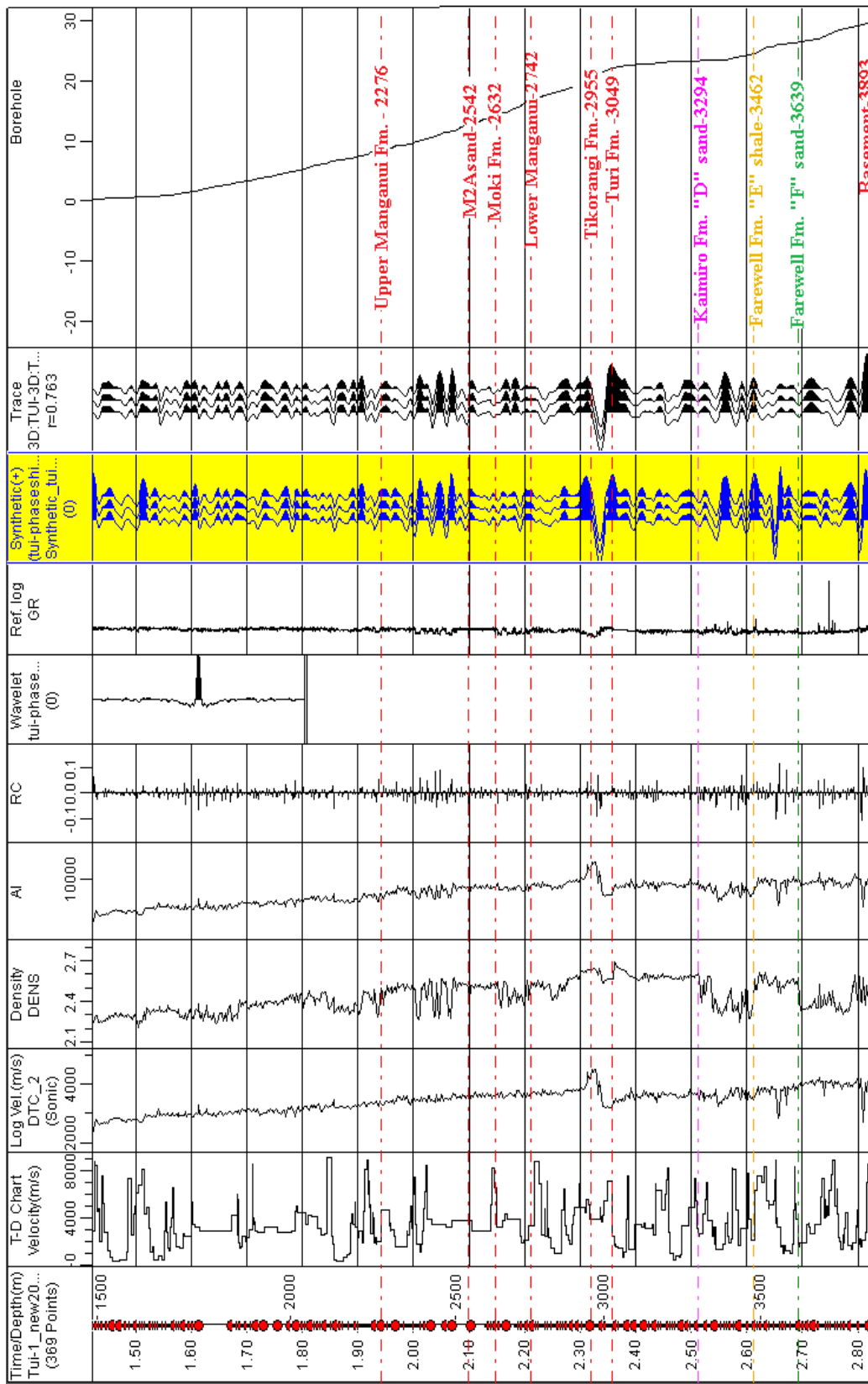


Figure 4.3. Synthetic generation and matching for Well Tui-1. The synthetic seismogram and the seismic trace match well.

4.3. FAULT INTERPRETATION

Thirty-two different minor faults were identified in the Tui-3D area. No major fault was found in the study area. Faults and fractures play a significant role in oil migration and accumulation. Therefore, if faulting continues through the Kapuni “E” Shale, oil could migrate vertically through the Kapuni “D” Sandstone (NZOP, 2004).

Faults were picked along the inline as unassigned because it helped to pick faults freely. Unassigned fault segments were then named using the base map or a 3D view. Horizons of the Farewell “E” Shale and Farewell “F” Sand with interpreted faults are shown in Figures 4.4 and 4.5, respectively. Figure 4.5 indicates that The Farewell “F” Sand onlaps to the basement near Well Tieke-1. Figure 4.6 shows faults and target horizons in a 3D view.

In the study area, interpreted thirty-two minor faults penetrated almost all the target formation layers. They are mostly observed near Wells of Taranui-1, Tieke-1, Amokura, Pateke, and Tui.

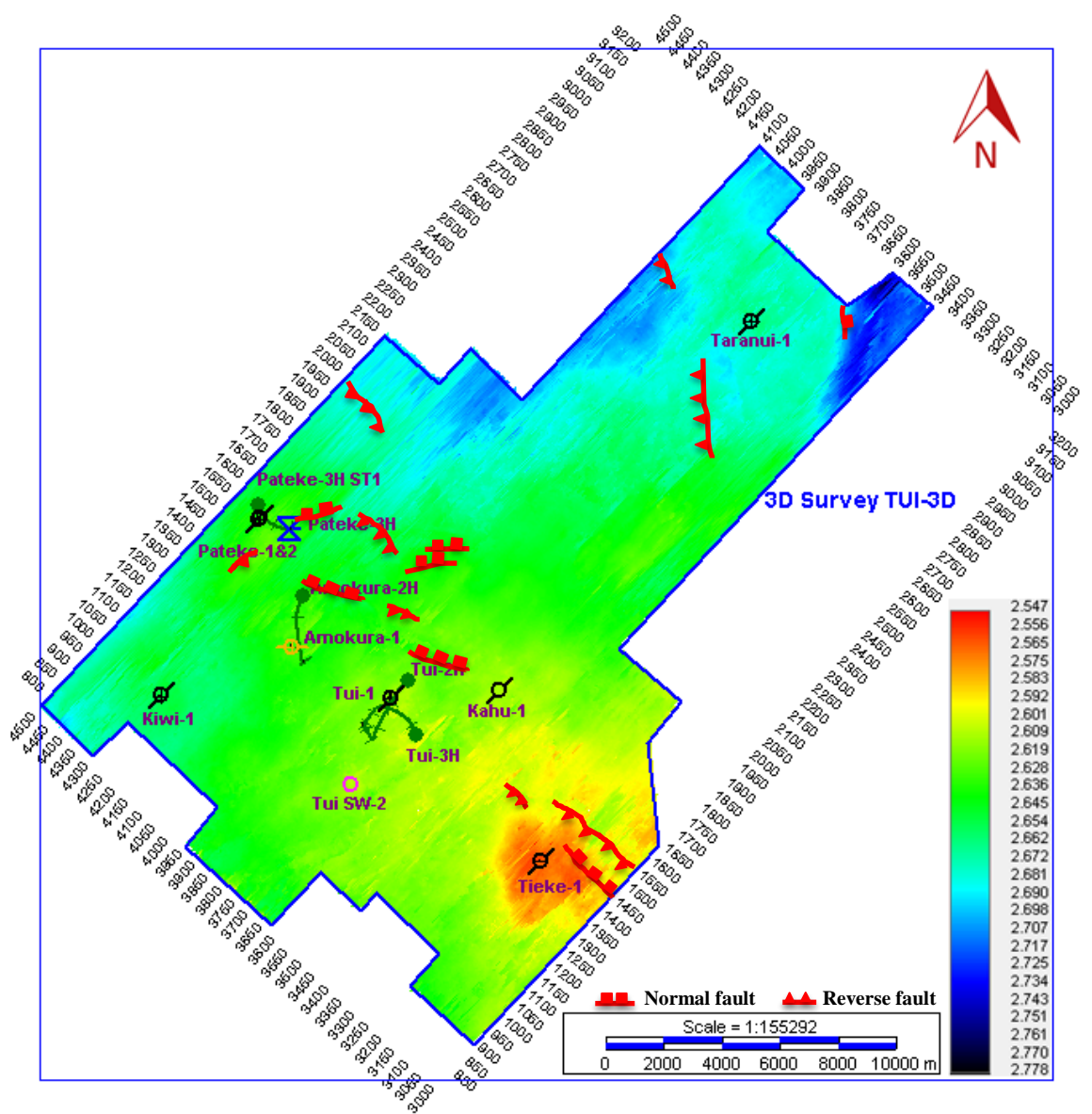


Figure 4.4. Time structure map of the Farewell “E” Shale with identified minor faults. The color bar shows the time values in seconds.

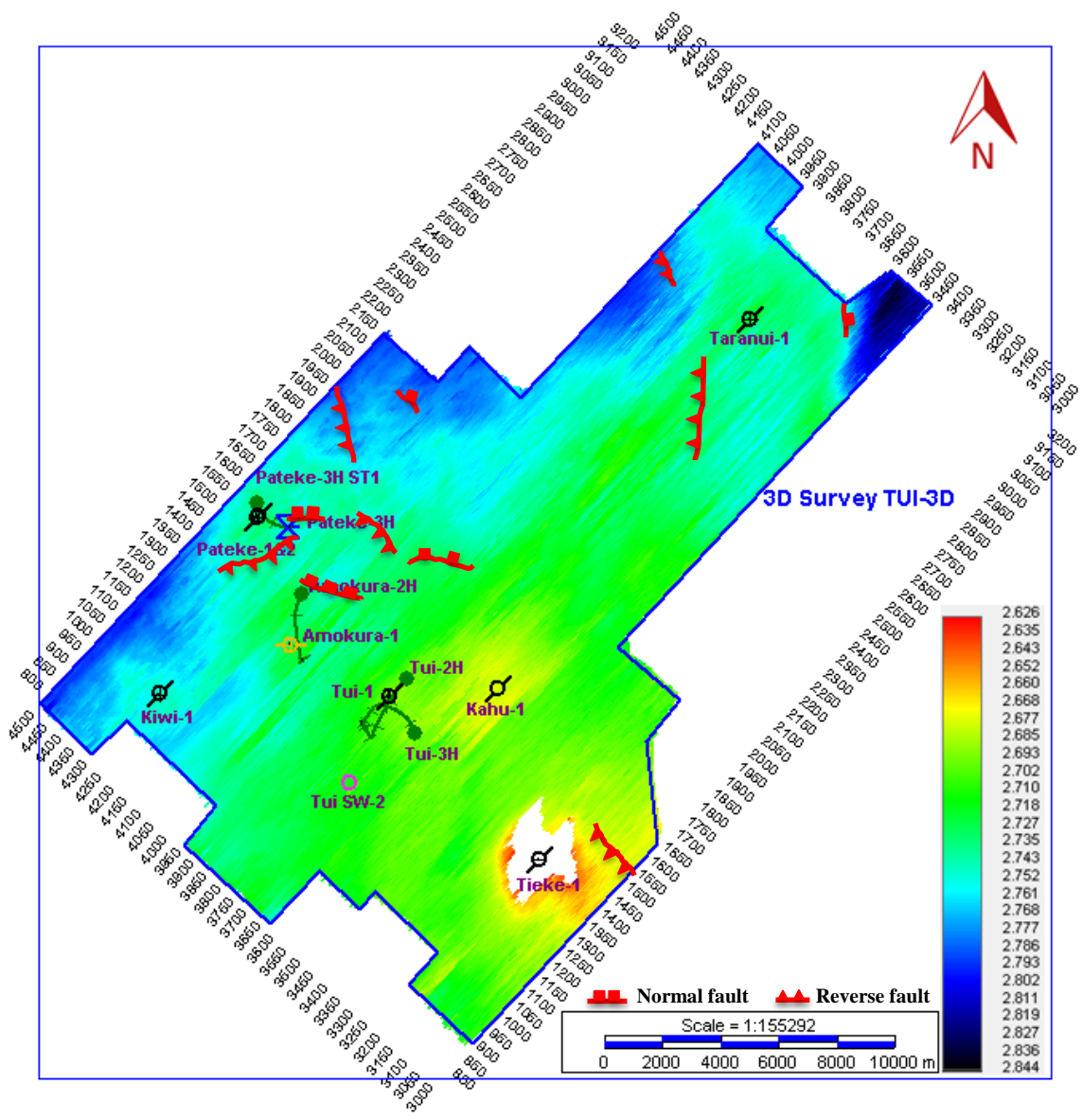


Figure 4.5. Time structure map of the Farewell “F” Sand Horizon with identified minor faults. The color bar shows the time values in seconds.

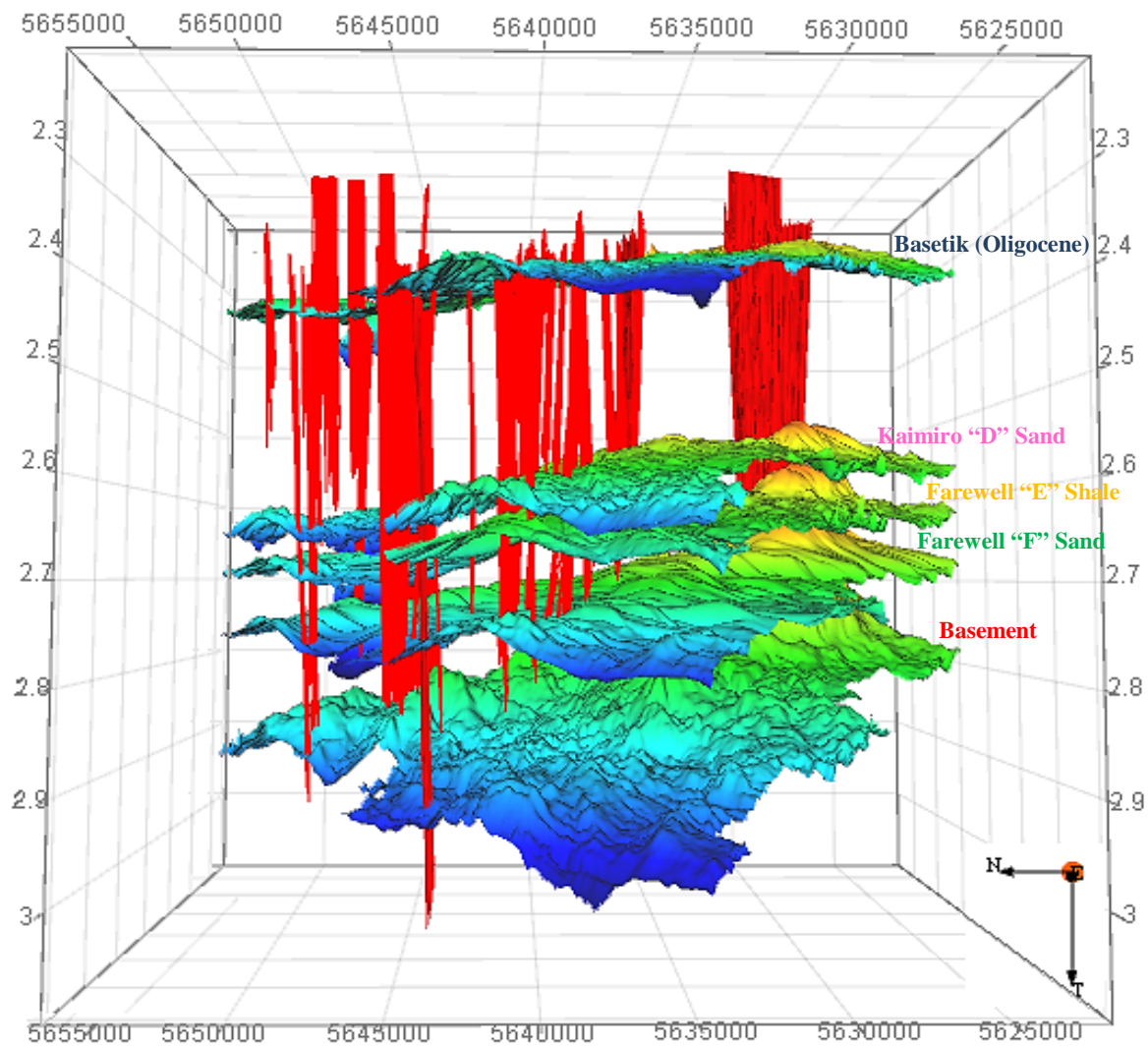


Figure 4.6. 3D cube shown thirty-two identified faults and five interpreted horizons. Red vertical surfaces illustrate minor faults. From top to bottom are horizons of Basetik (Oligocene), Kaimiro "D" Sand, Farewell "E" Shale, Farewell "F" Sand, and basement.

4.4. HORIZON INTERPRETATION

After performing the fault interpretation, seismic horizons were picked from the Tui-3D seismic data. The Autopick 2D hunt and manual methods were used for the horizon interpretation. The horizons were picked based on the knowledge of their stratigraphy and the formation tops provided by the wells within the study area. In addition, the seismic attribute of phase and amplitude similarity were taken into consideration for layer continuity for each horizon when the horizons were identified.

Five seismic horizons, which are Basetik (Oligocene) (base of the Tikorangi Formation), Kaimiro “D” Sand, Farewell “E” Shale, Farewell “F” Sand, and basement, were picked. The conditions of the picked horizons are listed in Table 4.1. Figures 4.7 and 4.8 illustrate five picked horizons with the matched synthetic seismogram. Basetik (Oligocene) constantly showed a very high amplitude over the study area at the base of the Tikorangi Formation with Oligocene age (unconformity). Kaimiro “D” Sand (Kapuni “D” Sandstone) is a potential reservoir in the field. Farewell “E” Shale (Kapuni “E” Shale) is the proven seal rock, and Farewell “F” Sand (Kapuni “F” Sandstone) is the proven carrier and reservoir rock in the research area. While picking Farewell “F” Sand horizon, the Farewell “E” Shale was used as a guide. The North Cape onlaps to the basement. As a result, this horizon was not observed in the entire area. The basement and North Cape are the base of the Farewell “F” Sand, and this base has a very high amplitude throughout the study field.

Table 4.1. Interpreted seismic horizons.

Horizon Name	Color	Relative Acoustic Impedance	Picked Seismic Reflector
Sea Floor	Brown	High	Peak
Basetik (Oligocene)	Dark Blue	Low	Trough
Kaimiro "D" Sand	Pink	Low	Trough
Farewell "E" Shale	Yellow	High	Peak
Farewell "F" Sand	Green	Low	Trough
North Cape	Black	Low	Trough
Basement	Red	High	Peak

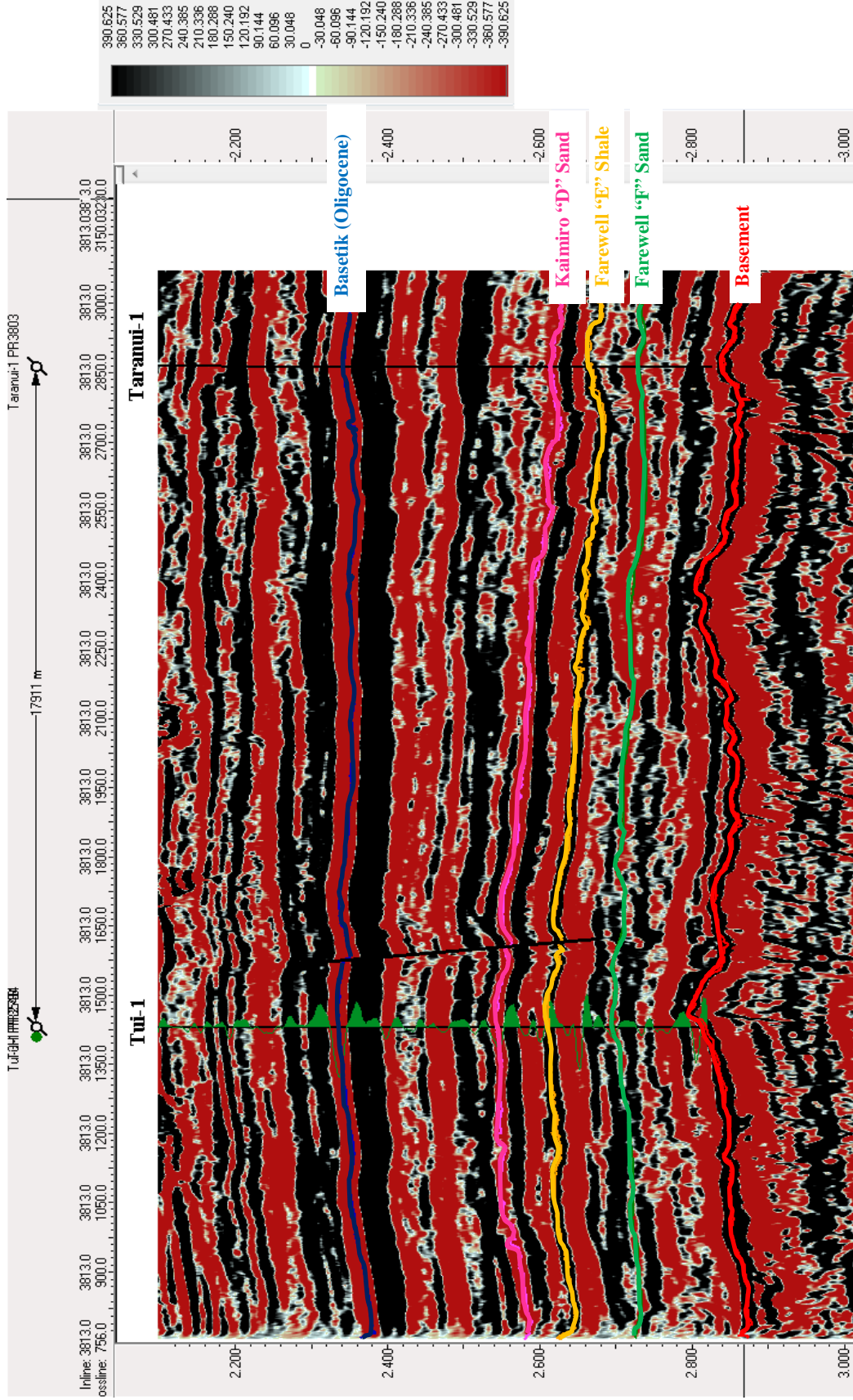


Figure 4.7. Vertical seismic section of Inline 3813. The synthetic seismogram was matched with the seismic traces to identify each horizon for target formation tops. The black line shows an interpreted fault near Well Tui-1 (28.3 km long section).

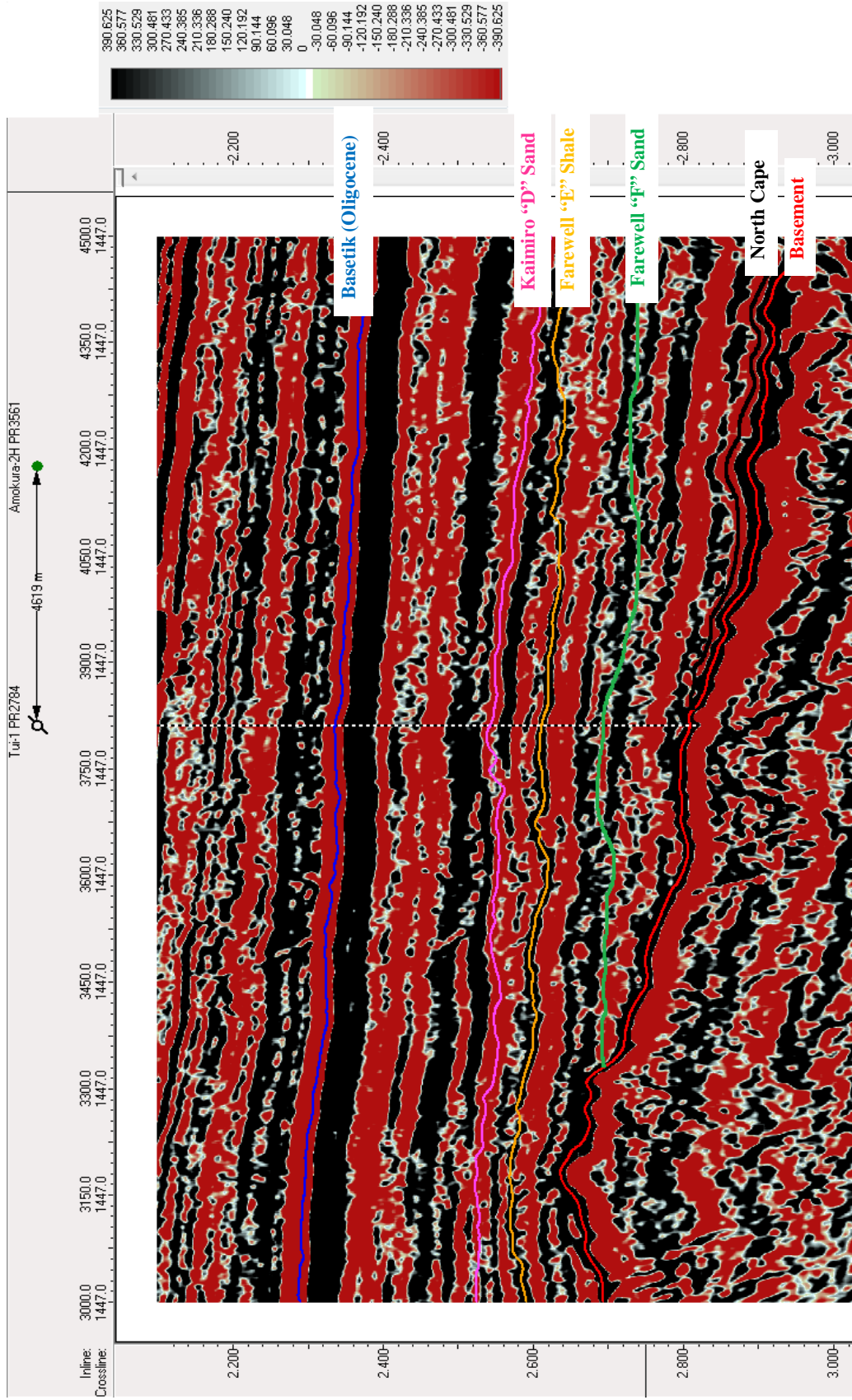


Figure 4.8. Vertical seismic section of Crossline 1447. The North Cape and Farewell "F" Sand onlap to the basement (18.75 km long section).

4.5. STRUCTURAL MAPPING

After the horizons were picked, time structure, average velocity, interval velocity, isopach, and depth maps were generated to conduct the structural interpretation.

4.5.1. Time Structural Map. When the horizons were picked, the time of each horizon was recorded to acquire time structure maps using the Gradient Projection algorithm, which calculates X and Y derivatives at the location of each data point. An interpolated value at a grid node was projected by an inverse distance to a power weighting (IHS, 2014).

The time structure maps for the Basetik (Oligocene), Kaimiro “D” Sand, Farewell “E” Shale, Farewell “F” Sand, and basement horizons are displayed in Figures 4.9, 4.10, 4.11, 4.12, and 4.13, respectively.

In the study area, the structure maps help to understand the dipping of the target horizons in seconds and to reveal many anticlines shown with arrows and a syncline. Generally, anticlines were observed near Wells Tieke-1 and Pateke and the dipping of the target horizons is toward the north to northwest. The results are as follows: 1) the structure map for the Basetik (Oligocene) shows a dipping toward the northwest (Figure 4.9). Low relief anticlines were observed near Wells Tieke-1, Taranui-1, and Pateke. A syncline was observed at the east side near Well Taranui-1, 2) the structure map for the Kaimiro “D” Sand shows a dipping toward the northwest (Figure 4.10). A low relief-broad anticline was observed around Well Tui-1 and other anticlines were observed near Wells Tieke-1 and Pateke, 3) the structure map for the Farewell “E” Shale shows a dipping toward the north (Figure 4.11). Anticlines are observable near Wells Kiwi-1, Tieke-1, Tui SW-2, Pateke, Tui, Amokura, and Taranui-1, 4) the structure map for the

Farewell “F” Sand shows a dipping toward the north and northwest (Figure 4.12). A prospect area, which is located at southwest near Well Taranui-1, was suggested to be drilled for future investigation. The Farewell “F” Sand onlaps to the basement near Well Tieke-1, 5) the structure map for the basement shows a dipping toward the northwest (Figure 4.13). Anticlines are observable near Wells Pateke, Tieke-1, and Taranui-1.

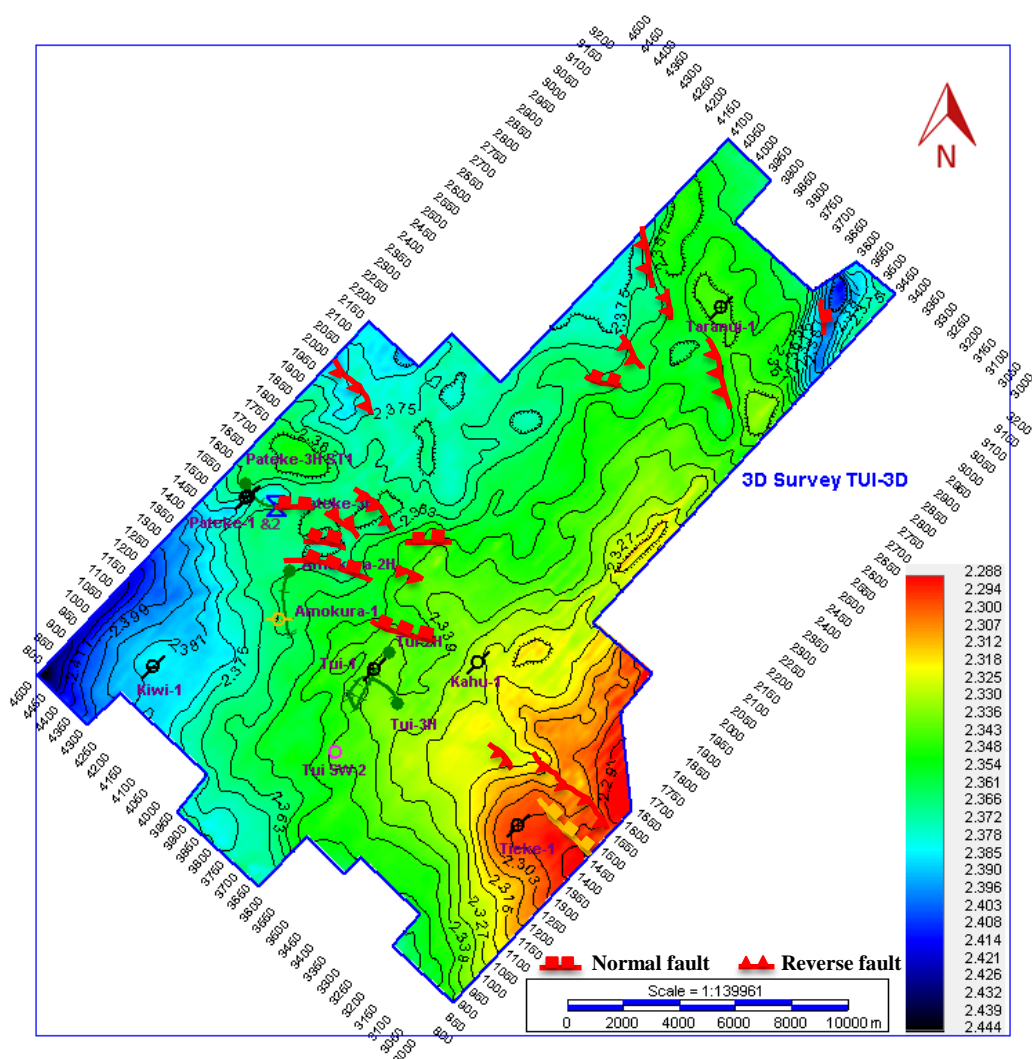


Figure 4.9. Time structure map of the Basetik (Oligocene) Horizon. The structure map displays a dipping toward the northwest. Low relief anticlines were observed near Wells Tieke-1, Taranui-1, and Pateke. A syncline was observed at the east side near Well Taranui-1. The color bar shows the time values in seconds.

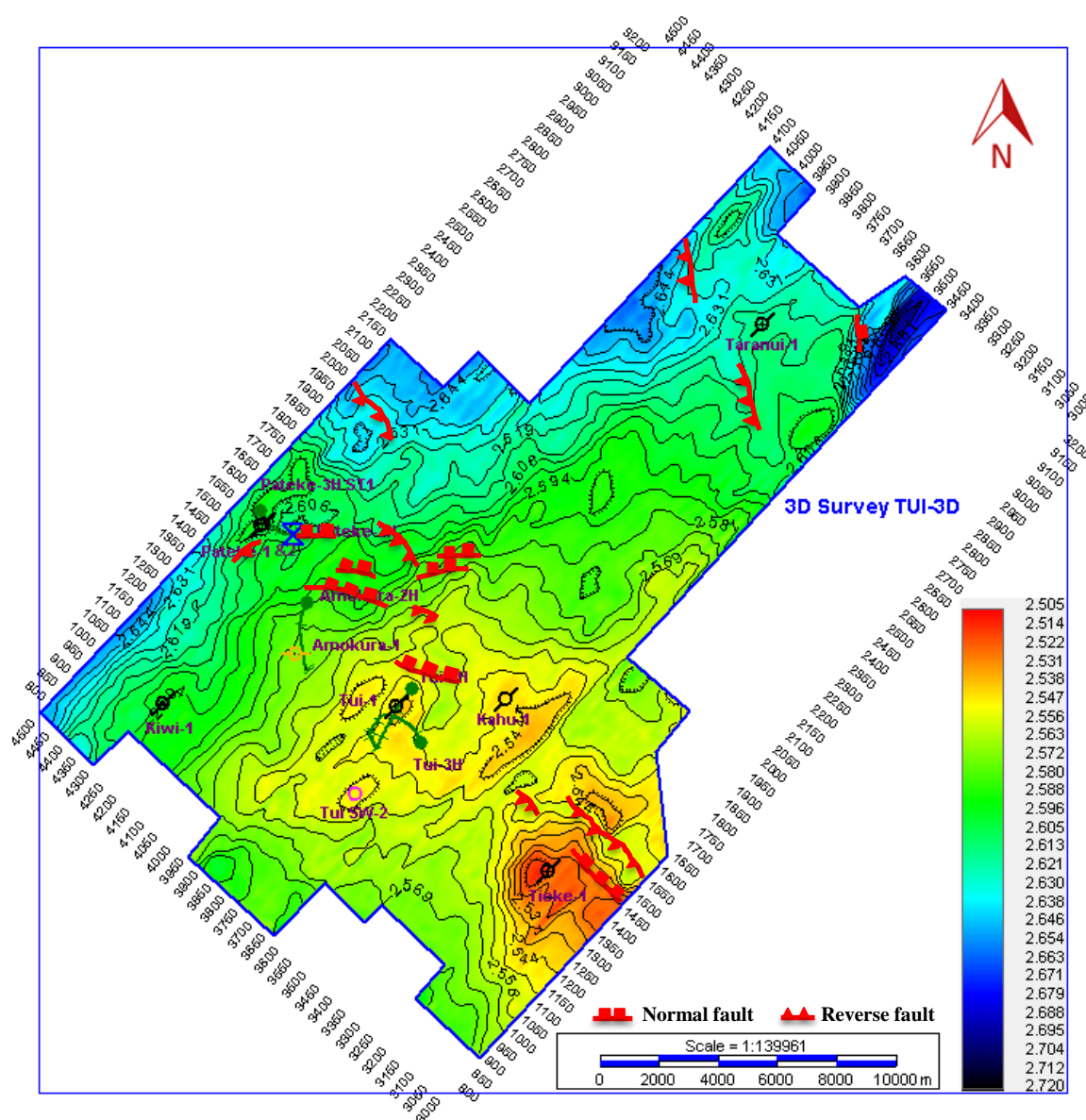


Figure 4.10. Time structure map of the Kaimiro “D” Sand Horizon. The structure map displays a dipping toward the northwest. A low relief- broad anticline was observed around Well Tui-1 and other anticlines were observed near Wells Tieke-1 and Pateke. A syncline was observed at the east side near Well Taranui-1. The color bar shows the time values in seconds.

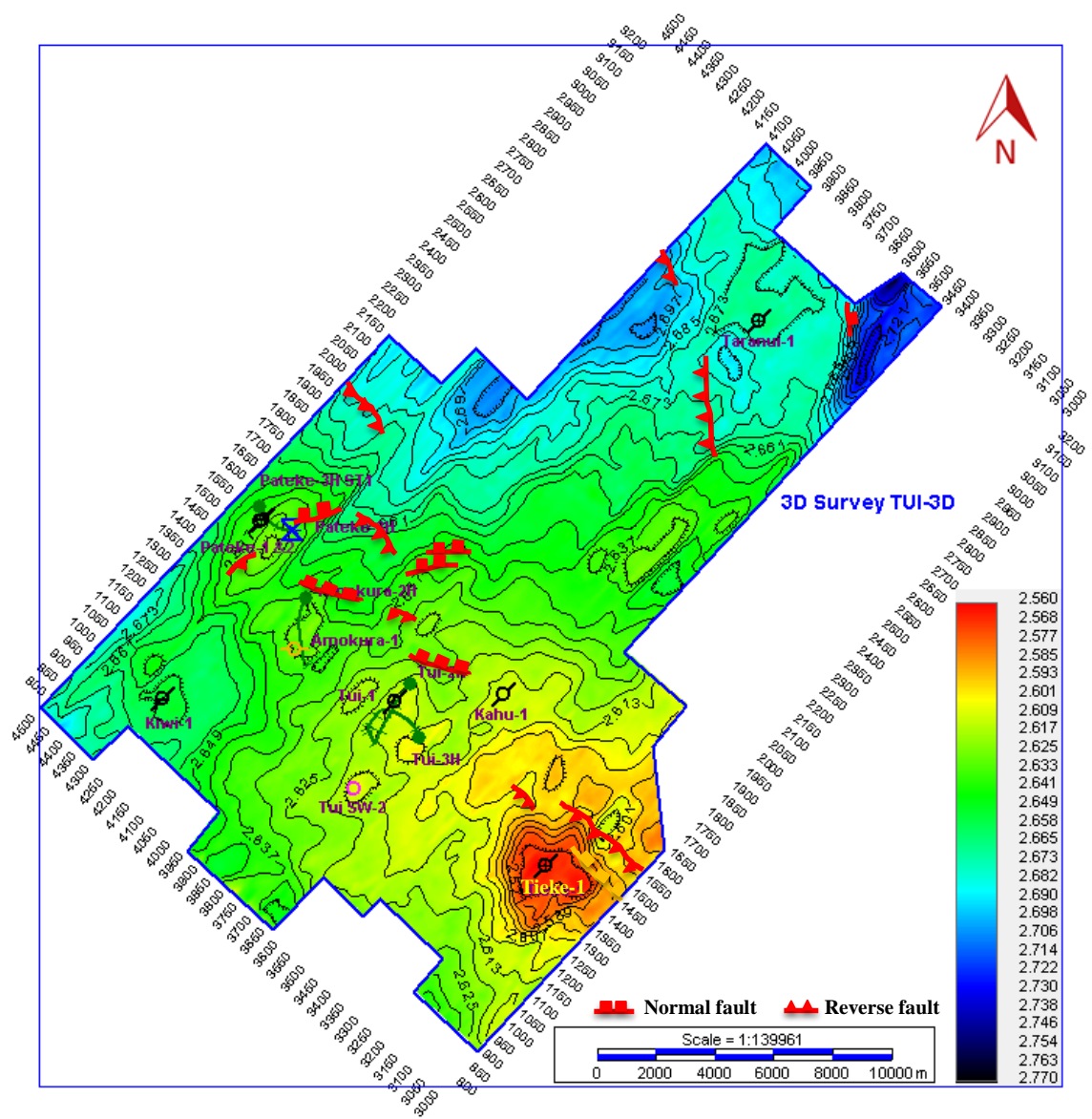


Figure 4.11. Time structure map of the Farewell “E” Shale Horizon. The structure map displays a dipping toward the north. An anticline shown in red was observed around Well Tieke-1, which is located south of the area. Other anticlines are observable near Wells Kiwi-1, Tui SW-2, Pateke, Tui, Amokura, and Taranui-1. The color bar shows the time values in seconds.

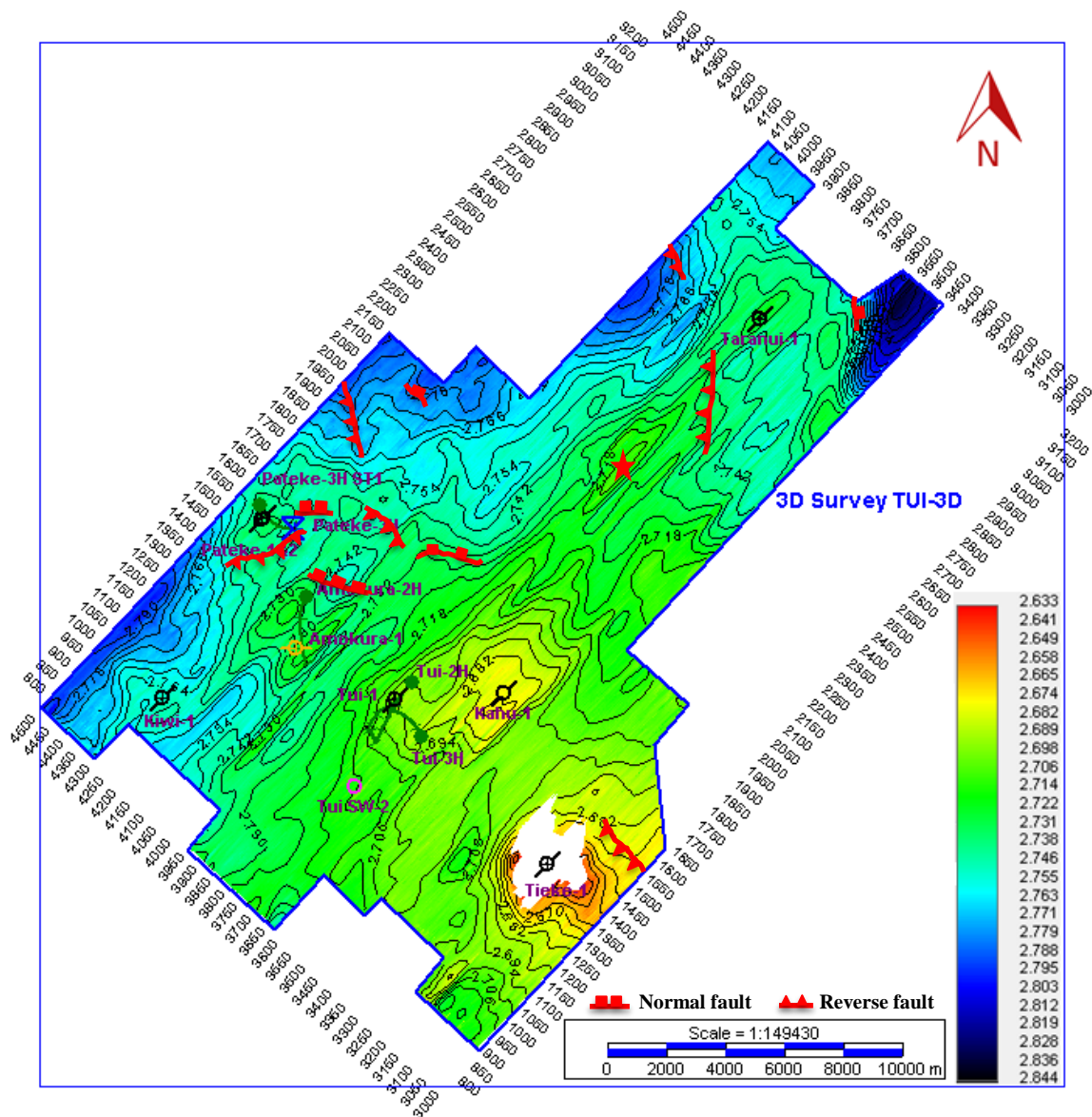


Figure 4.12. Time structure map of the Farewell “F” Sand Horizon. The structure map displays a dipping toward the north and northwest. An anticline from the basement shown in white was observed around Well Tiede-1, which is located south of the area. The Farewell “F” Sand Horizon onlaps to the basement near Well Tiede-1. An anticline shown with a star, is the prospect to be drilled for further investigation. The color bar shows the time values in seconds.

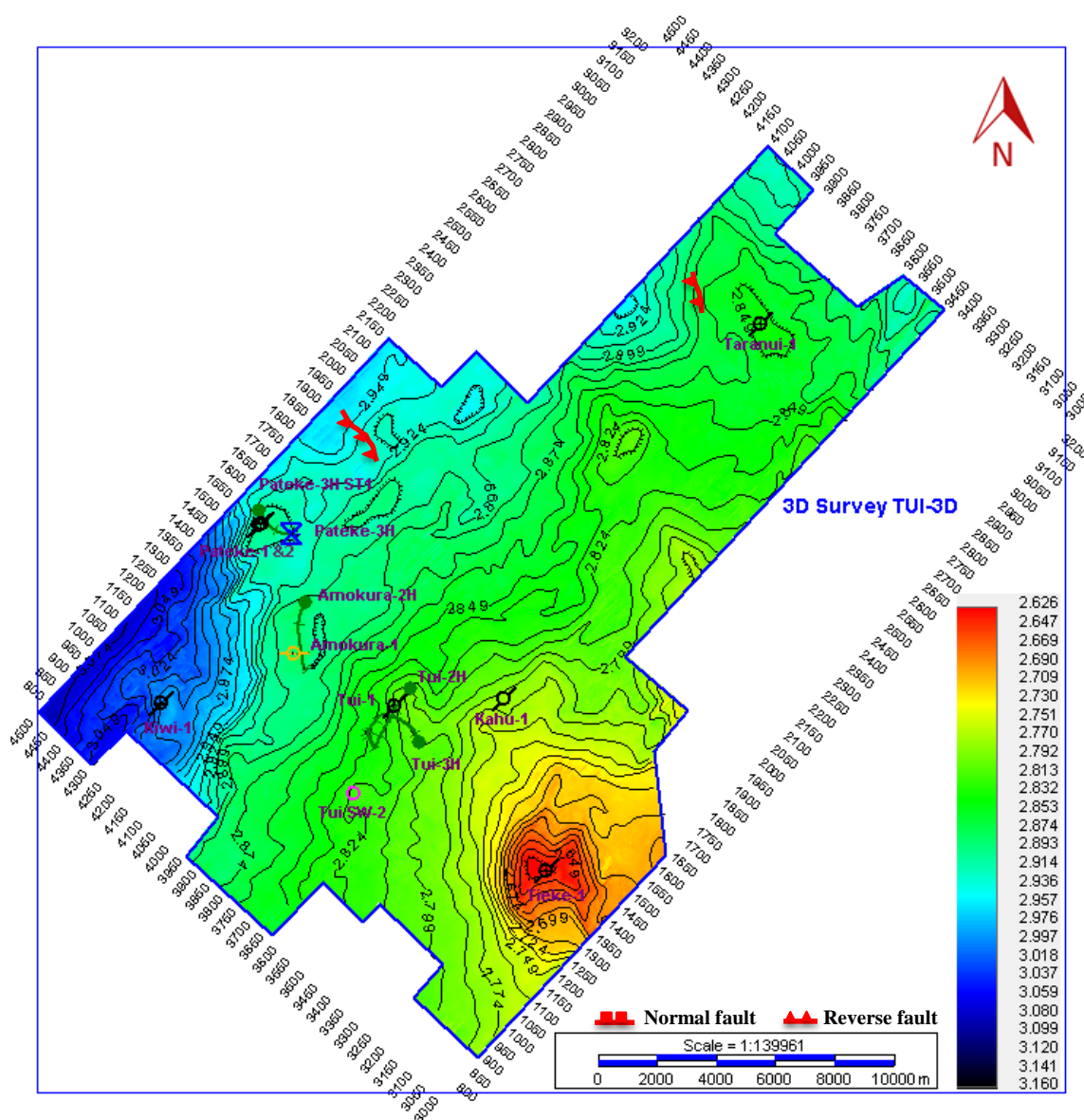


Figure 4.13. Time structure map of the basement Horizon. The structure map displays a dipping toward the northwest. An anticline shown in red was observed around Well Tieke-1, which is located south of the area. Other anticlines are observed near Wells Pateke and Taranui-1. The color bar shows the time values in seconds.

4.5.2. Depth Map by Average Velocity. A depth structure map shows the geometry of each horizon and is very important to see horizons in values of depth instead of time. In order to generate depth structure maps, average velocity information is needed

for each horizon. To calculate average velocity, the following equation was used (IHS, 2014):

$$\text{Average velocity} = (2 * Df) / (T), \quad (1)$$

where Df is the depth value from the formation top, and T is the two-way travel time coming from the time surface (Figure 4.14). This equation was used for all the chosen wells and acquired velocity points. The average velocity maps were generated, using those velocity points and the inverse distance to a power gridding algorithm (IHS, 2014).

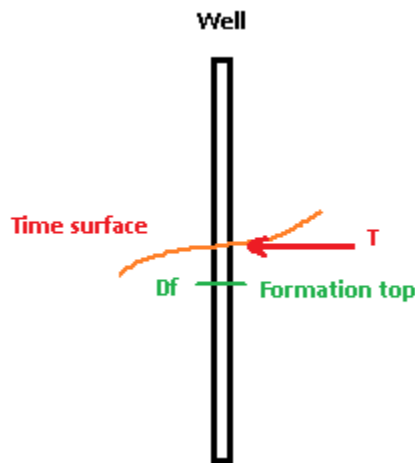


Figure 4.14. Illustration of average velocity generation. The correlation between formation top and time surface is shown.

The average velocity maps for the Basetik (Oligocene), Kaimiro “D” Sand, Farewell “E” Shale, Farewell “F” Sand, and basement are displayed in Figures 4.15, 4.16, 4.17, 4.18, and 4.19, respectively.

Average velocity maps indicate that the velocity decreases toward the northwest for the target horizons except the basement, which has the velocity decreasing toward the northeast. The lowest value of the average velocity for the target horizons is around Well Pateke-1 except the basement, which has the lowest velocity around Well Kahu-1. Velocities of the Basetik (Oligocene) Horizon vary between 2478 m/s and 2587 m/s (Figure 4.15). Velocities vary between 2590 m/s and 2662 m/s for the Kaimiro “D” Sand Horizon (potential reservoir) (Figure 4.16). For the Farewell “E” Shale Horizon (cap rock), velocities vary between 2605 m/s and 2671 m/s (Figure 4.17). Velocities of the Farewell “F” Sand Horizon (reservoir) vary between 2671 m/s and 2736 m/s (Figure 4.18). Velocities of the basement Horizon vary between 2730 m/s and 2791 m/s (Figure 4.19).

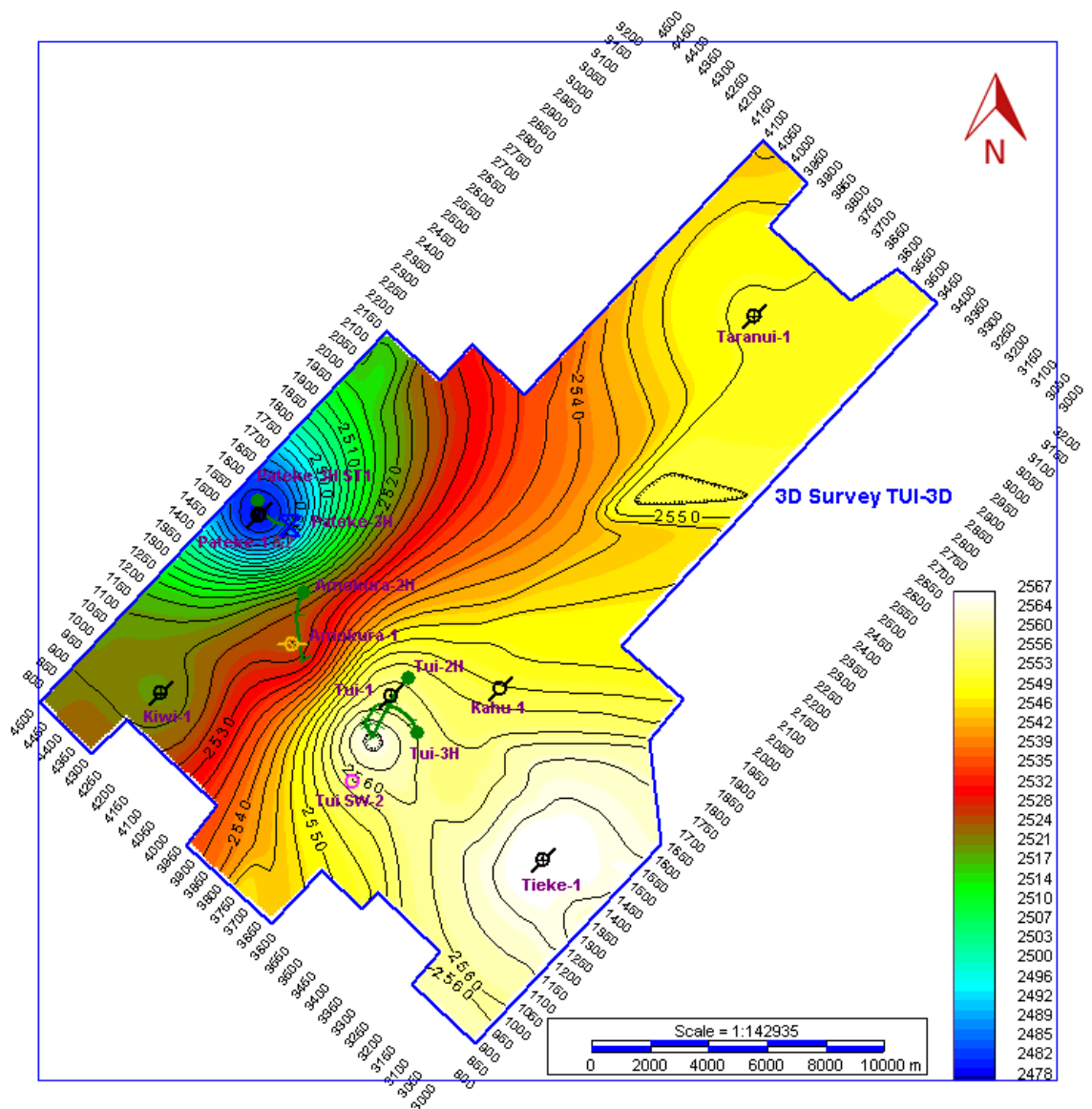


Figure 4.15. Average velocity map of the Basetik (Oligocene) Horizon. Velocities range from 2478 m/s to 2587 m/s. The lowest velocity is around Well Pateke-1, and the highest velocity is around Well Tieke-1. The average velocity decreases toward the northwest.

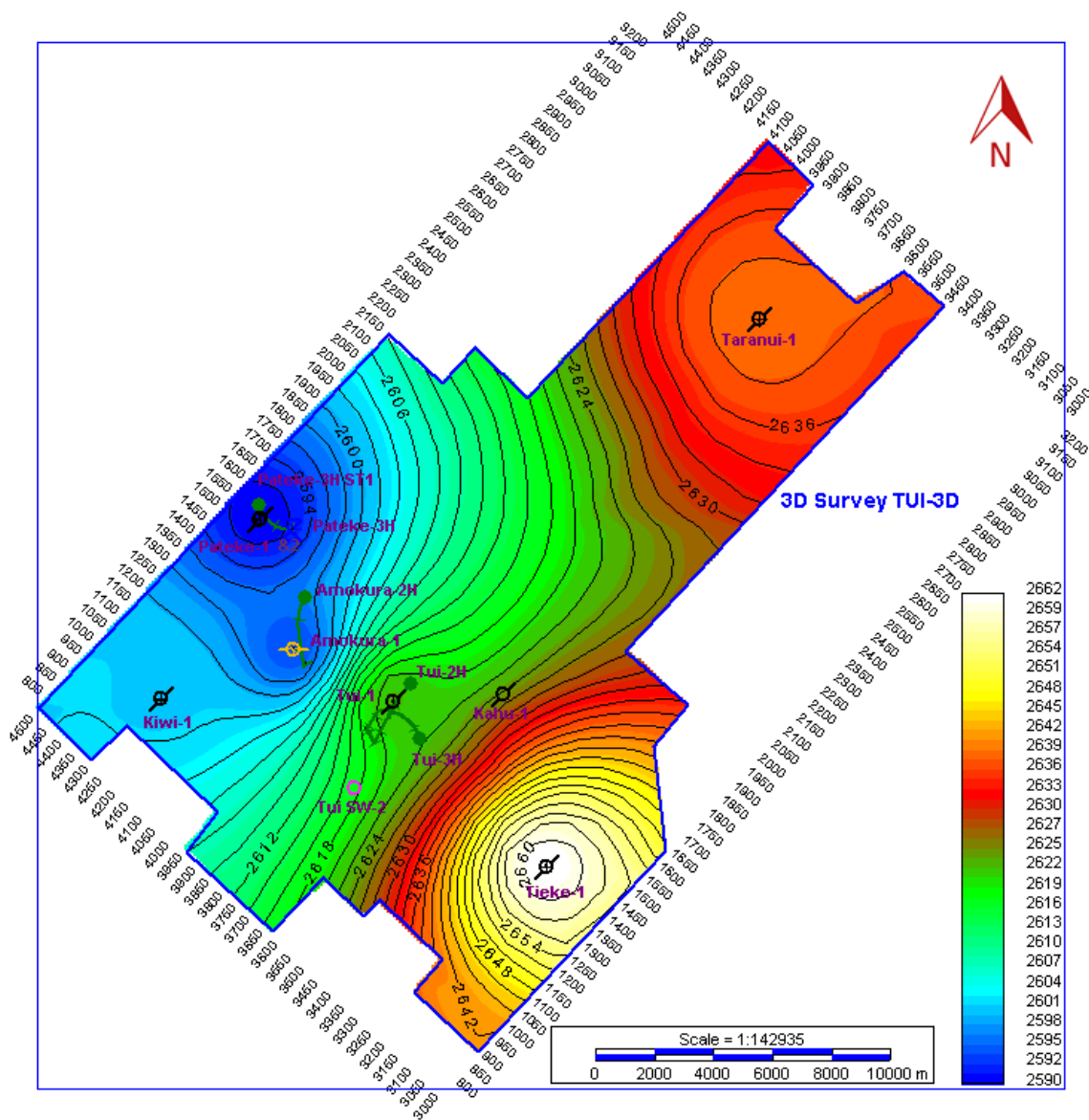


Figure 4.16. Average velocity map of the Kaimiro “D” Sand Horizon. Velocities range from 2590 m/s to 2662 m/s. The lowest velocity is around Well Pateke-1, and the highest velocity is around Well Tieke-1. The average velocity decreases toward the northwest.

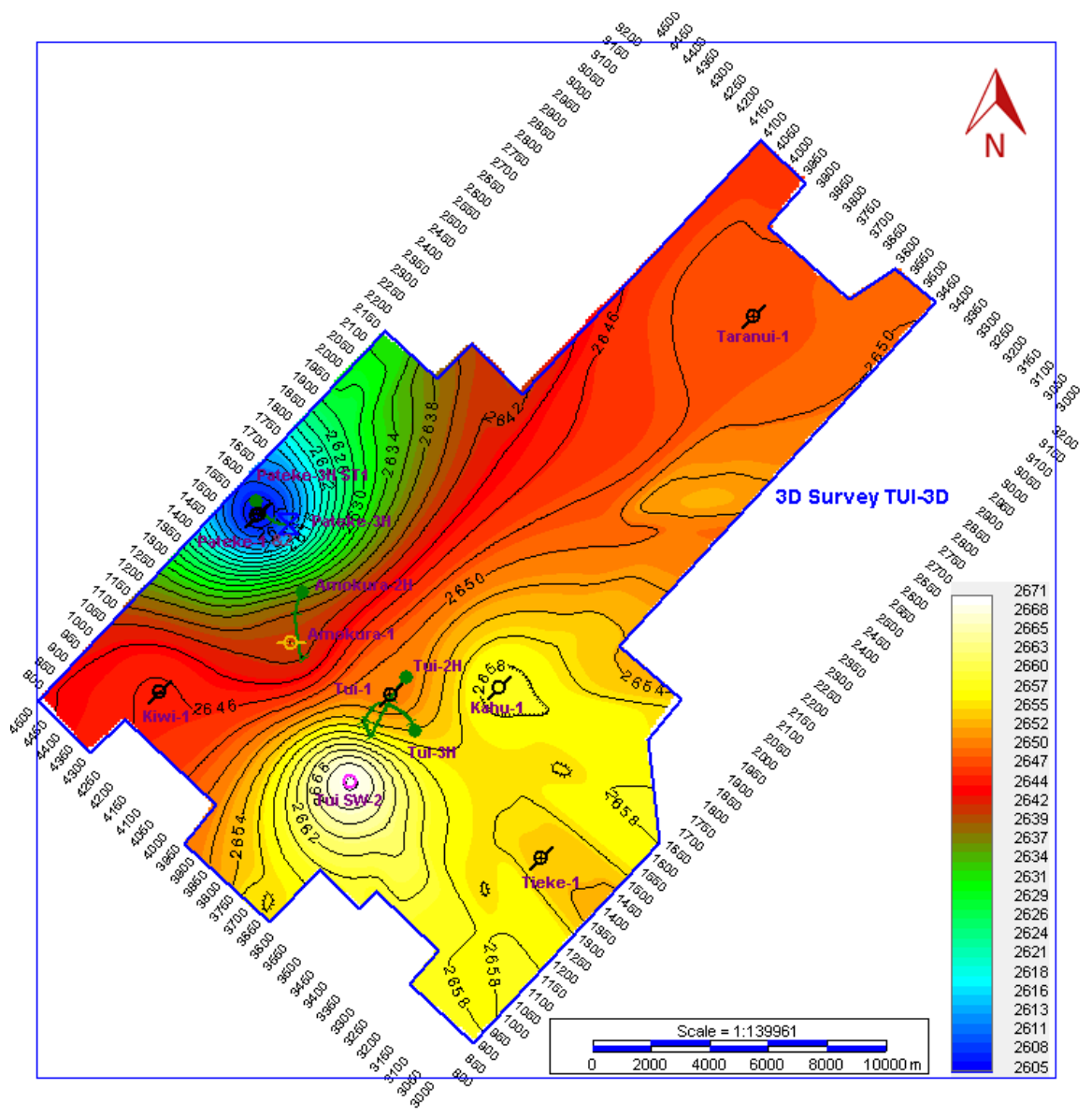


Figure 4.17. Average velocity map of the Farewell “E” Shale Horizon. Velocities range from 2605 m/s to 2671 m/s. The lowest velocity is around Well Pateke-1, and the highest velocity is around Well Tui SW-2. The average velocity decreases toward the northwest.

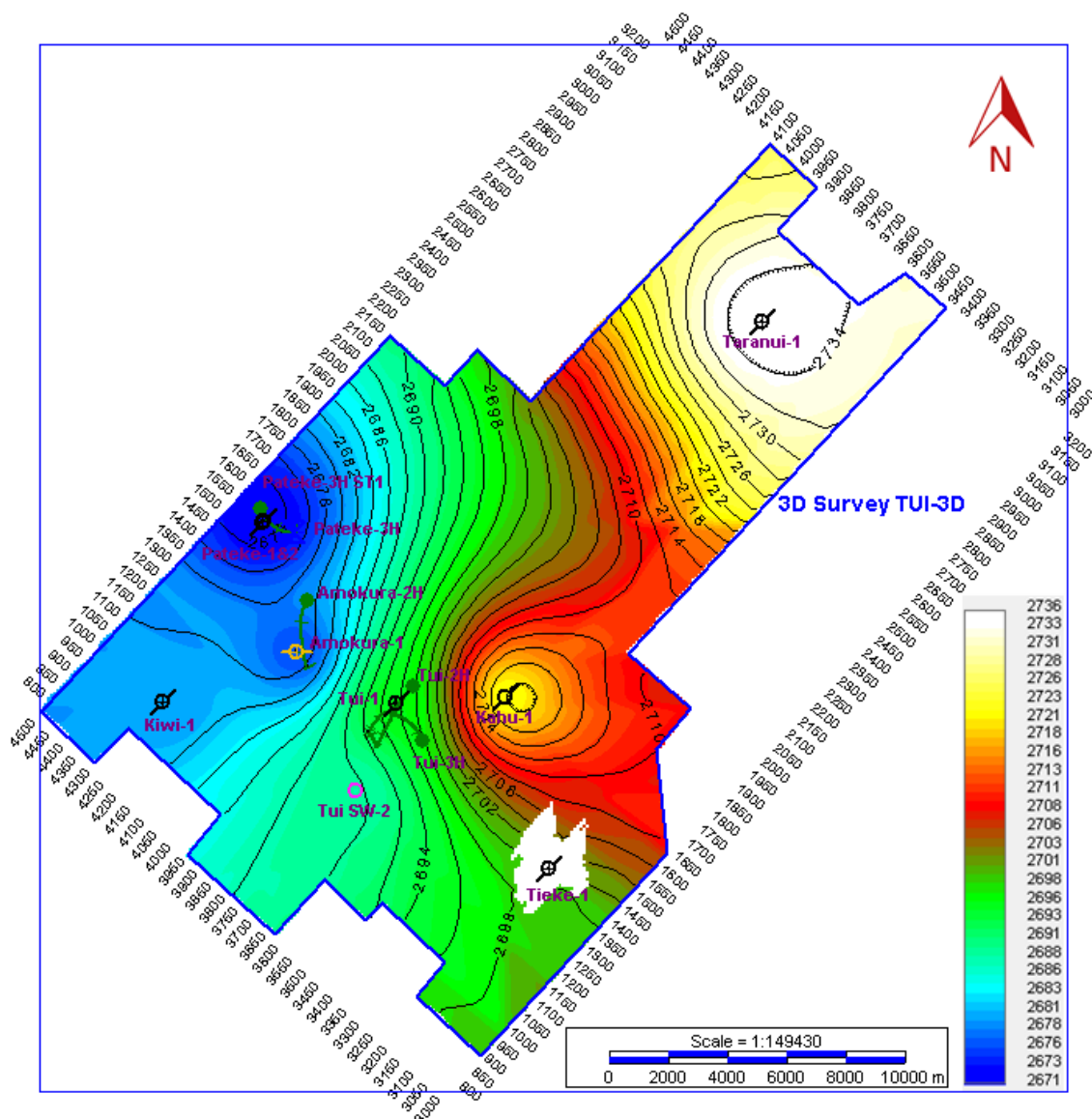


Figure 4.18. Average velocity map of the Farewell “F” Sand Horizon. Velocities range from 2671 m/s to 2736 m/s. The lowest velocity is around Well Pateke-1, and the highest velocity is around Well Taranui-1. The Farewell “F” Sand onlaps to the basement shown in white at the Tieke-1 well. The average velocity decreases toward the northwest.

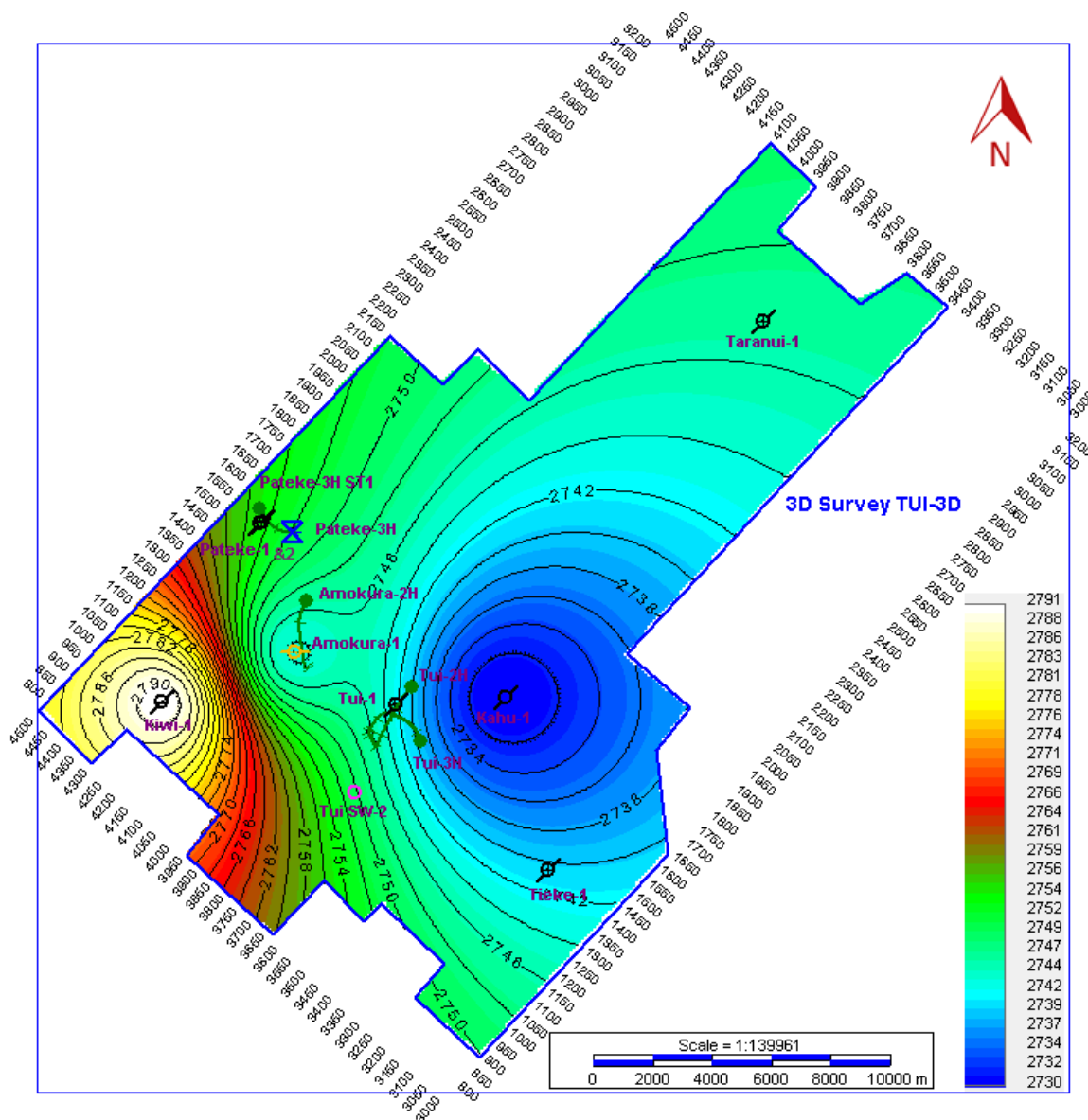


Figure 4.19. Average velocity map of the basement Horizon. Velocities range from 2730 m/s to 2791 m/s. The lowest velocity is around Well Kahu-1, and the highest velocity is around Well Kiwi-1. The average velocity decreases toward the northeast.

After the average velocity maps were constructed, the depth maps were generated by multiplying the average velocity values by the time surface values (IHS, 2014). The depth structure maps are displayed for the Basetik (Oligocene), Kaimiro “D” Sand, Farewell “E” Shale, Farewell “F” Sand, and basement horizons in Figures 4.20, 4.21,

4.22, 4.23, and 4.24, respectively. The 3D view of the depth maps for the Kaimiro “D” Sand, Farewell “E” Shale, Farewell “F” Sand, and basement are shown in Figure 4.25.

In the study area, the depth maps help to visualize the dipping of the target horizons in meters and to reveal many anticlines shown with arrows and a syncline. The results are as follows: 1) the depth map for the Basetik (Oligocene) Horizon represents Oligocene unconformity (Figure 4.20). Anticlines are observable near Wells Kiwi-1, Taranui-1, and Pateke and a synclinal is observable east of Well Taranui-1, 2) the depth map for the Kaimiro “D” Sand Horizon indicates a dipping toward the northeast (Figure 4.21). A low relief- broad anticline was observed around Well Tui-1, and other anticlines were observable around Wells Tieke-1 and Pateke, 3) the depth map for the Farewell “E” Shale Horizon indicates a dipping toward the north (Figure 4.22). Anticlines were observable around Wells Tieke-1, Taranui-1, Pateke, and Tui-1, 4) the depth map for the Farewell “F” Sand Horizon indicates a dipping toward the north (Figure 4.23). The map reveals that Wells Tui-1, Amokura-1 and Pateke-1&2 have a low relief anticline, structural traps, for oil accumulation. An anticline from the basement shown in white was observable around Well Tieke-1, 5) the depth map for the basement Horizon indicates a dipping toward the northwest (Figure 4.24). An anticline was observable near Well Tieke-1, 6) a 3D view of the target horizons indicate a dipping generally toward the north (Figure 4.25). An anticline was observed at the south of the study area.

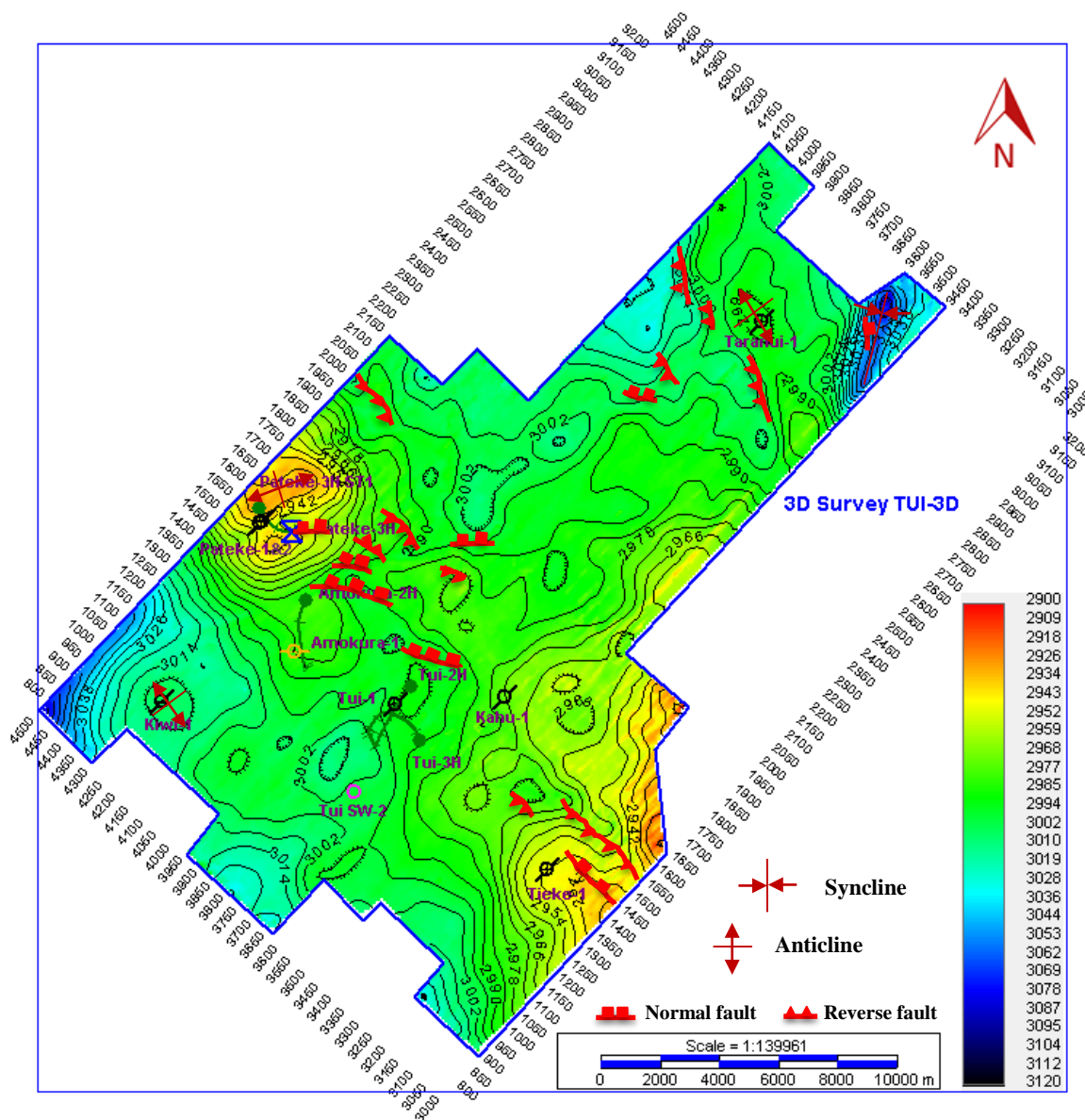


Figure 4.20. Depth map of the Basetik (Oligocene) Horizon. The depth map represents Oligocene unconformity of roughly 10 million years between 2,980 and 2,990 m (Stroud et al., 2003). Anticlines are observable near Wells Kiwi-1, Taranui-1, and Pateke and a synclinal is observable east of Well Taranui-1. The color bar shows the depth values in meters.

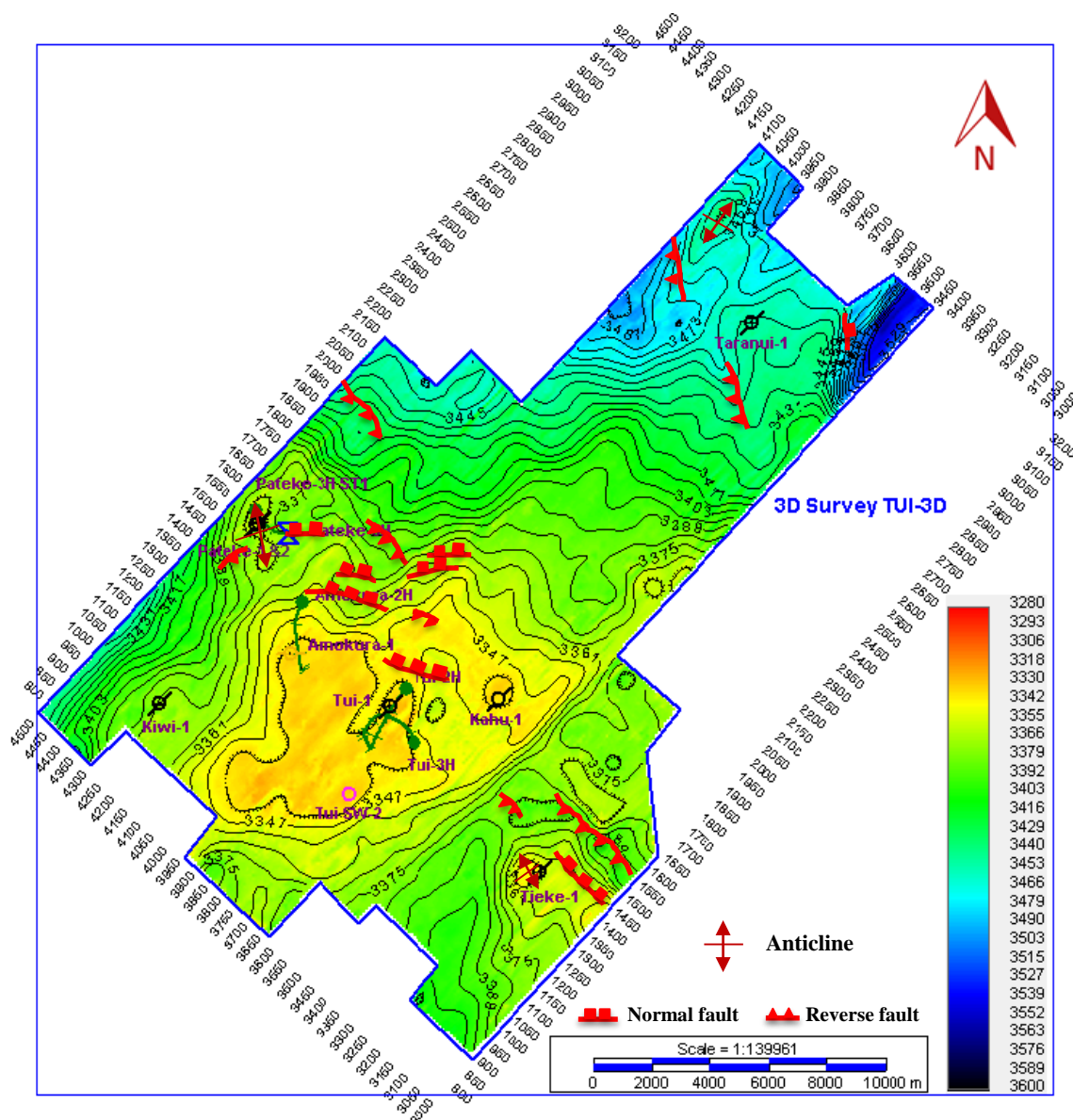


Figure 4.21. Depth map of the Kaimiro "D" Sand Horizon. The depth map illustrates a dipping toward the northeast. This horizon is a potential reservoir in the area. A low relief-broad anticline was observed around Well Tui-1, and other anticlines were observable around Wells Tieke-1 and Pateke. The color bar shows the depth values in meters.

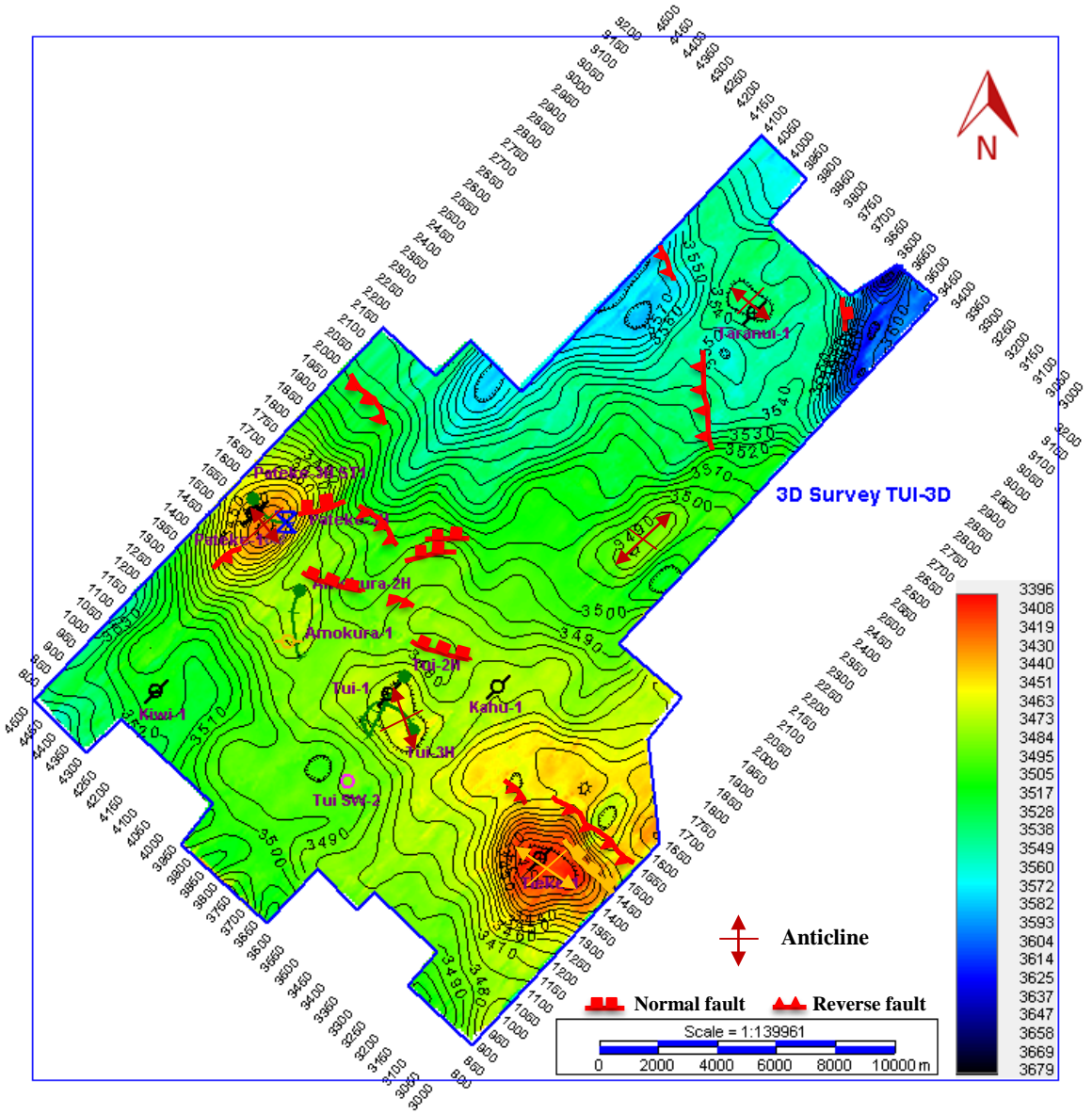


Figure 4.22. Depth map of the Farewell “E” Shale Horizon. The depth map illustrates a dipping toward the north. The Farewell “E” Shale consists of mostly siltstone and clay and behaves as a cap rock. Anticlines were observable around Wells Tieke-1, Taranui-1, Pateke, and Tui-1. The color bar shows the depth values in meters.

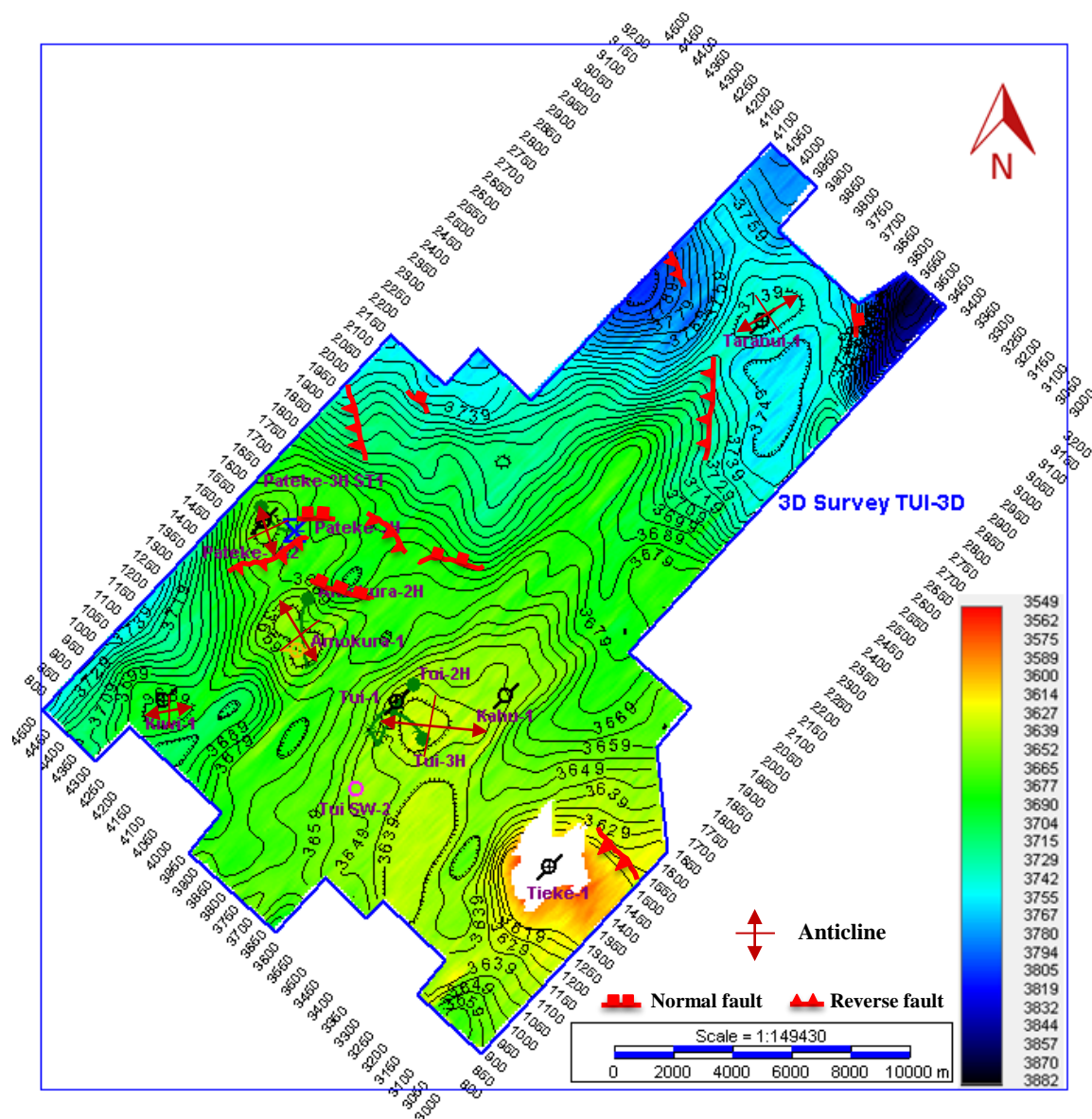


Figure 4.23. Depth map of the Farewell “F” Sand Horizon. The depth map illustrates a dipping toward the north. This map reveals that Wells Tui-1, Amokura-1 and Pateke-1&2 have a low relief anticline, structural traps, for oil accumulation. An anticline from the basement shown in white was observable near Well Tieke-1, which is located south of the area. The Farewell “F” Sand onlaps to the basement. The color bar shows the depth values in meters.

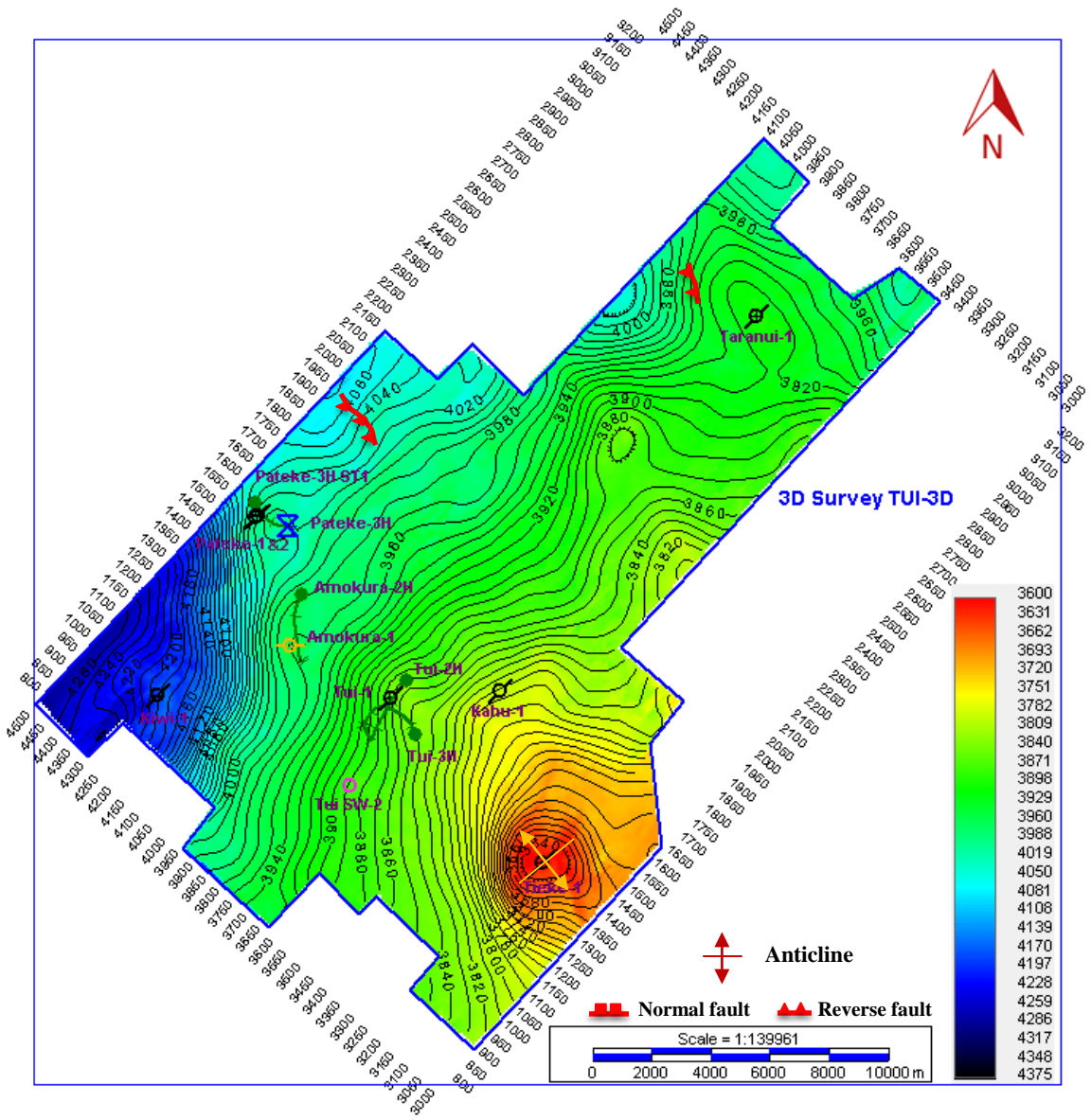


Figure 4.24. Depth map of the basement Horizon. The depth map illustrates a dipping toward the northwest. An anticline was observable around Well Tieke-1, which is located south of the area. The color bar shows the depth values in meters.

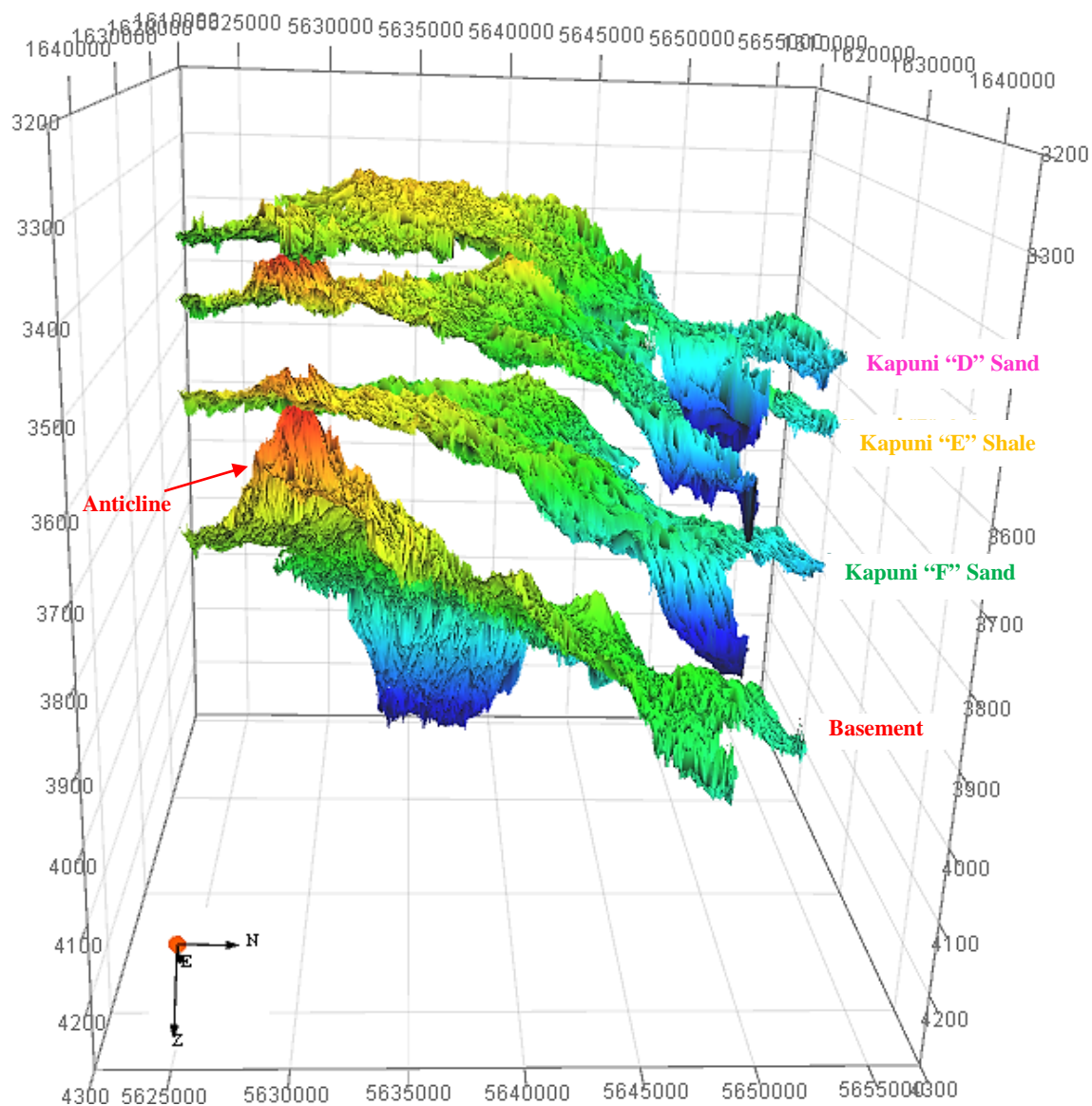


Figure 4.25. 3D depth view of four horizons which are Kapuni "D" Sand (Kaimiro "D" Sand), Kapuni "E" Shale (Farewell "E" Shale), Kapuni "F" Sand (Farewell "F" Sand), and basement. The 3D cube shows a dipping generally toward the north. An anticline shown with arrow was observed at the south of the study area.

4.5.3. Time-Depth Conversion. A time-depth conversion was conducted to the seismic data to get more realistic results and images of the horizons and wells. A time-

depth conversion was processed by correlating two types of grids, i.e. depth and time. A vertical seismic slice of Inline 3813 is shown in depth values in Figure 4.26.

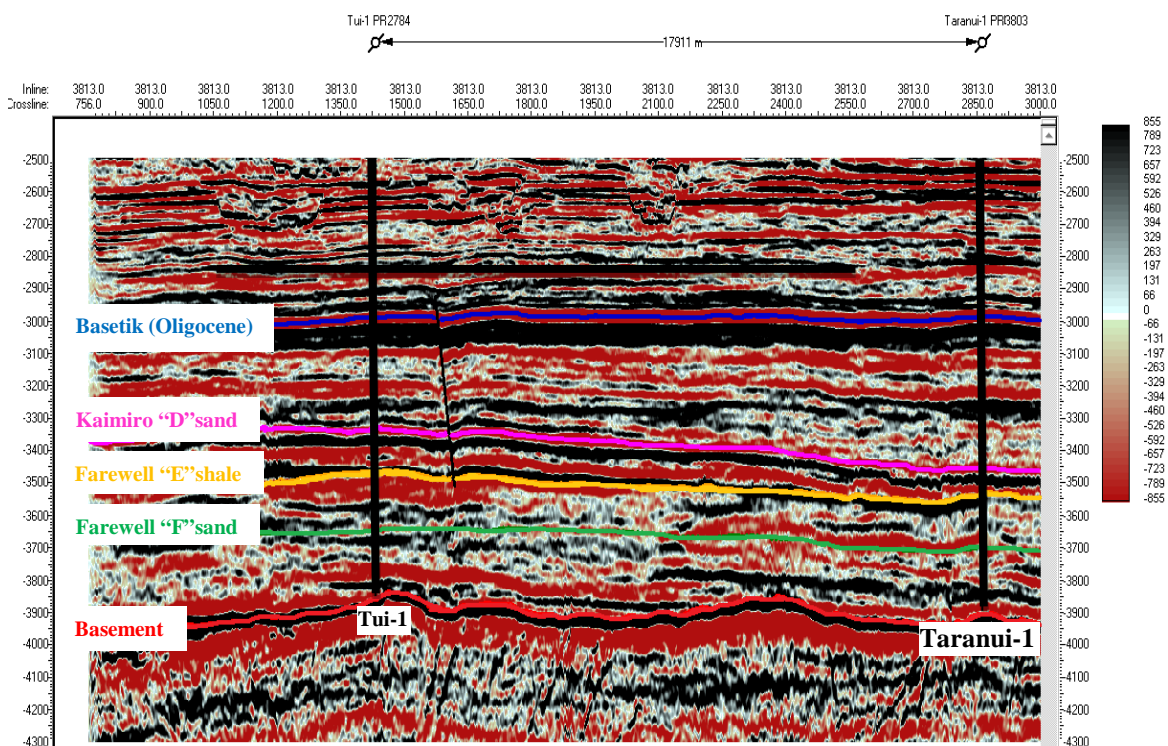


Figure 4.26. Vertical seismic section of Inline 3813 in depth. The color bar shows the amplitude values. A fault is interpreted near the Tui-1 well with a black line. The depth is subsea and in meters. The time can be found in Figure 4.7 (28 km long section).

4.5.4. Isopach Map. An isochron map shows the time difference between two horizons. An interval velocity map is needed to generate an isopach map. An isopach map shows the thickness of each targeted horizon. It can be constructed by multiplying these two maps (IHS, 2014).

4.5.4.1. Interval velocity map. The interval velocity was calculated using the following equation (IHS, 2014):

$$\text{Interval Velocity} = (F2-F1) * 2 / (T2-T1), \quad (2)$$

where F2 is the depth of the upper formation top, F1 is the depth of the lower formation top, T2 is the two way travel time of the upper time surface, and T1 is the two way travel time of the lower time surface (Figure 4.27).

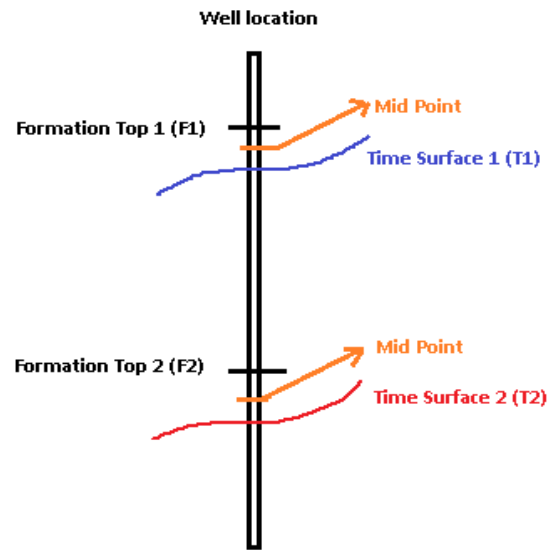


Figure 4.27. Illustration displaying formation tops and time surfaces used to calculate the interval velocity.

The interval velocity was calculated using two time surfaces and two formation tops at a specific well. This process was repeated at each well in the study area, and velocity control points were acquired. After these calculations, X and Y locations were calculated using the midpoints shown in Figure 4.27. Most of the wells in the study area were deviated, which is why midpoints were used to get X and Y locations. The first midpoint was the intersection of the upper formation top and the upper time surface, and the second midpoint was the intersection of the lower formation top and the lower time

surface. The two midpoints were averaged to obtain final X and Y locations for the interval velocity value (IHS, 2014). All velocity points, final X and Y values, and the inverse distance to a power gridding algorithm were used to generate interval velocity maps.

The interval velocity maps for the Kaimiro “D” Sand, Farewell “E” Shale, and Farewell “F” Sand are shown in Figures 4.28, 4.29, and 4.30, respectively.

Interval velocity maps show that velocities vary between 3122 m/s and 3952 m/s for the Kaimiro “D” Sand Horizon (potential reservoir) (Figure 4.28). For the Farewell “E” Shale Horizon (cap rock), velocities vary between 3687 m/s and 4507 m/s (Figure 4.29). Velocities of the Farewell “F” Sand Horizon (reservoir) vary between 3532 m/s and 4163 m/s (Figure 4.30).

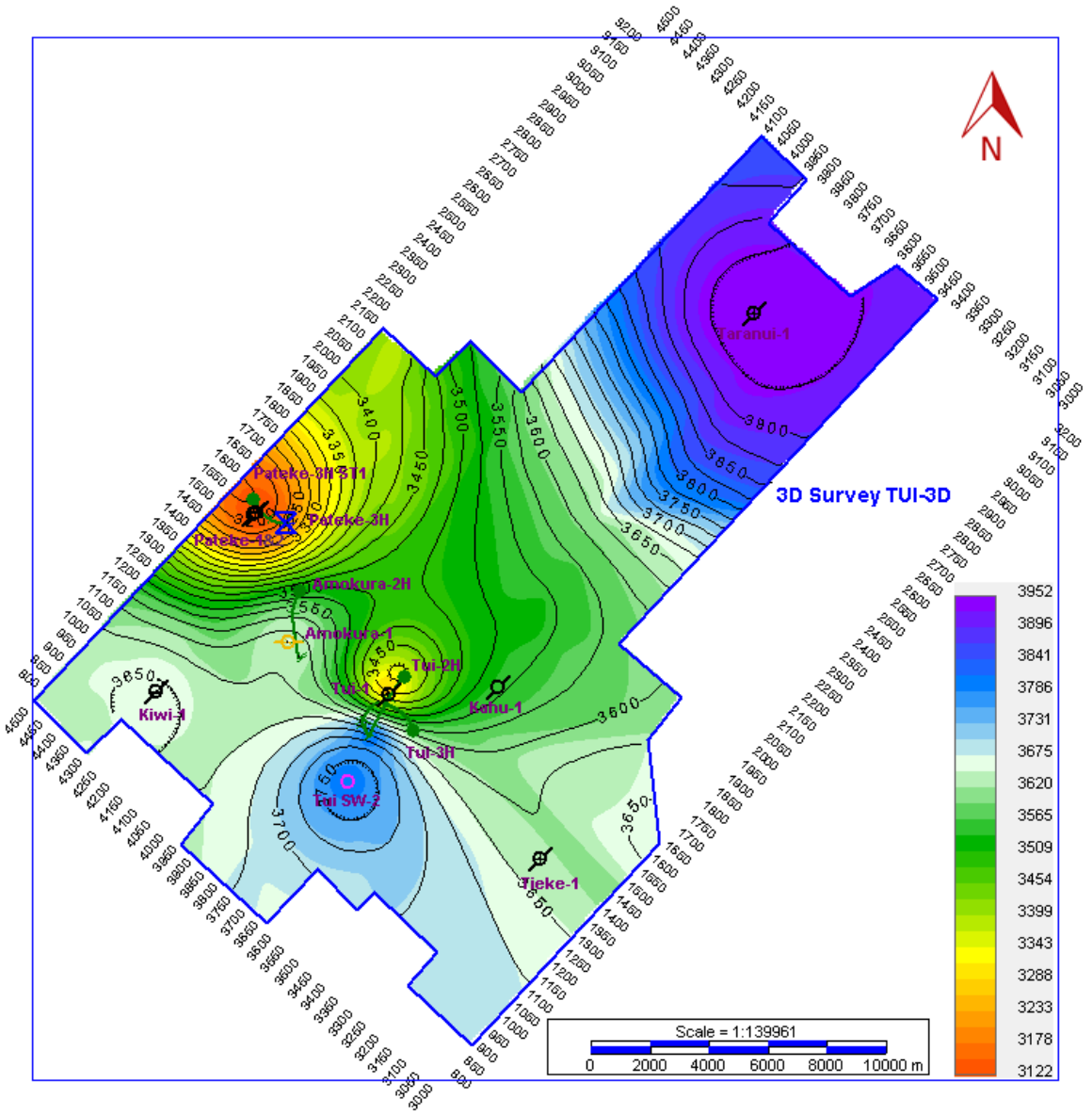


Figure 4.28. Interval velocity map of the Kaimiro “D” Sand. The lowest value is around Well Pateke, and the highest value is around Well Taranui-1. Velocities range from 3122 m/s to 3952 m/s.

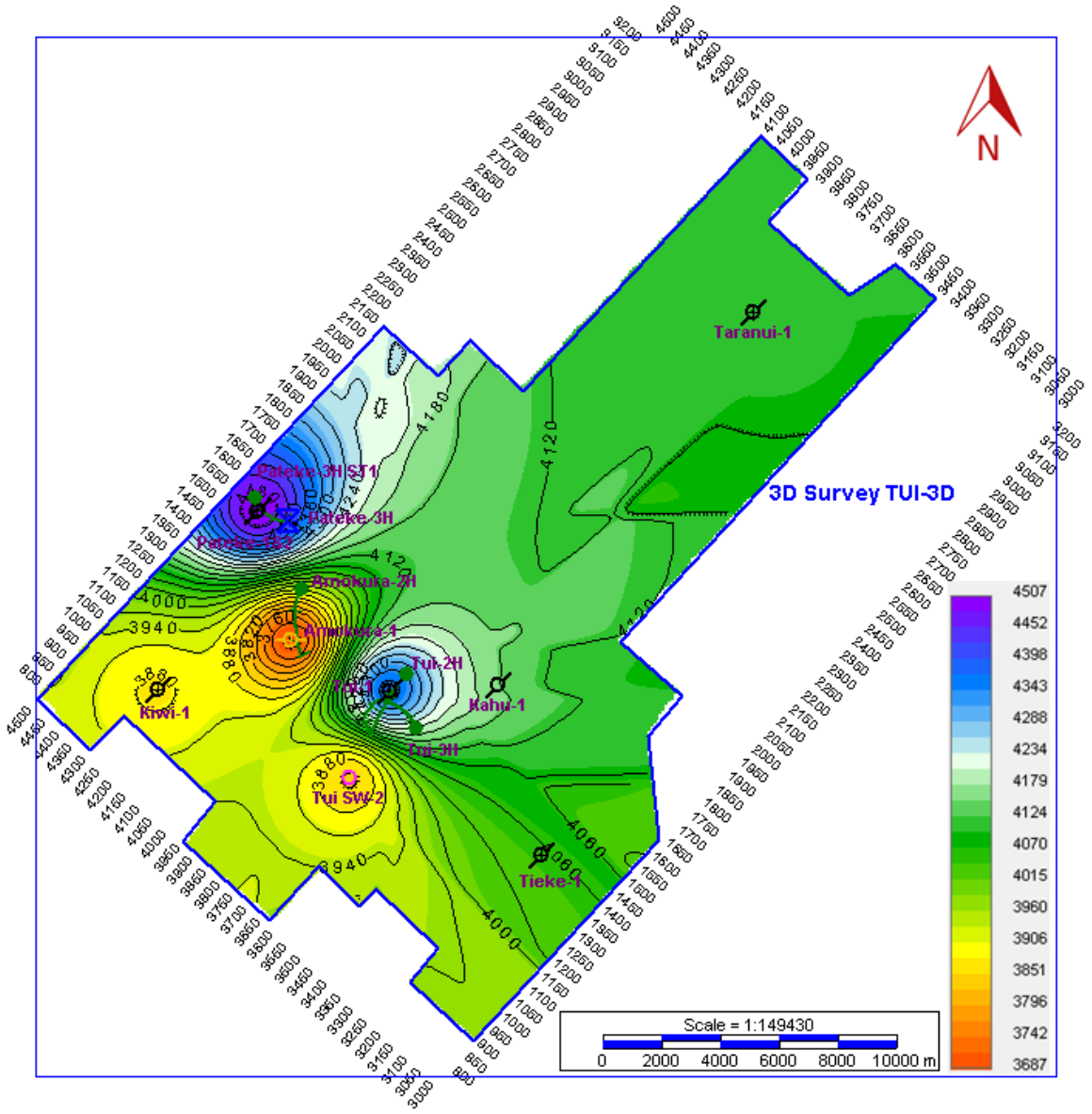


Figure 4.29. Interval velocity map of the Farewell “E” Shale. The lowest value is around Well Amokura-1, and the highest value is around Well Pateke-1. Velocities range from 3687 m/s to 4507 m/s.

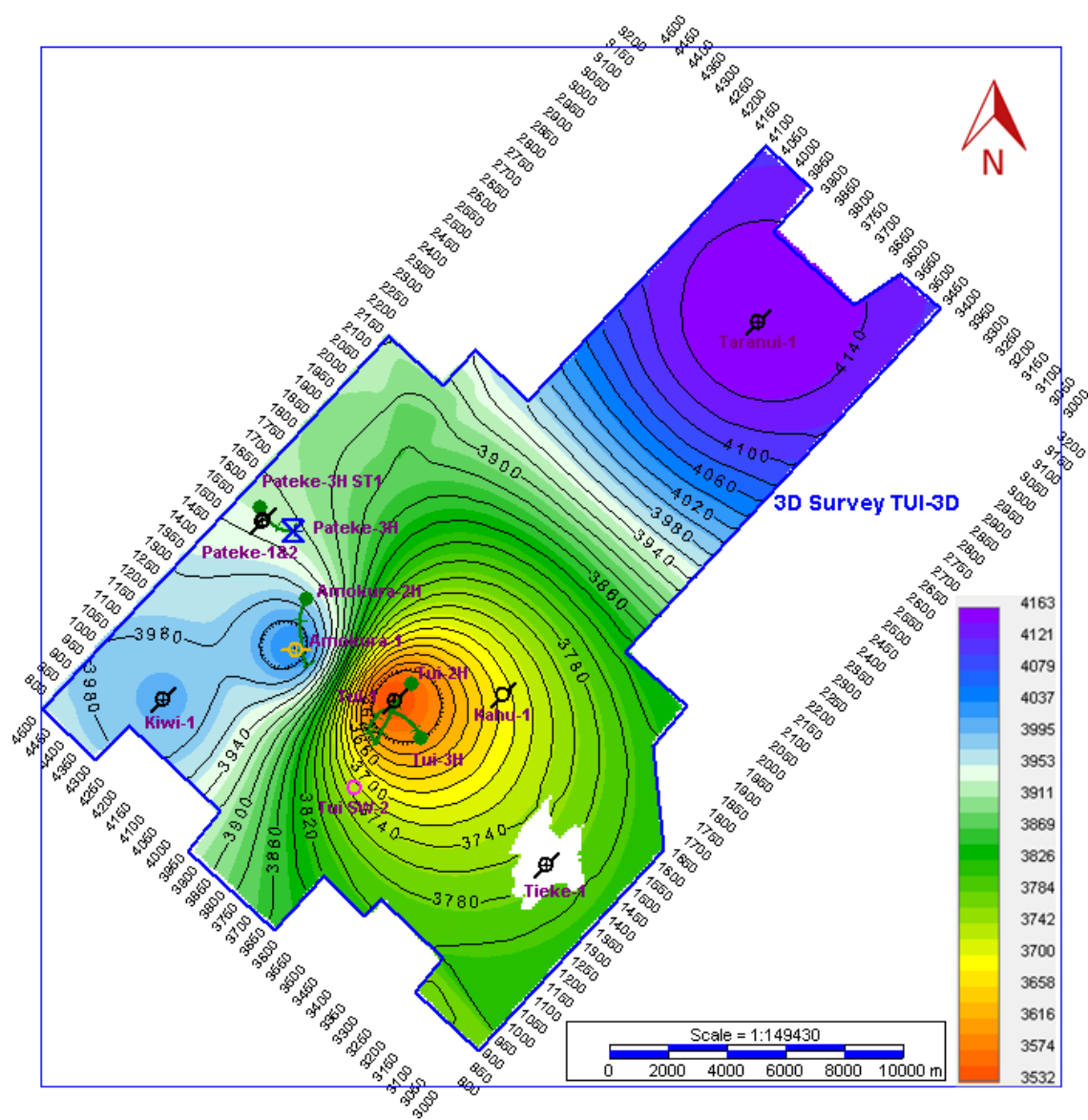


Figure 4.30. Interval velocity map of the Farewell “F” Sand. The lowest value is around Well Tui-1, and the highest value is around Well Taranui-1. The Farewell “F” Sand onlaps to the basement shown in white at the Tieke-1 well. Velocities range from 3532 m/s to 4163 m/s.

4.5.4.2. Isopach map. Isopach map can be used to analyze seismic stratigraphic features and depositional systems. It shows the thickness variations for the target formations.

The isopach maps for the Kaimiro “D” Sand, Farewell “E” Shale, and Farewell “F” Sand are displayed in Figures 4.31, 4.32, and 4.33, respectively.

The isopach map of the Kaimiro “D” Sand indicates that the thinnest area is around Well Pateke (Figure 4.31). For the Farewell “E” Shale, the thickness increases toward the southwest (Figure 4.32). The thickest area is around the Pateke wells and the thinnest area is around Well Taranui-1. The thickness of the Farewell “F” Sand increases toward the northwest (Figure 4.33). The thickest area is around Well Pateke and the thinnest area is around Well Tieke-1.

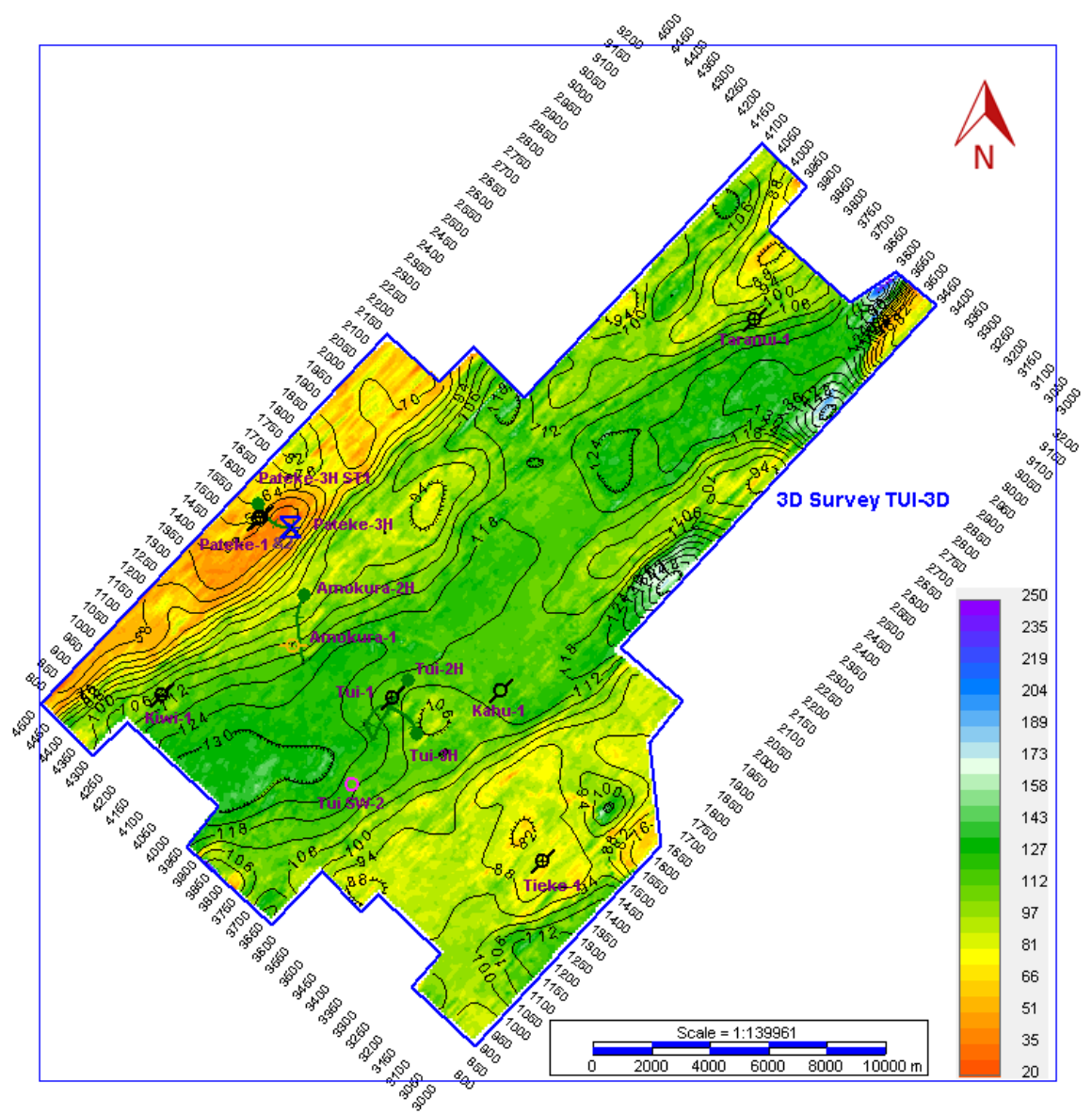


Figure 4.31. Isopach map of the Kaimiro “D” Sand. The map shows the thickness in meter. Sediment accumulation became thinner toward the west. The thickness ranges from 20 m to 250 m.

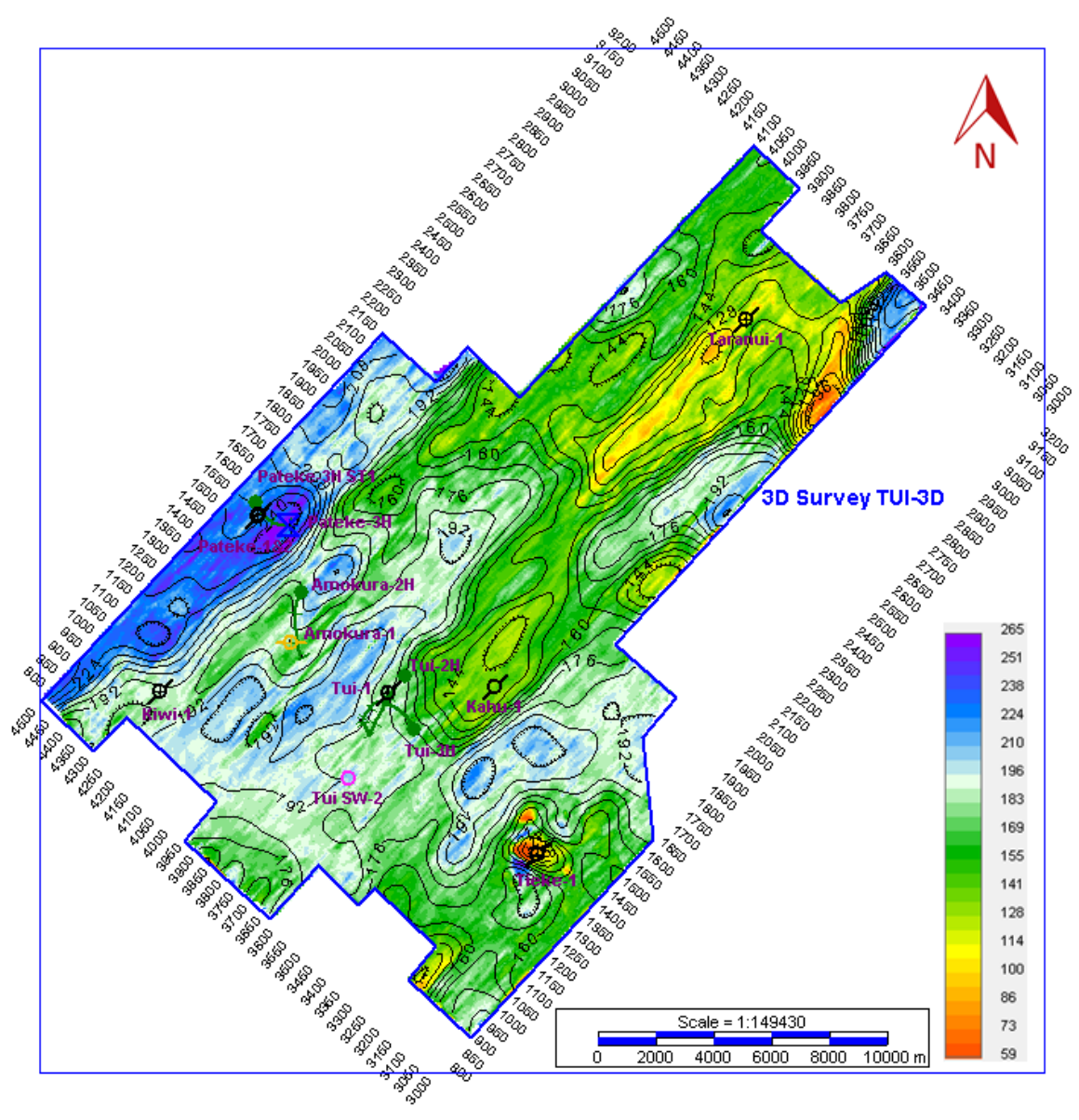


Figure 4.32. Isopach map of the Farewell “E” Shale. The map shows the thickness in meter. The values range from 59 m to 265 m. The horizon becomes thicker toward the southwest.

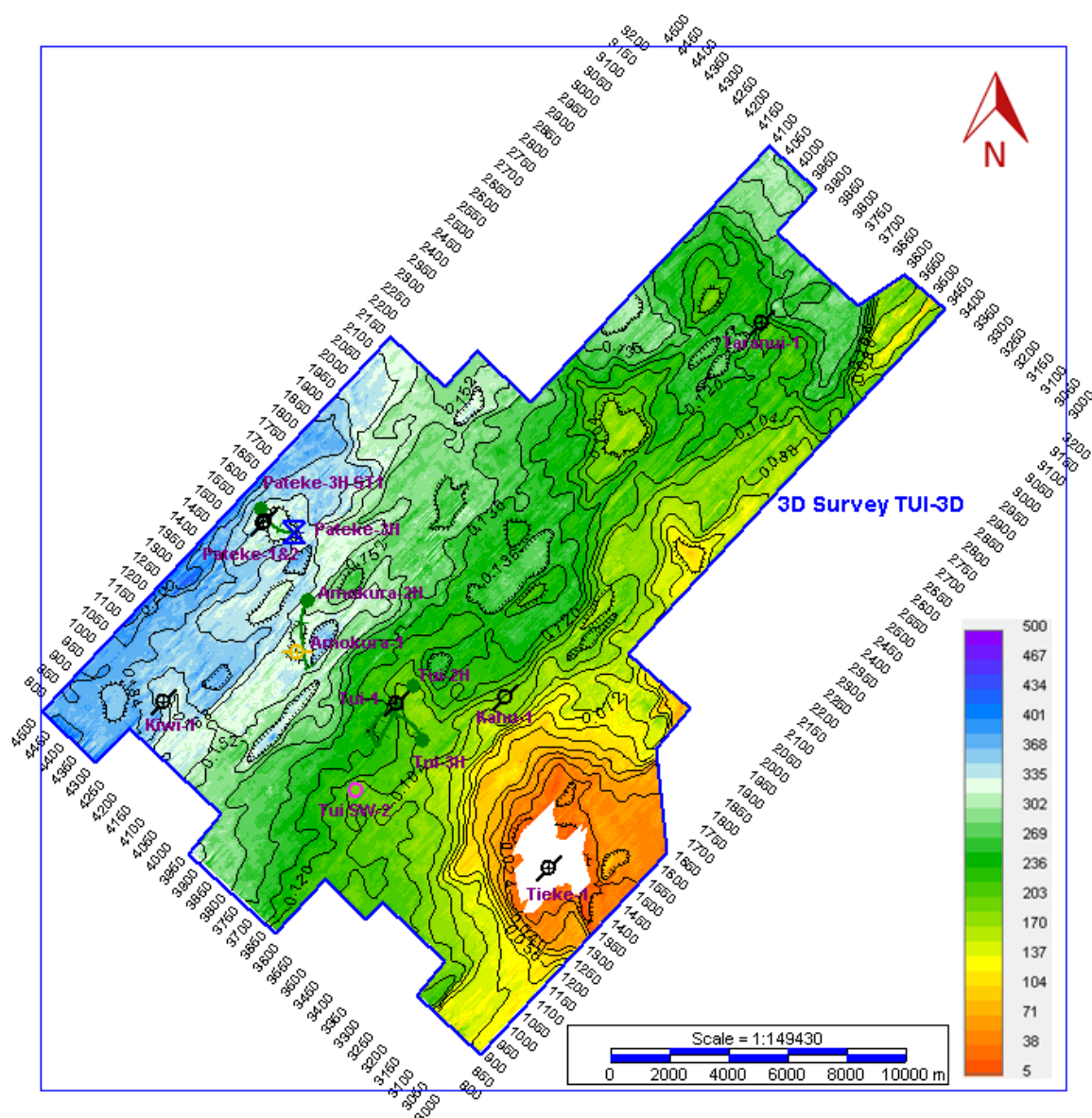


Figure 4.33. Isopach map of the Farewell “F” Sand. The map shows the thickness in meter. The horizon becomes thicker toward the northwest. The Farewell “F” Sand onlaps to the basement as shown in white near Well Tieke-1. The color bar shows the depth values in meters.

5. SEISMIC STRATIGRAPHIC ANALYSIS

Some stratigraphic features of the shallow formations, channels in the Moki “A” Sand, gullies in the Giant Foresets, and a channel within the Farewell “F” Sand were identified after seismic attribute analyses to understand the depositional environment.

5.1. SEISMIC ATTRIBUTES

A seismic attribute provides enhanced information for subtle geological and geophysical features by extracting more information from seismic data. Some of the seismic attribute volumes, such as chaos, local flatness, and sweetness, were generated in this study using the Petrel 2014 software and imported back to the Kingdom 2015 to interpret geologic features such as channels, gullies, and lineaments.

5.1.1. Local Flatness. Local flatness is a structural as well as a stratigraphic attribute, which is connected to seismic textures and helps to identify faults, channel infills, and vertical features. Flatness guides the interpretation of vertical and dipping seismic events. When the events are planar, there is no discontinuity. The generated volume values range from 0 to 1, becoming non-planar towards to 1 as it approaches. This attribute should be used to examine time slices instead of seismic sections (Pereira, 2009).

5.1.2. Chaos. The attribute of chaos refers to the lack of organization within seismic data in the dip and azimuth method of estimation. Low constancy refers to a chaotic pattern. Chaotic patterns are used to identify faults, salt bodies, gas chimneys, and channels. The generated volume of chaos is scaled from 0 to 1 with 1 being the most chaotic (Pereira, 2009).

5.1.3. Sweetness. Sweetness is an attribute used for recognizing sands and sandstones in 3D seismic data in terms of clastic successions (Hart, 2008). It was first depicted by Radovich and Oliveros (1998) and is defined as a combination of the envelope (reflection strength) and instantaneous frequency. Taner and Sheriff (1977) defined reflection strength and instantaneous frequency as complex attributes. When high amplitude and low frequency occur, the sweetness shows a high value (Figure 5.1). The sweetness attribute is affected by tuning effects and fluid in pores because they are the factors that change instantaneous frequency or envelope (Hart, 2008).

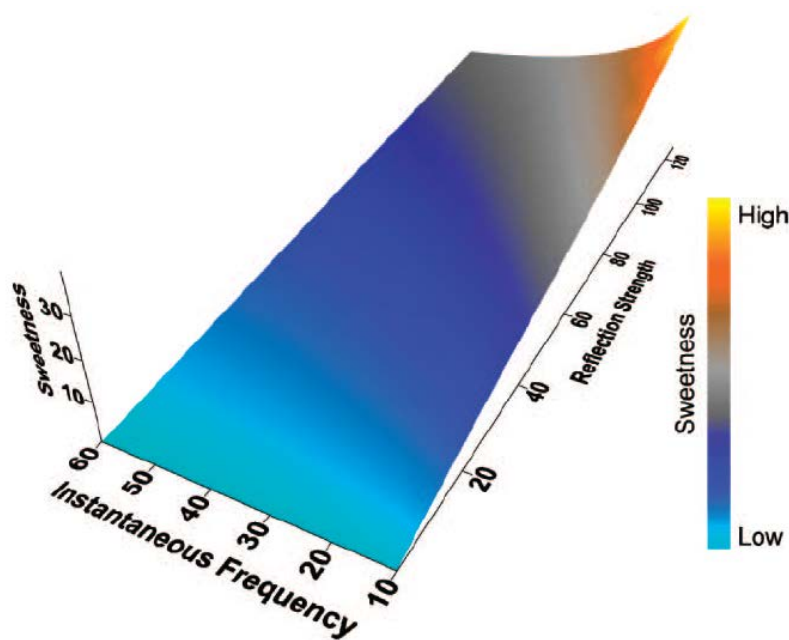


Figure 5.1. Sweetness attribute shown as surface. The attribute is composed of instantaneous frequency and reflection strength (Hart, 2008).

5.2. STRATIGRAPHIC FEATURES

Horizon slices were generated by the tracked horizons. Seismic attributes such as chaos, local flatness, and sweetness were applied to the horizons to assist stratigraphic feature delineation.

5.2.1. Gullies in Giant Foresets Formation. Gullies were found by picking Horizon A in the Giant Foresets Formation (GFF) (Figures 5.2 and 5.3). GFF was deposited in a slope to shelfal environment and is Pliocene to Pleistocene in age (Pilaar & Wakefield, 1978). After seismic attributes were applied, gullies were observed clearly in horizon slices (Figures 5.4 and 5.5). They are oriented along the northwest-southeast and straight to low sinuous. Figure 5.6 displays gullies in a 3D cube. Horizon A shows a dipping toward the northwest. The gullies are up to 12 km, roughly 10 to 70 m deep, from 20 m to 500 m wide, U-shaped, and approximately parallel to each other (Figure 5.6B).

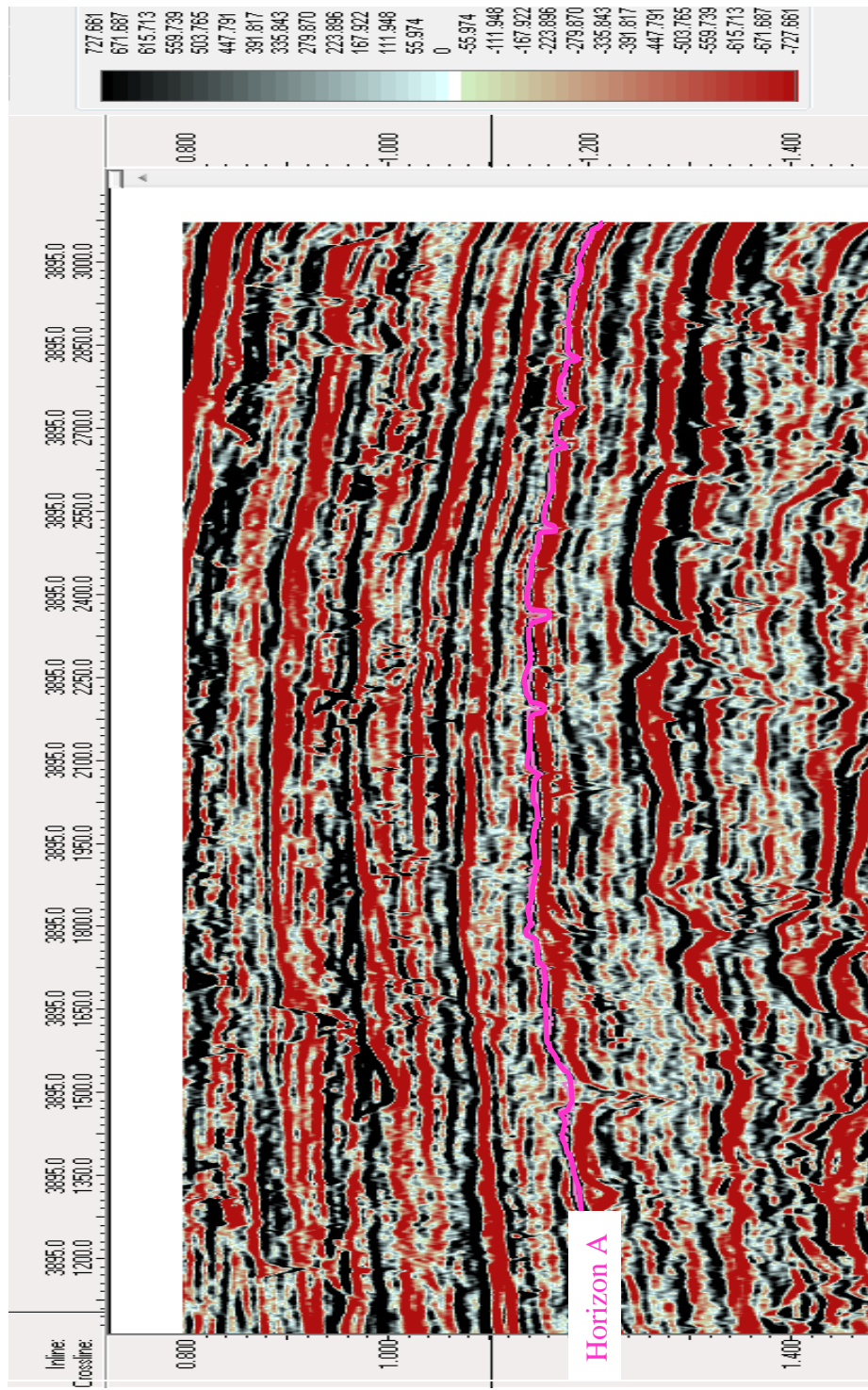


Figure 5.2. Vertical seismic section of Inline 3895 showing Horizon A (pink) (25.9 km long section).

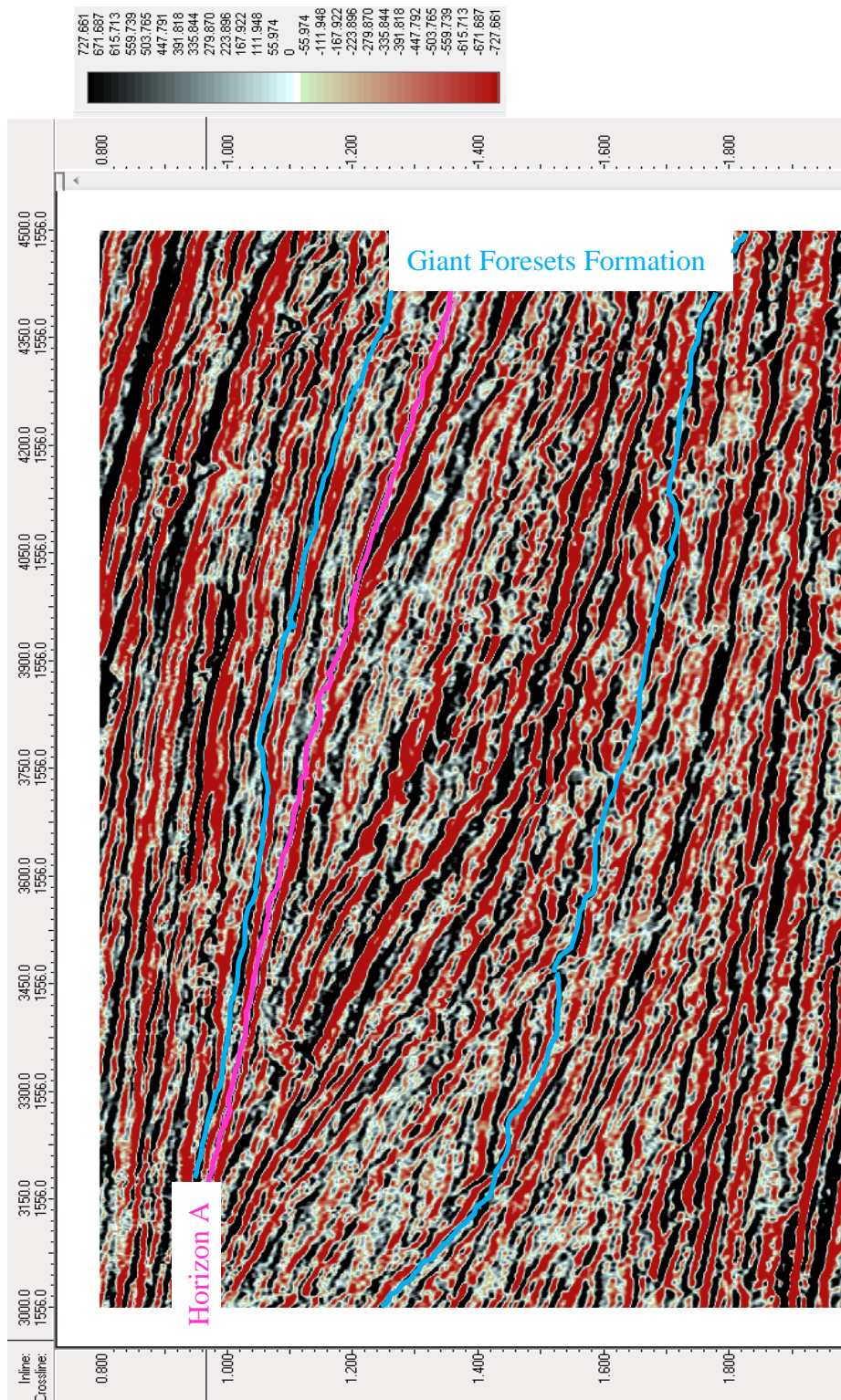


Figure 5.3. Vertical seismic section of Crossline 1556 showing Horizon A (pink). The Horizon A was deposited within the Giant Foresets Formation in a slope to shelfal environment and is Pliocene to Pleistocene in age (Pliaar & Wakefield, 1978) (18.75 km long section).

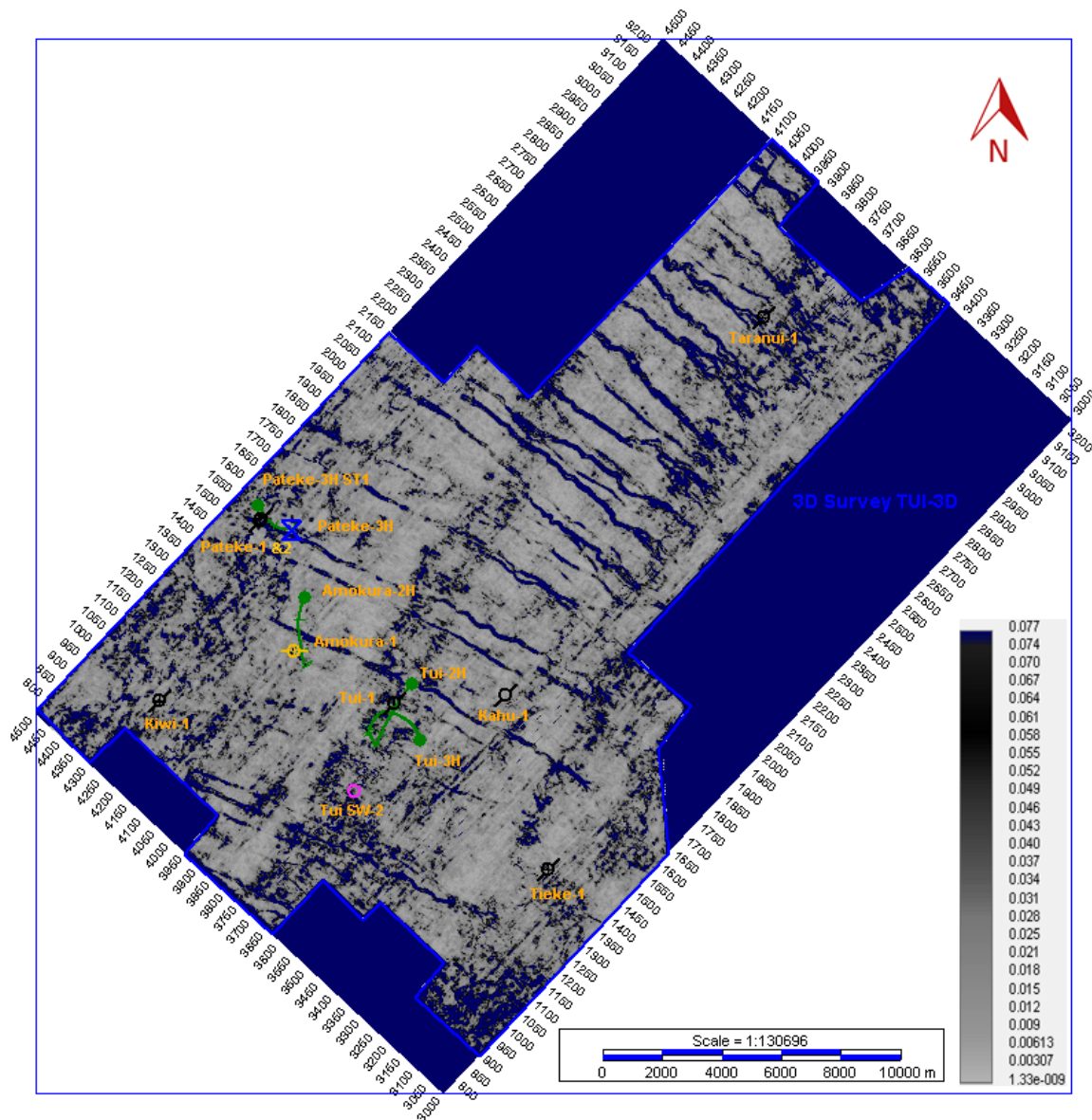


Figure 5.4. Horizon slice of chaos attribute of Horizon A showing gullies. The gullies are oriented along the northwest-southeast direction with a length of up to 12 km.

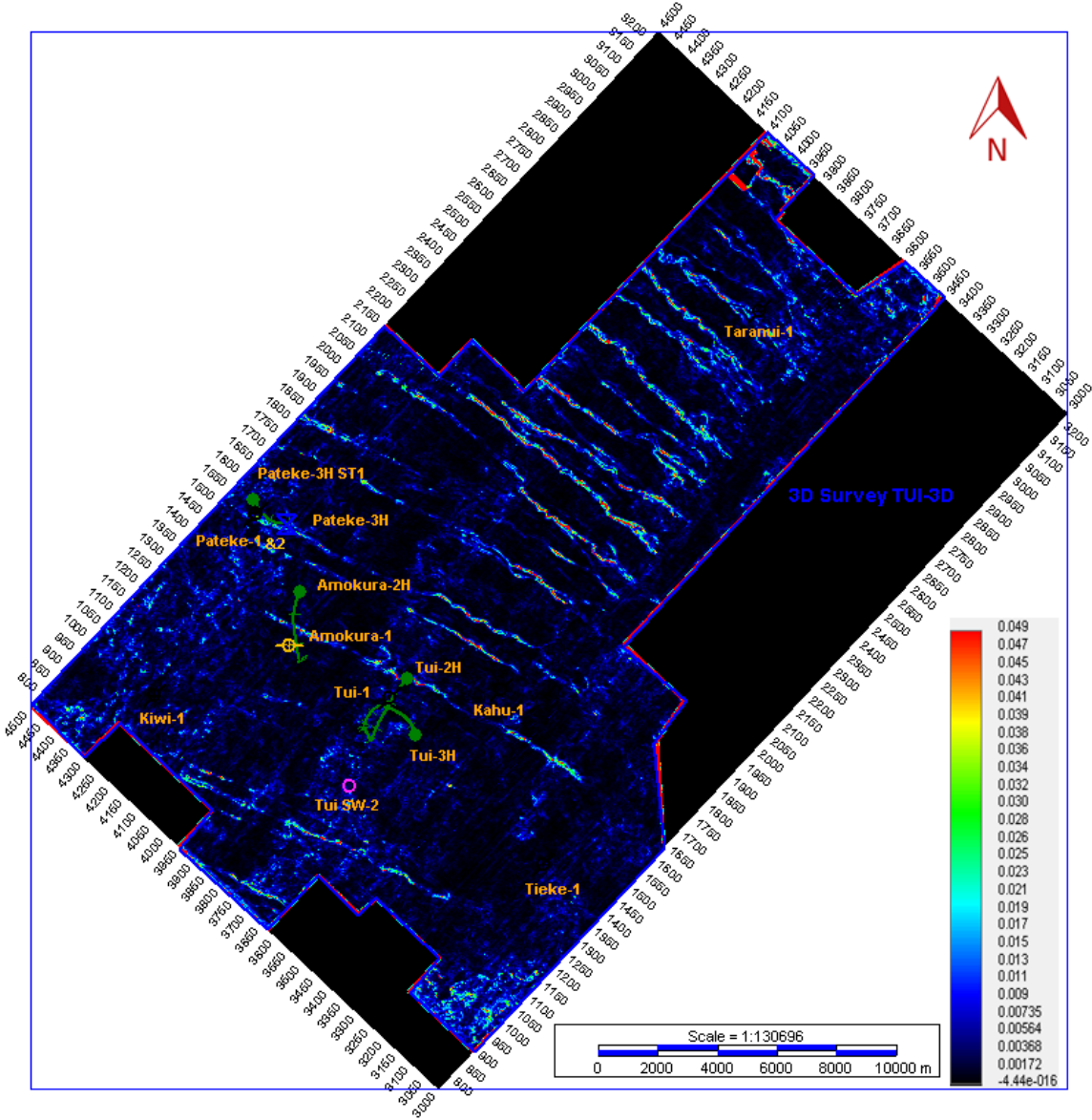
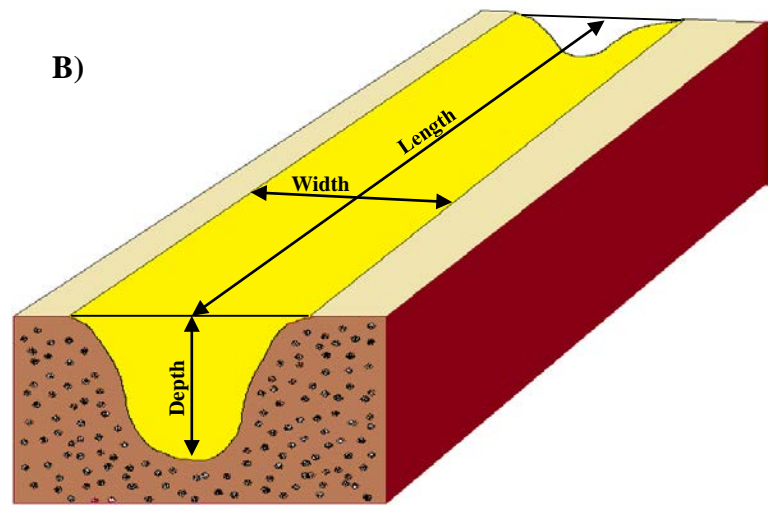
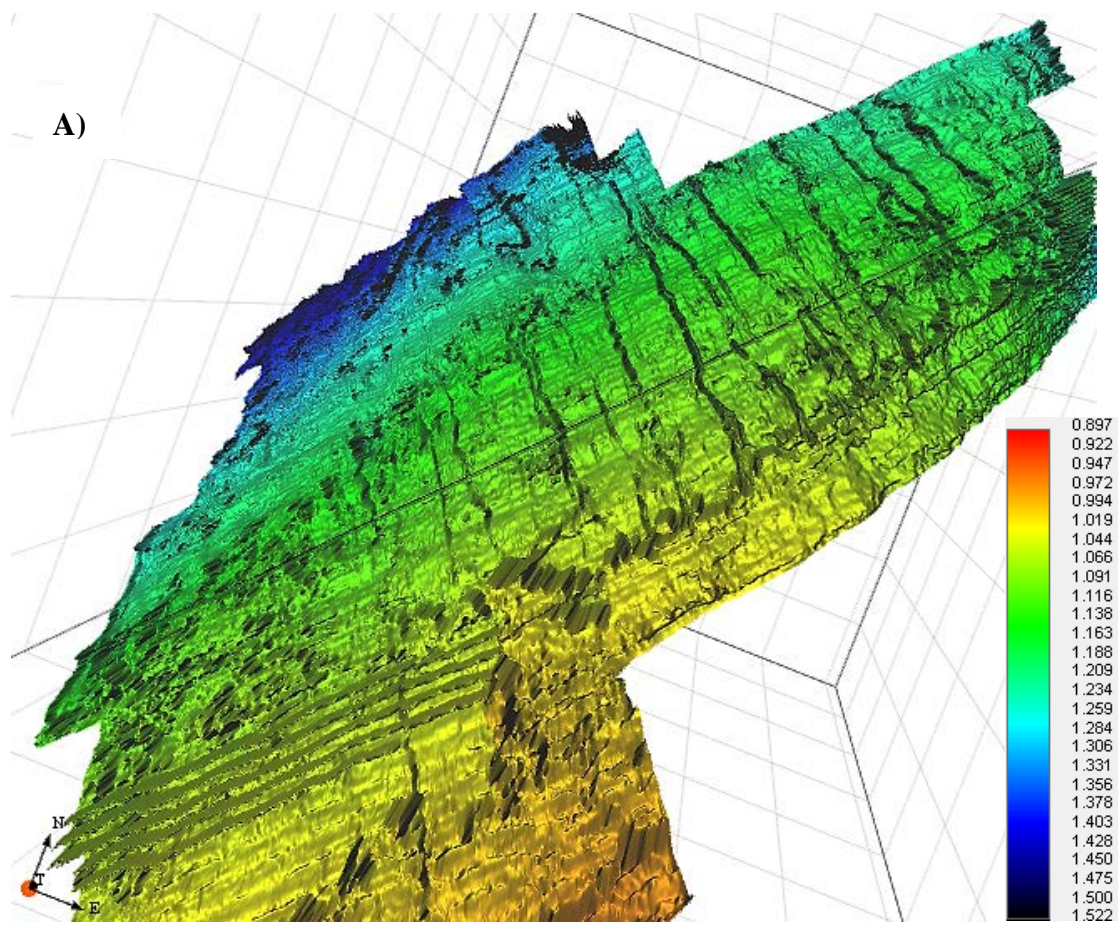


Figure 5.5. Horizon slice of local flatness attribute of Horizon A showing gullies. The gullies are oriented along the northwest-southeast direction, straight to low sinuous, and approximately parallel to each other.



Gullies are roughly 10-70 m deep, 20 m to 500 m wide, U-shaped, and up to 12 km long.

Figure 5.6. Gullies in Horizon A shown in a 3D view. A) A closer look of Horizon A is displayed in a 3D cube. It shows a dipping toward the northwest. B) Schematic illustration indicates depth, width, shape, and length of a gully.

5.2.2. A Channel System in the Farewell “F” Sand. A channel, which is named Kahu, was observed on horizon slice of the Farewell “F” sand. Well Kahu-1 was drilled to observe features of the Kahu channel (AWE, 2010). According to well report (PR 4272), the Kahu channel acts as a seal because it has shaly infill. The Farewell “F” Sand was deposited in a fluvial system with Paleocene-Early Eocene in age (Strogen et al., 2010).

The horizon slice of the Farewell “F” Sand clearly shows the Kahu Channel in Figure 5.7. Additionally, Figure 5.8 shows possible trap for oil accumulation of the Farewell “F” Sand where the horizon and the Kahu channel coincide (AWE, 2009).

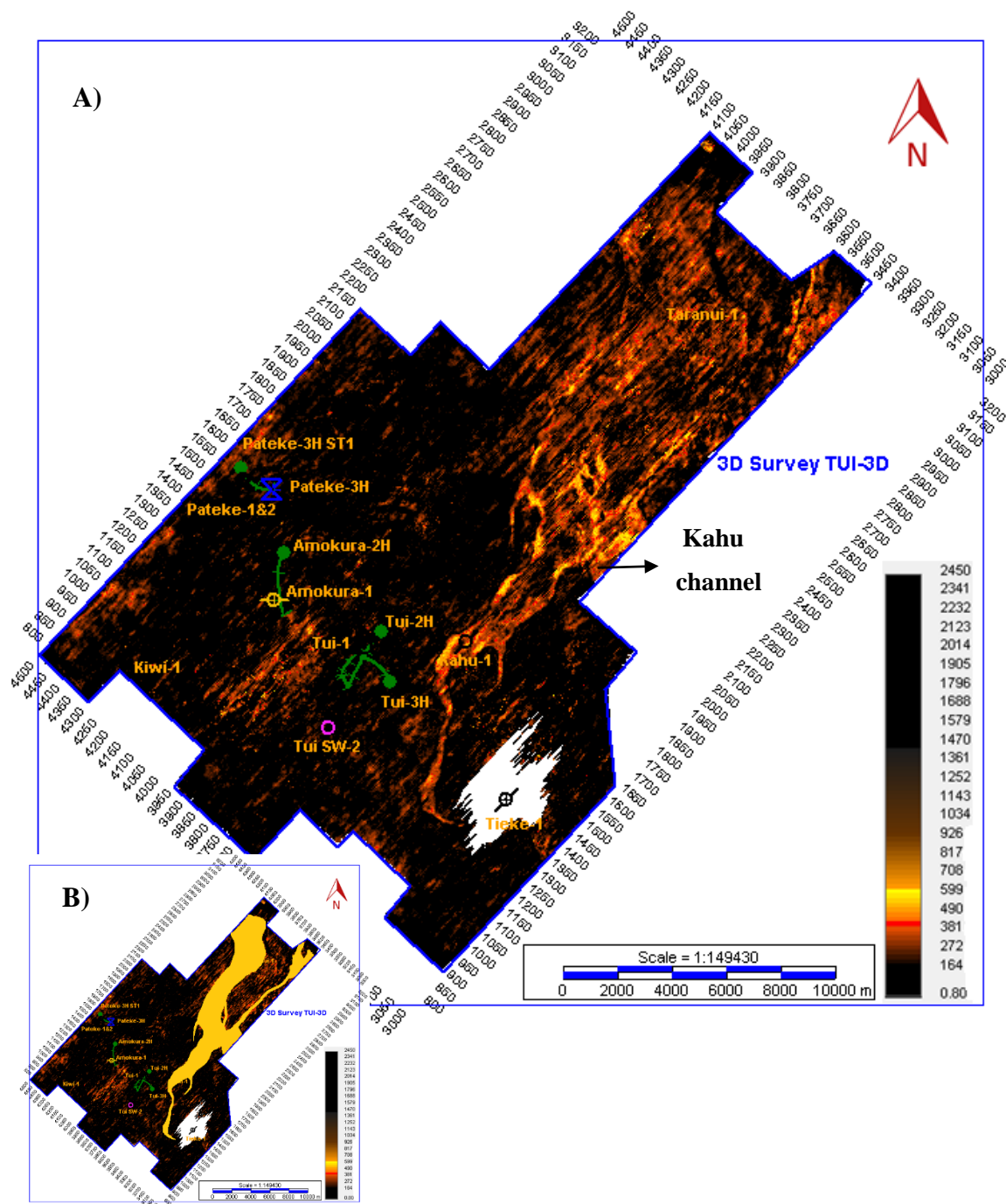


Figure 5.7. Sweetness attribute of horizon slice showing the top of the Farewell “F” Sand. A) An anticline from the basement, shown in white, was observable near Well Tiekē-1, which is located in the south of the area. The horizon slice clearly reveals the Kahu channel F sand sequence. The Kahu channel is a poor quality reservoir, but it has the ability to provide a good seal due to shaly infill. B) The Kahu channel was highlighted in yellow.

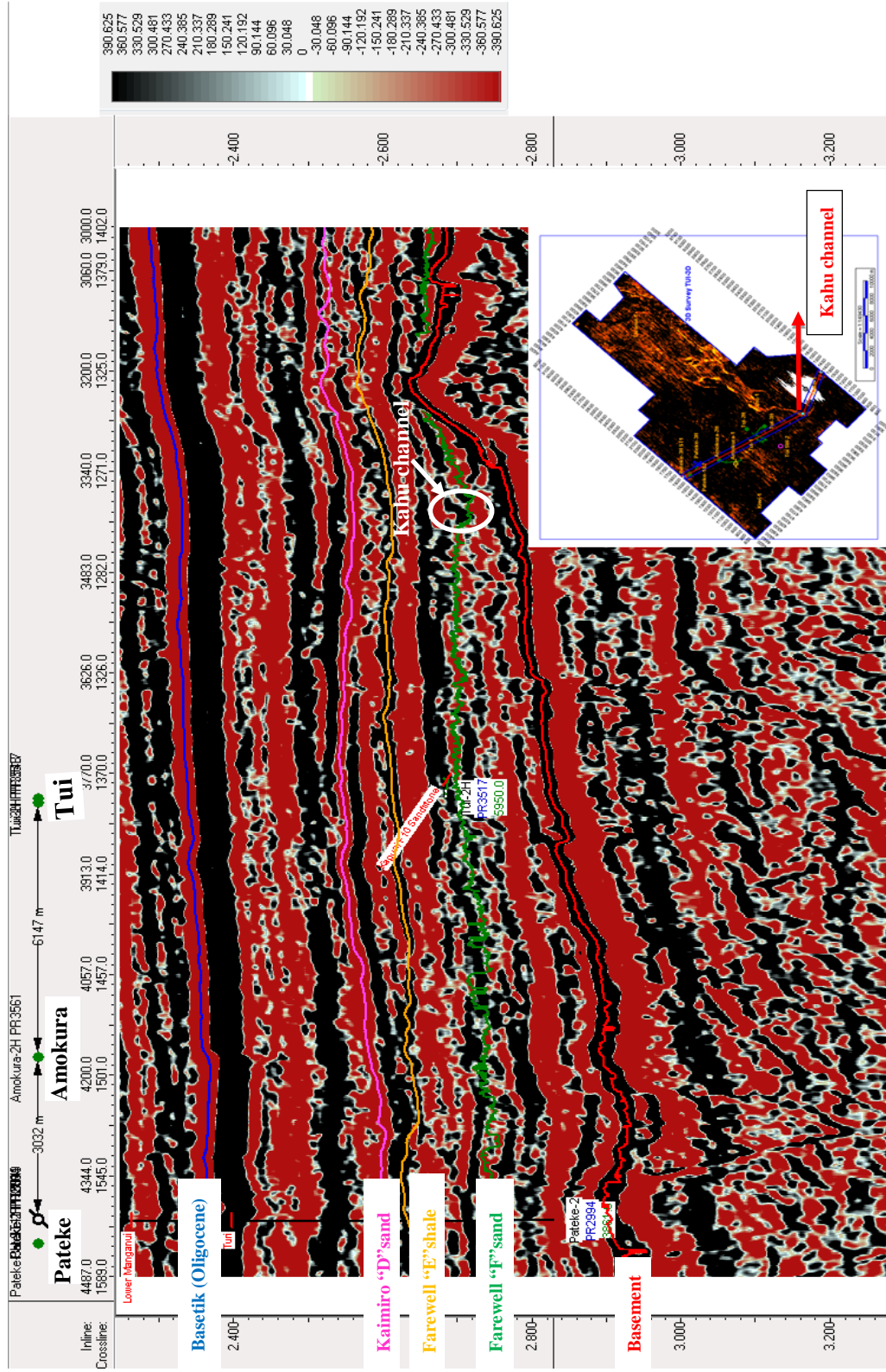


Figure 5.8. Arbitrary line showing the target horizons and Kahu channel. The Farewell "F" Sand onlaps to the basement and there might be a possible trap where the Kahu channel and Farewell "F" Sand coincide (AWE, 2009).

5.2.3. Channels in Moki “A” Sandstone Formation. Many channels were identified using time slice (Figure 5.9) and a vertical seismic section (Figure 5.10) in the Moki “A” Sand Formation. They are NW-SE trending meandering channels, which have high to moderate sinuosity and high ratio of width/depth. Seismic attribute of chaos was used to better display channels (Figure 5.11). In addition, Figure 5.12 shows the channels using Inline 3827 and time slice at 2.092 s.

The Moki “A” Sand is the upper part of the Moki Formation, the Mid-Miocene sandstone sequence, and was accumulated in base-of-slope turbidites (Engbers, 2002).

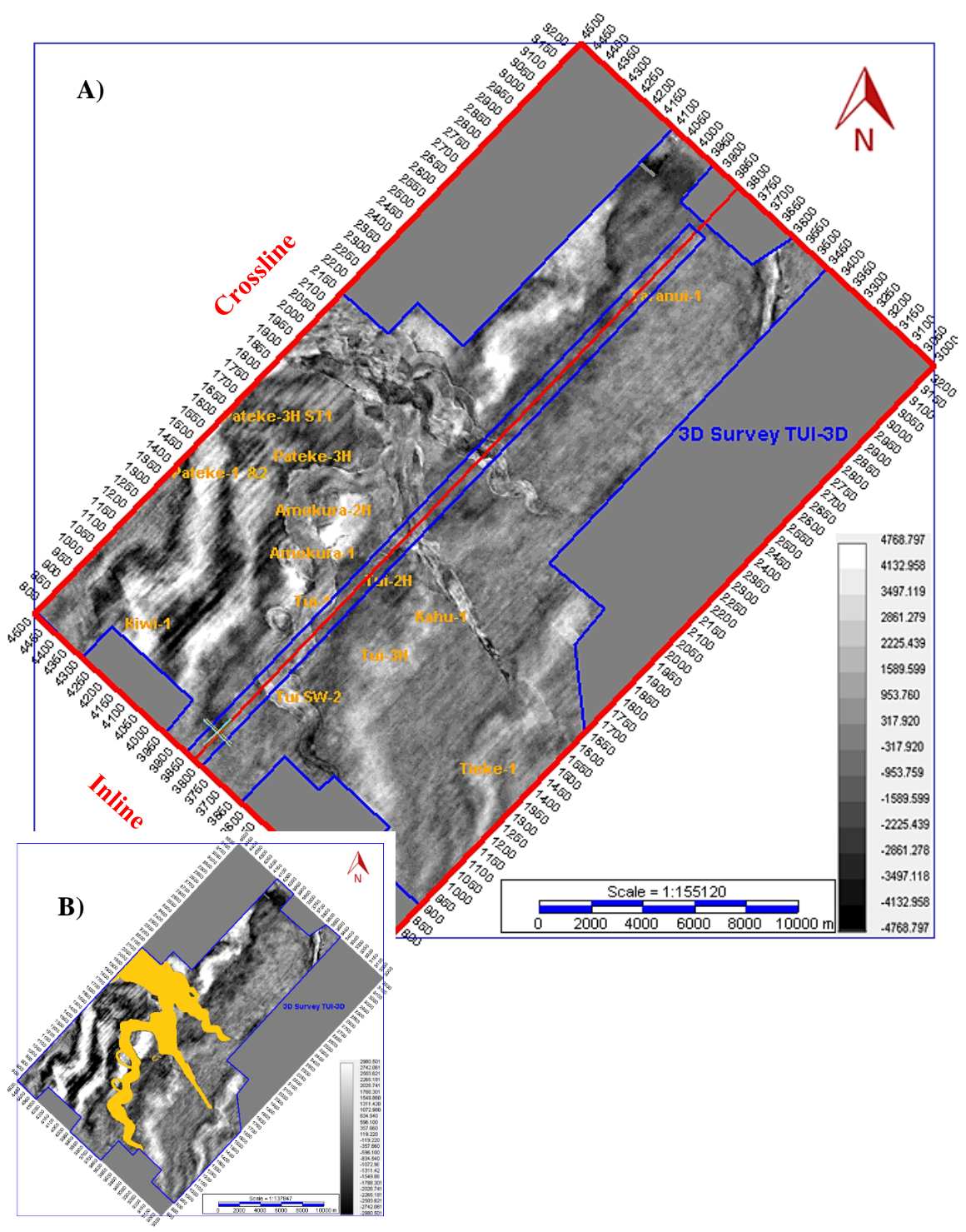


Figure 5.9. Channels in the Moki "A" Sand. The bar shows the amplitude variations. A) Time slice at 2.092 s displays channels. B) Channels are highlighted in yellow.

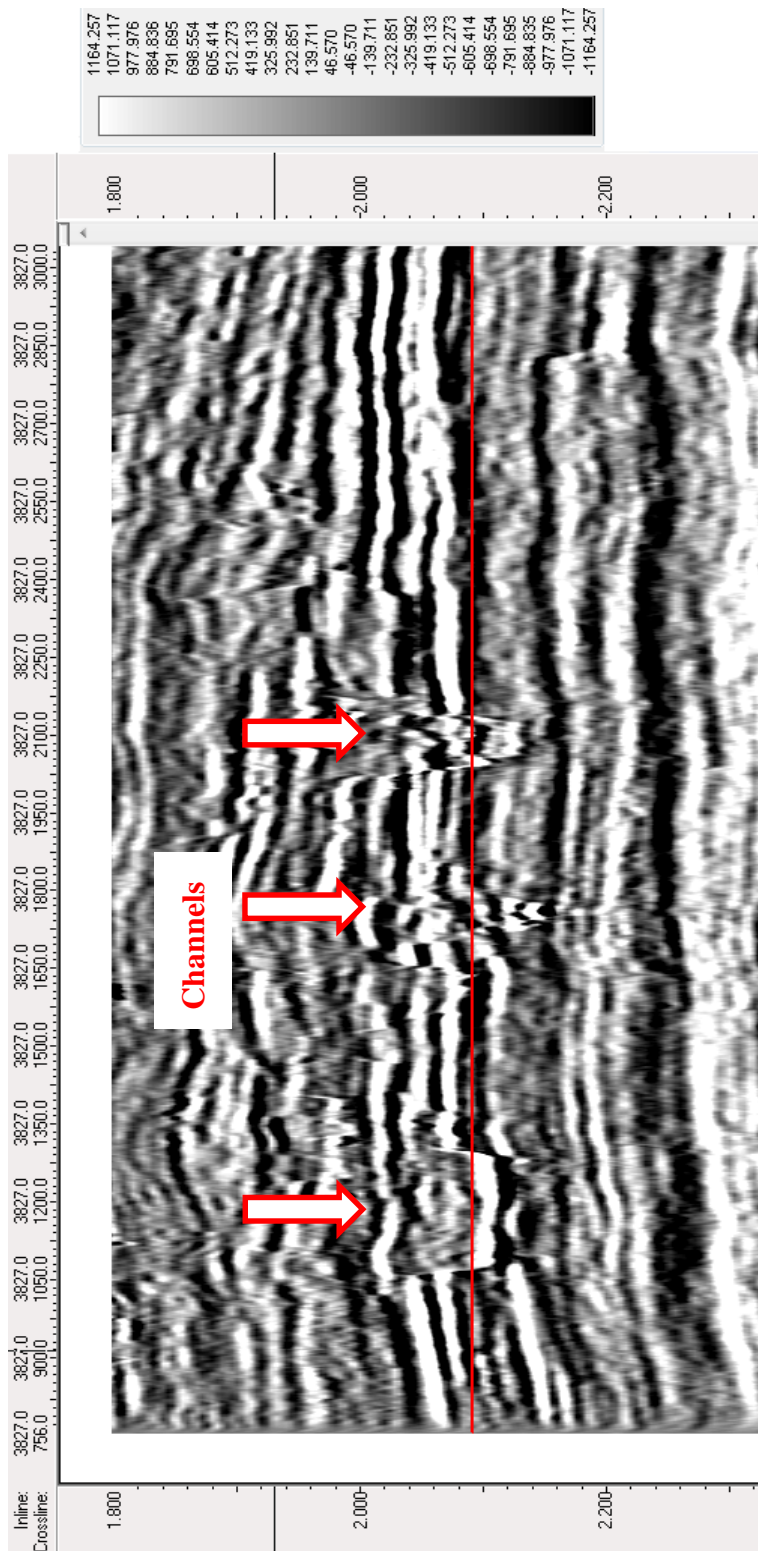


Figure 5.10. Vertical seismic section of Inline 3827 showing different channels. The bar shows the amplitude values. Channels have high width/depth ratio. The red line illustrates the time slice at 2.092 s, shown in Figure 5.11 (28.4 km long section).

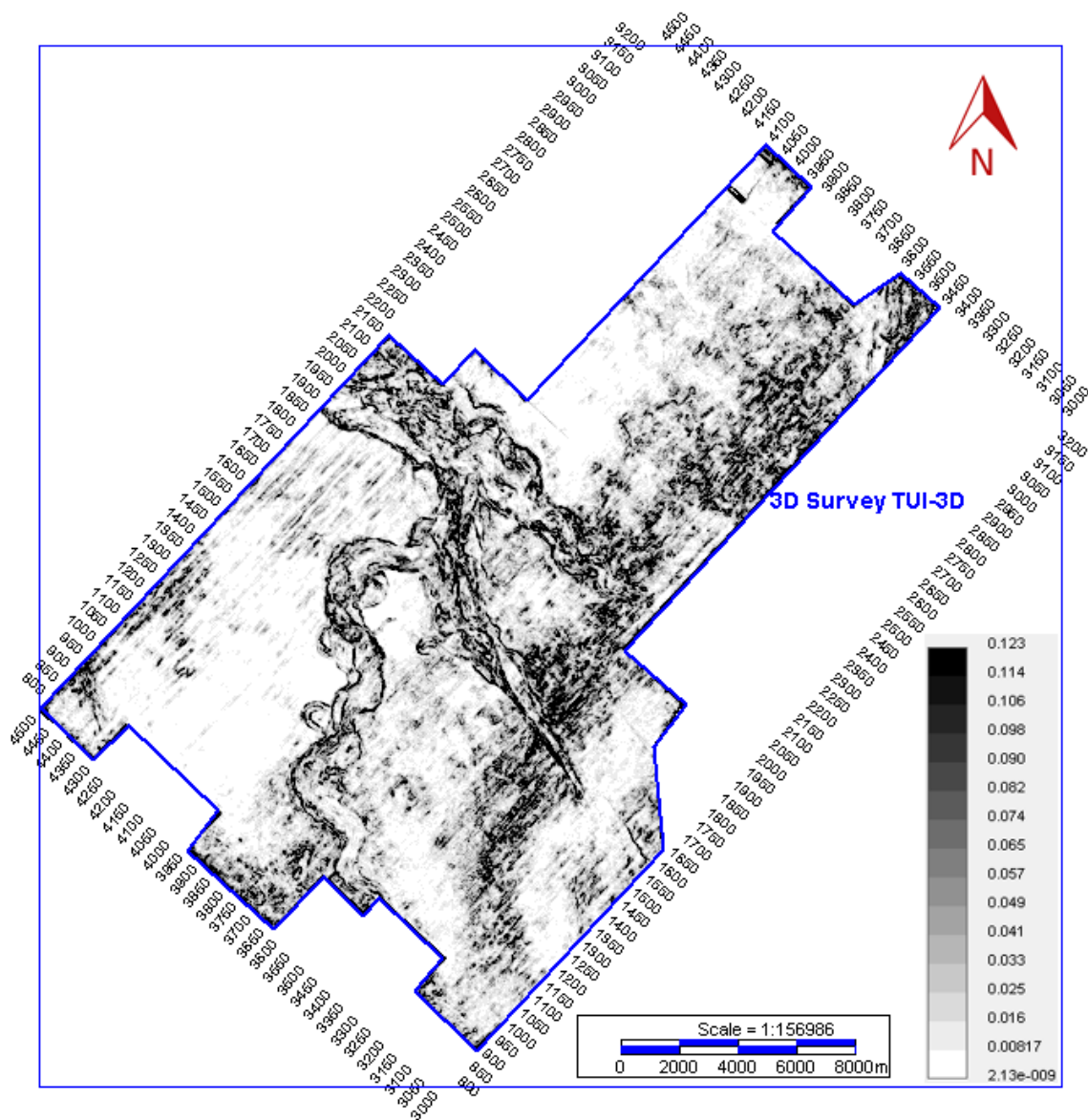


Figure 5.11. Chaos slice at 2.092 s showing channels in the Moki “A” Sand. NW-SE trending meandering channels are observable.

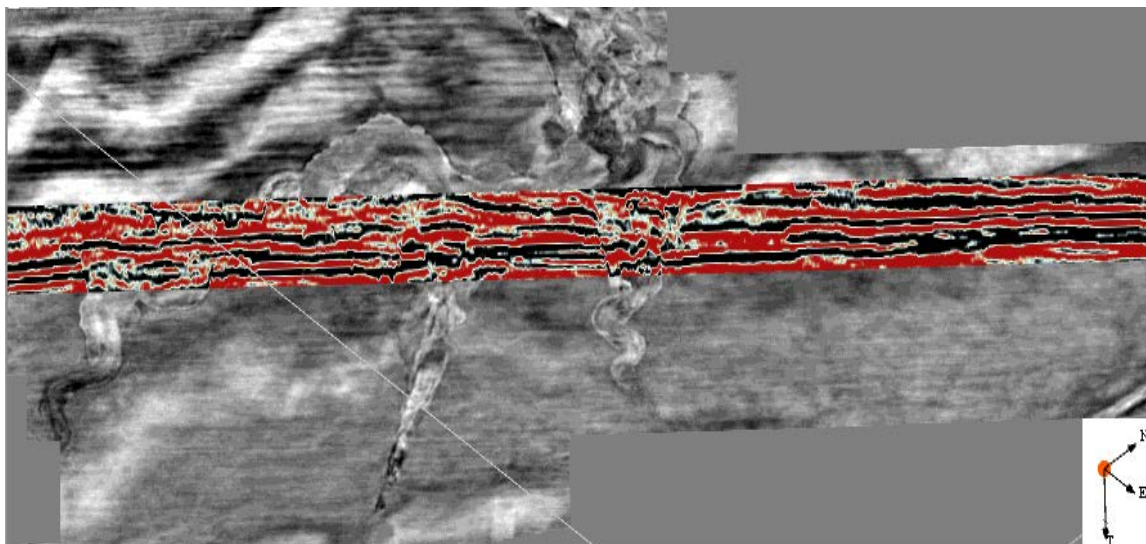


Figure 5.12. Inline 3827 and time slice at 2.092 s showing channels in the Moki “A” Sand.

5.2.4. A Canyon and Lineaments in Shallow Formation. A canyon (Figures 5.13 and 5.14) and lineaments (Figure 5.15) were revealed using time slices in the shallower (recent) part of the data. A canyon has high width/depth ratio and it is at southwest of the area, straight to low sinuous, NW-SE oriented, roughly 2 km wide, 260 m deep, and 10 km long. Time slices display lineament features, which were only found in Well Tui SW-2, and the only possible cause for that is loose coarse sand, which has a shoreface and a dip of c. 2° (Figure 5.16) (AWE, 2012). Two lineament features were displayed in Inline 3595 (Figure 5.15) and the time slice at 0.312 s (Figure 5.17).

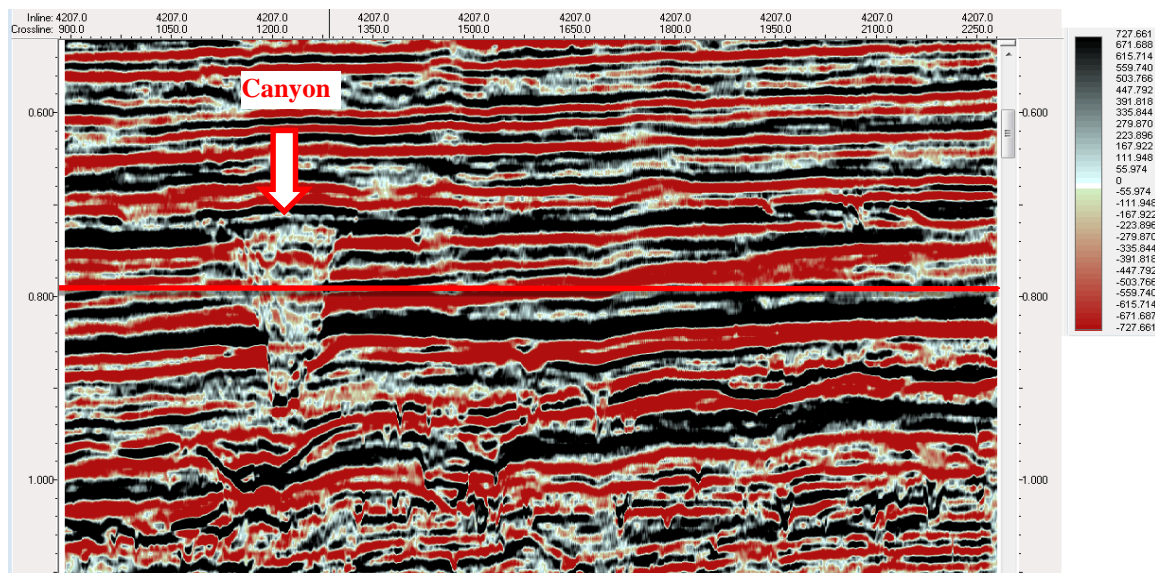


Figure 5.13. Vertical seismic section of Inline 4207 showing a canyon, which is roughly 2 km wide, 260 m deep, and 10 km long. The color bar shows the amplitude values (17.5 km long section).

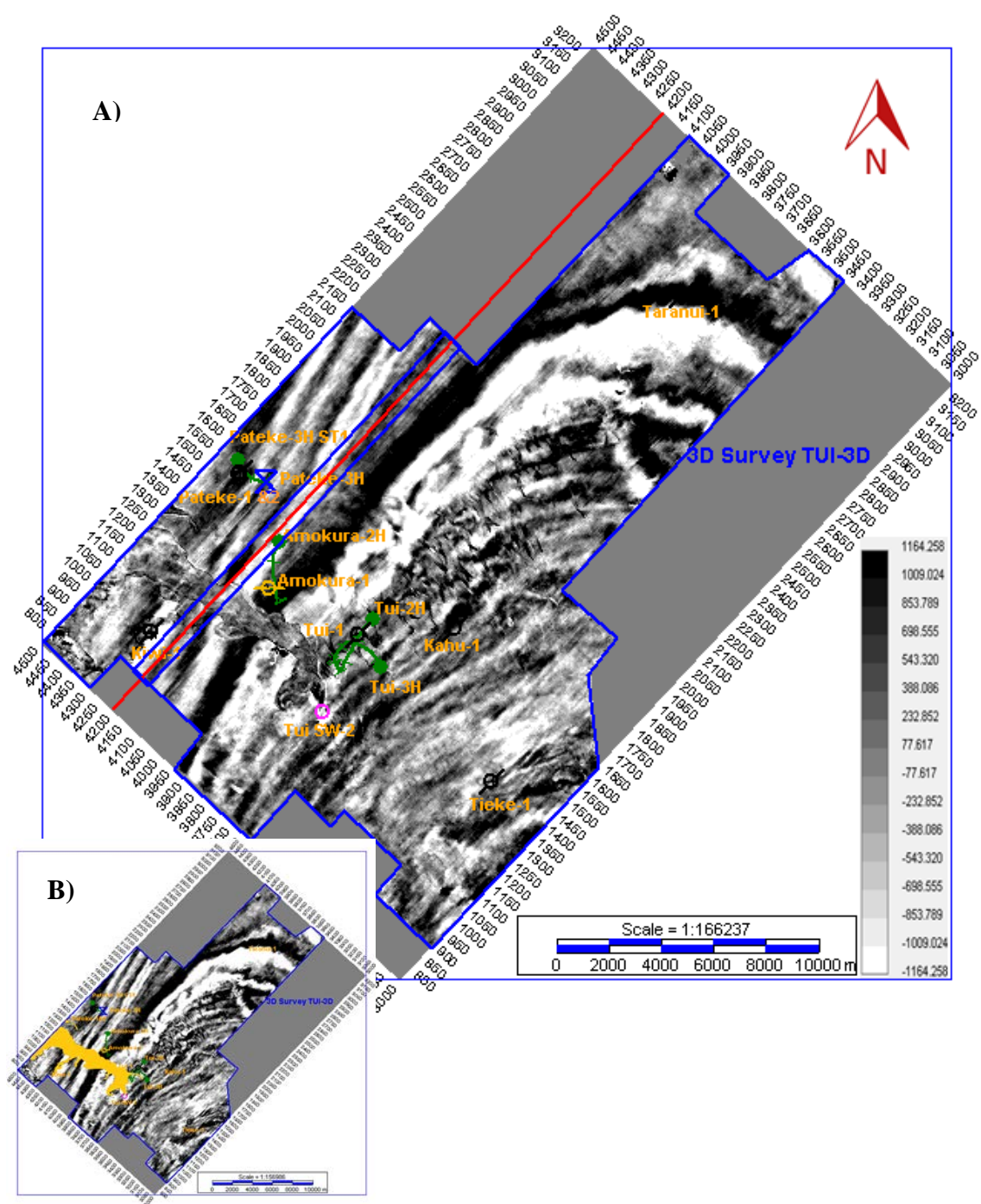


Figure 5.14. Time slice at 0.792 s showing the canyon. A) The canyon is observed at southwest of the area, straight to low sinuous, and NW-SE oriented. B) The canyon is highlighted in yellow.

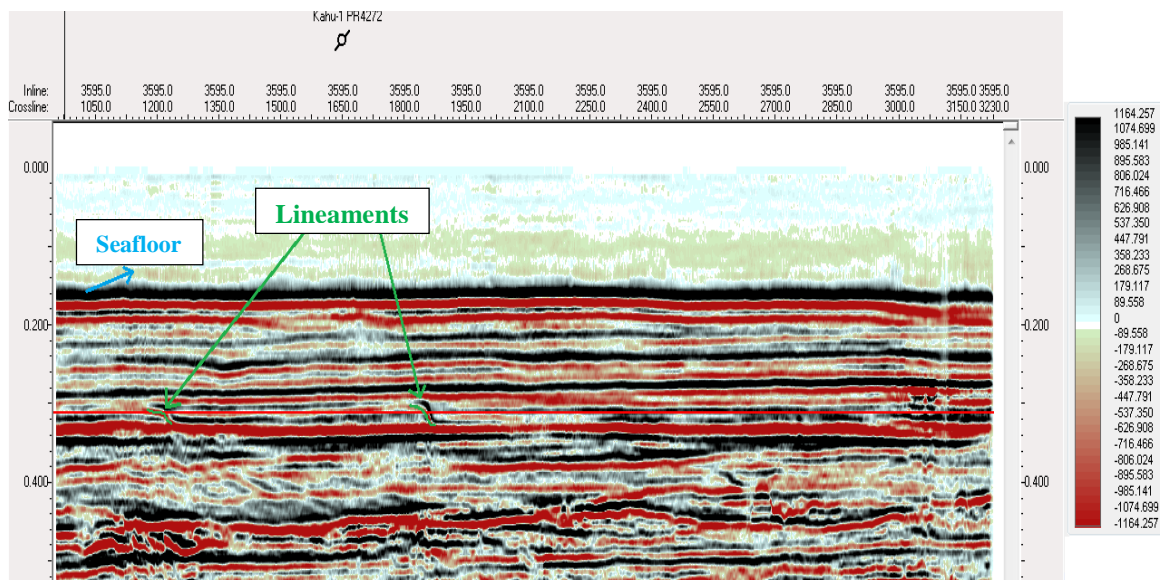


Figure 5.15. Vertical seismic section of Inline 3595 showing sea-floor and two lineament features. The color bar shows amplitude values (28.3 km long section).



Figure 5.16. Mobile and unconsolidated sand sample that was recovered from Well Tui SW-2. It may cause the lineament features shown in Figures 5.15 and 5.17 (AWE, 2012).

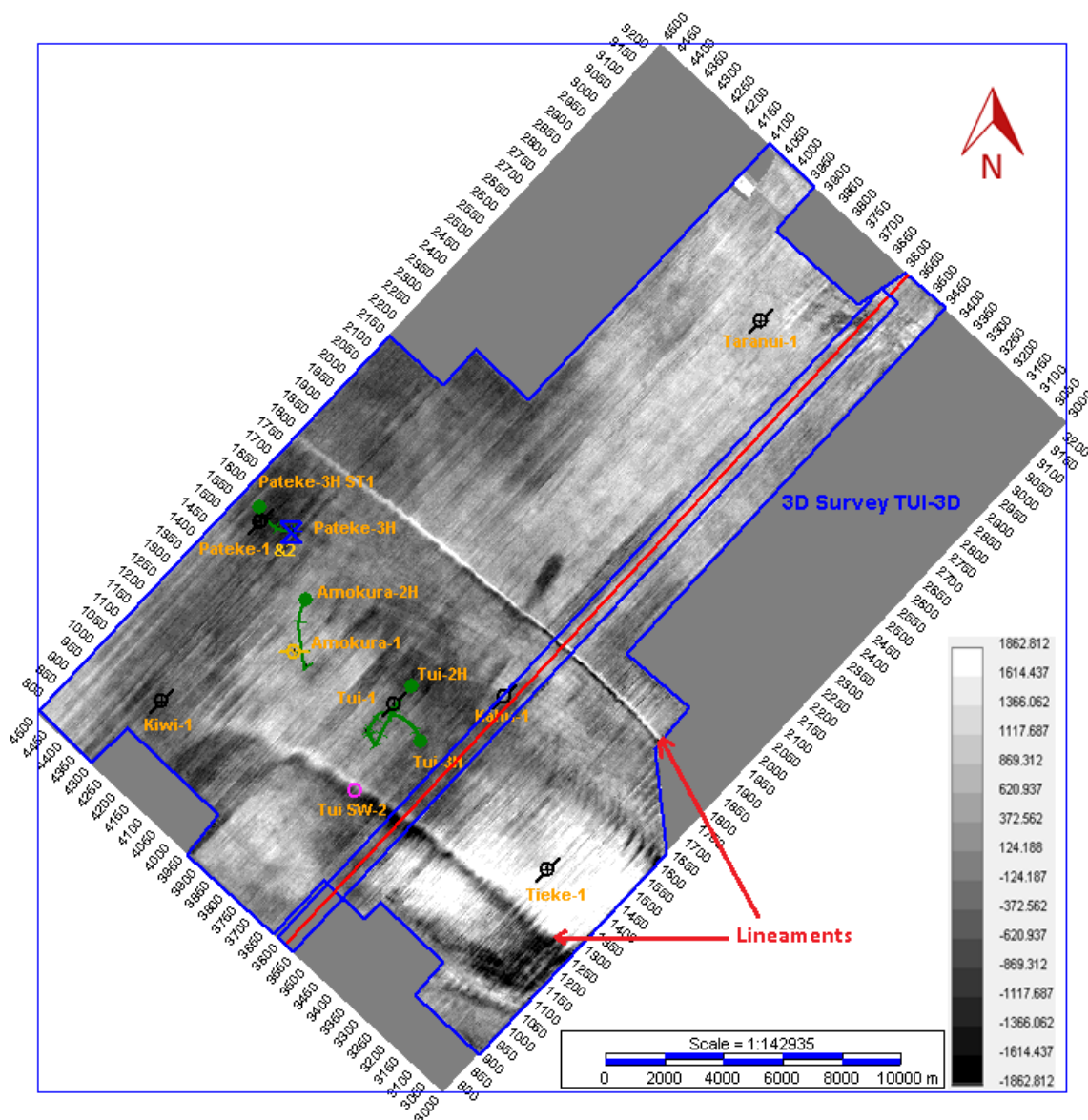


Figure 5.17. Time slice at 0.312 s showing the two lineaments indicated in Figure 5.15. The bar shows the amplitude values.

5.3. SEISMIC STRATIGRAPHY

Seismic stratigraphy is used to obtain stratigraphic information from seismic data. In this study, the main unconformity was identified using well data and formation tops. Five different seismic facies and channel reflection units were observed throughout the

data. The seismic reflection terminations and clinoform were identified. Finally, a well-logging correlation (Chapter 6), petrophysical analysis (Chapter 6), and depositional environment analysis were conducted.

Stratigraphic and depositional features such as lithofacies changes, geological time correlations, depositional and burial histories, and unconformities can be obtained from seismic stratigraphy.

Figure 5.18 shows Oligocene unconformity of about 10 million years between 2,980 and 2,990 m (Stroud et al., 2003). Base of the Tikorangi Formation (Basetik Horizon) represents this unconformity. Prograding patterns that show the slope surface are called clinoforms (Boggs, 2006). Figure 5.19 demonstrates clinoform surfaces identified in the Giant Foresets.

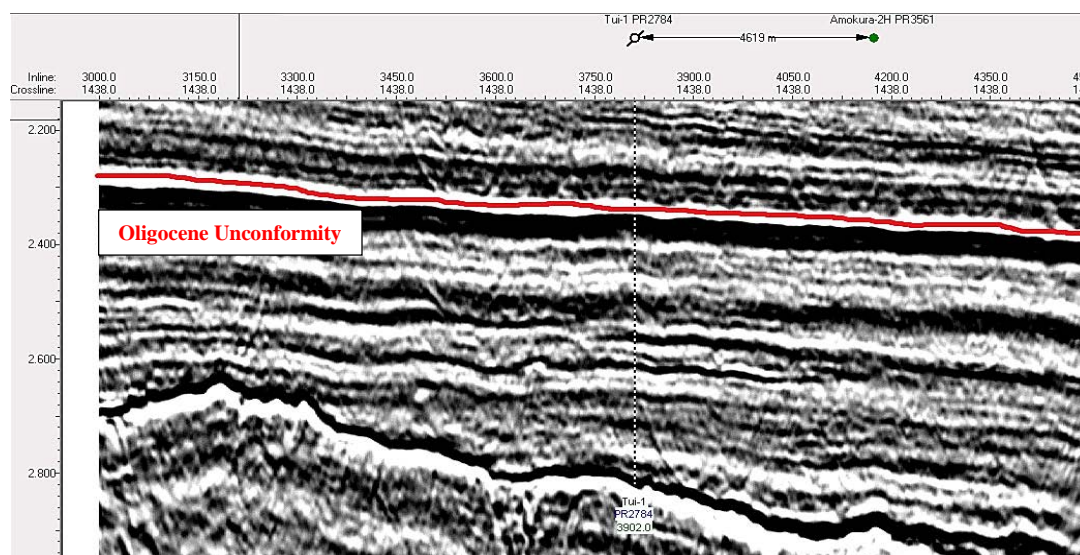


Figure 5.18. Crossline 1438 showing Oligocene unconformity of about 10 million years between 2,980 and 2,990 m (Stroud et al., 2003).

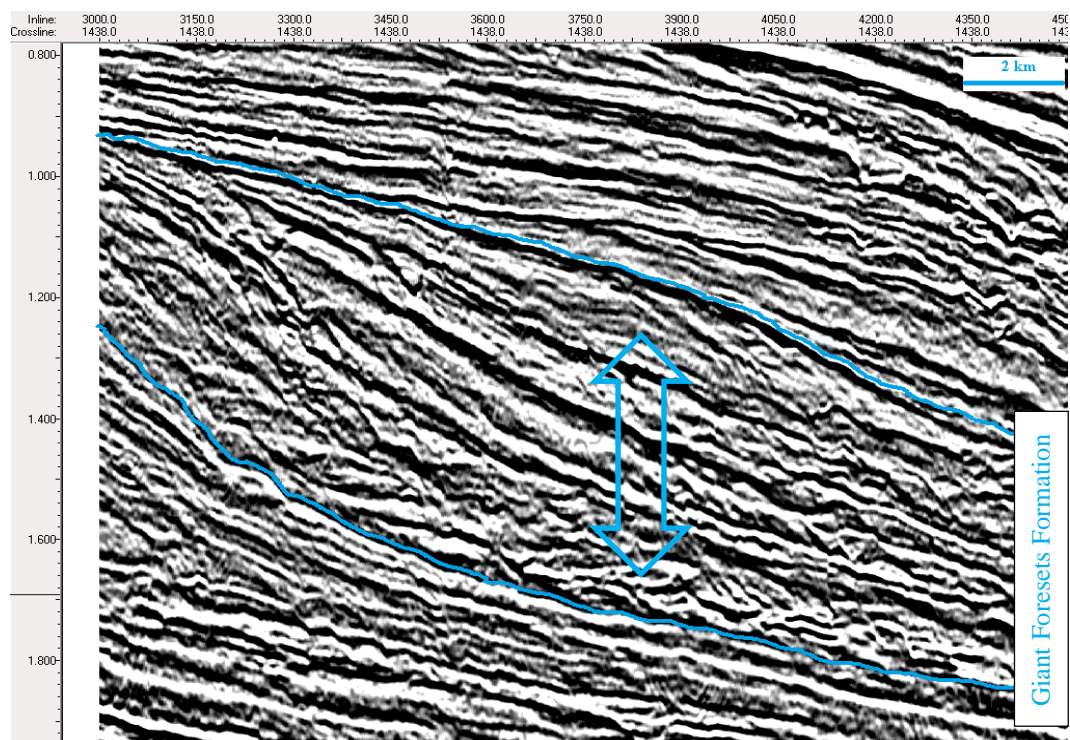


Figure 5.19. Clinoform surfaces showing prograding patterns in the Giant Foresets Formation (Crossline 1438).

The interpretation of reflection termination patterns may help to identify discontinuities over the discontinuity surfaces because discontinuities are usually great reflectors, and they generally set rock units apart from each other. Onlap and downlap are seen over discontinuities, and toplap, truncation, and apparent truncation happen under discontinuities (Vail, 1987). Figure 5.20 displays identified seismic reflection terminations in the study area. The onlap geometries were observed on the sequence 1, which is top of the basement, the toplap geometries were observed on the sequence boundary 2, which is top of the Giant Foresets Formation, and the onlap geometries were observed on the sequence 3, which is above the Giant Foresets Formation.

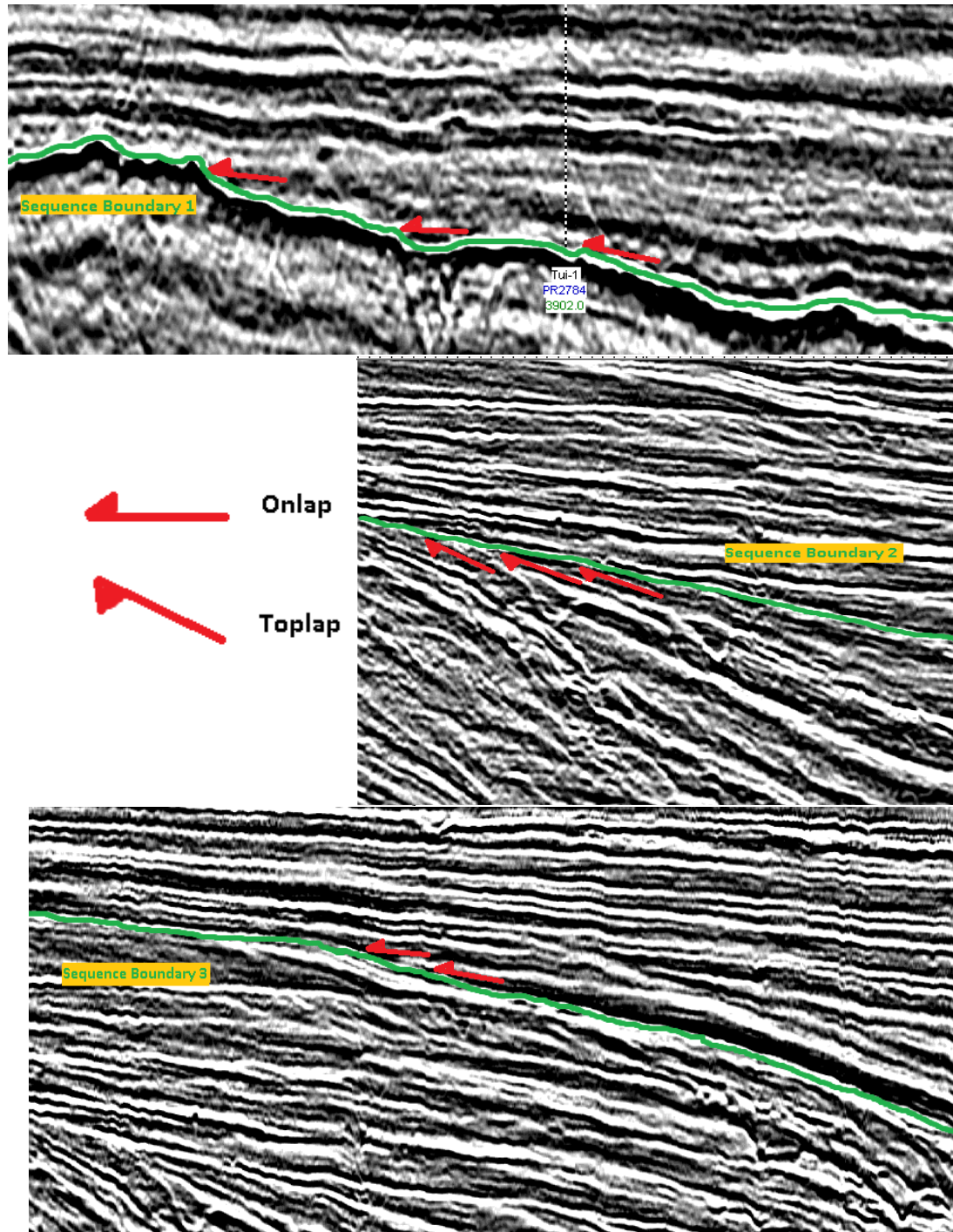
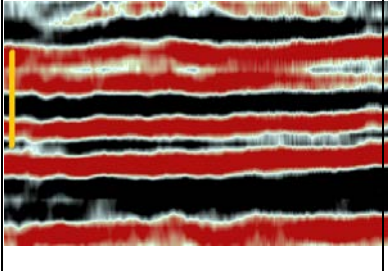
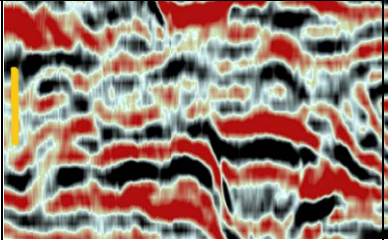
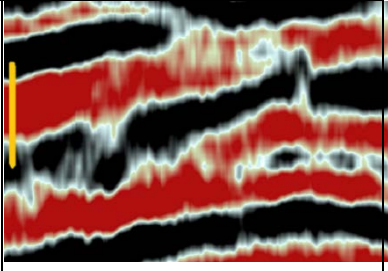
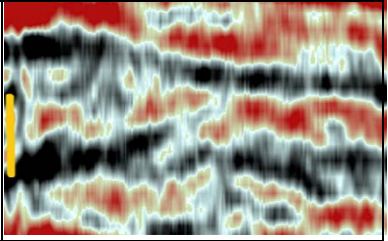
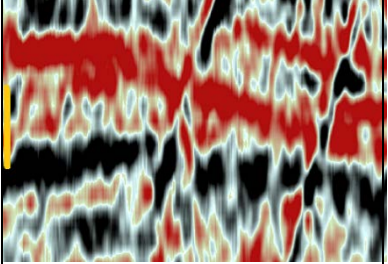


Figure 5.20. Seismic reflection termination patterns on seismic sections. Almost all Crosslines show these patterns in the study area.

Five different seismic facies were identified in study area (Table 5.1). These facies can be observed over the research area. SF1 seismic facies display a parallel, continuous high-amplitude reflection unit. This type of facies is observable mostly in the recent unit and the Miocene Moki Sandstone. SF2 seismic facies show a wavy-to-hummocky, discontinuous, and medium-to-low amplitude reflection unit. This type of facies can be observed mostly in the Plio-Pleistocene sequence. SF3 seismic facies display a subparallel continuous high-to-medium amplitude reflection unit. This type of facies is observed mainly in the Kapuni “E” Shale between two sandstones, which are the Kaimiro “D” Sand (Kapuni “D” Sand) and Farewell “F” Sand (Kapuni “F” Sand). SF4 seismic facies represent a subparallel, disrupted, and low-amplitude reflection unit. This type of facies can be observed mostly in the Paleocene Kapuni “D” and “F” sands, which were deposited in a shallow marine environment with uniform deposition rates. SF5 seismic facies display a chaotic, medium-to-low amplitude reflection unit. This type of facies is observable mainly in the granitic Late Cretaceous basement.

Inline 3806 indicates channels that have chaotic and medium-to-low amplitude reflection unit (Figure 5.21). Inline 4247 shows channels that have chaotic and low amplitude reflection unit (Figure 5.22). Figures 5.23 and 5.24 illustrate channels on time slices shown in Figures 5.21 and 5.22, respectively.

Table 5.1. The five different seismic facies identified in the study area.

Seismic Facies	Reflection Geometry	Amplitude Characteristics	Spatial Distribution	Example (Vertical yellow bars represent 40 ms)
SF1	Parallel continuous	High amplitude	Mostly seen at the recent unit and the Miocene Moki Sandstones	
SF2	Wavy to hummocky discontinuous	Medium to low amplitude	Occurs mainly at the Plio-Pleistocene sequence	
SF3	Subparallel continuous	High to medium amplitude	Mostly seen at the Kapuni "E" Shale between two sandstones	
SF4	Subparallel disrupted	Low amplitude	Present at the Paleocene Kapuni "D" and "F" Sandstones	
SF5	Chaotic	Medium to low amplitude	Occurs mainly in the Late Cretaceous basement	

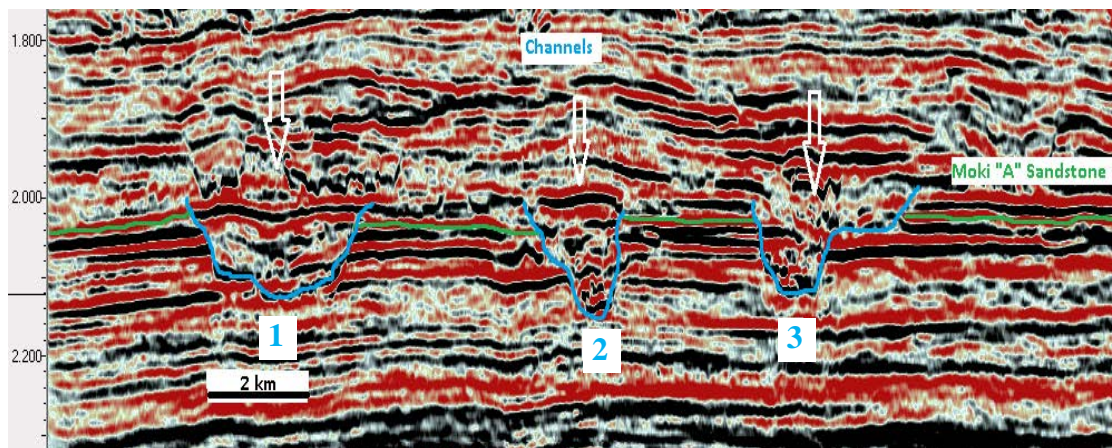


Figure 5.21. Inline 3806 illustrating incised channels in the Moki “A” Sand. Chaotic and medium-to-low amplitude reflection unit are observed for the channel’s infill.

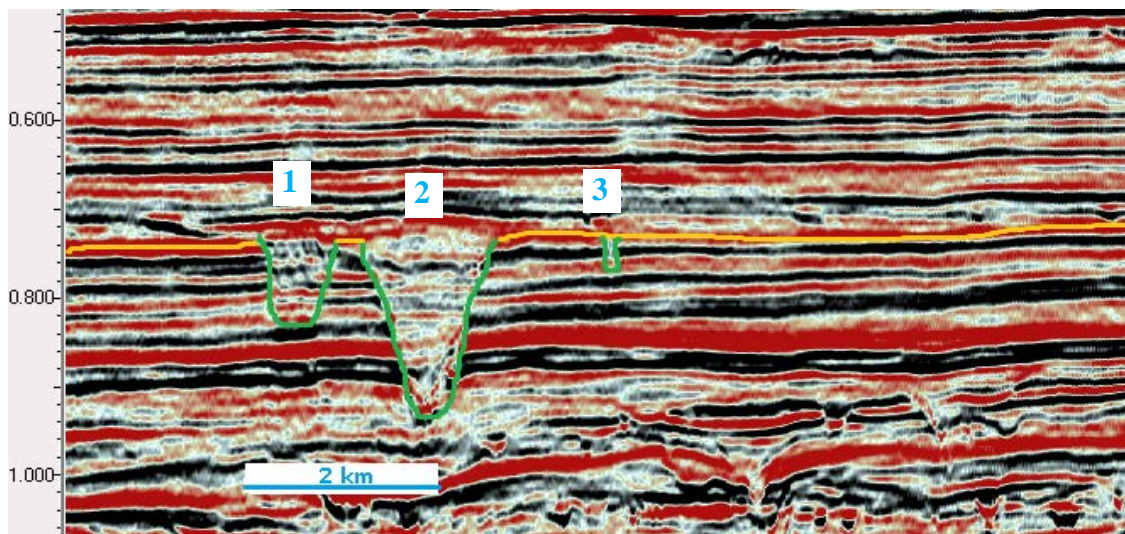


Figure 5.22. Inline 4247 showing incised channels. Chaotic and low-amplitude reflection unit are observed for the channel’s infill.

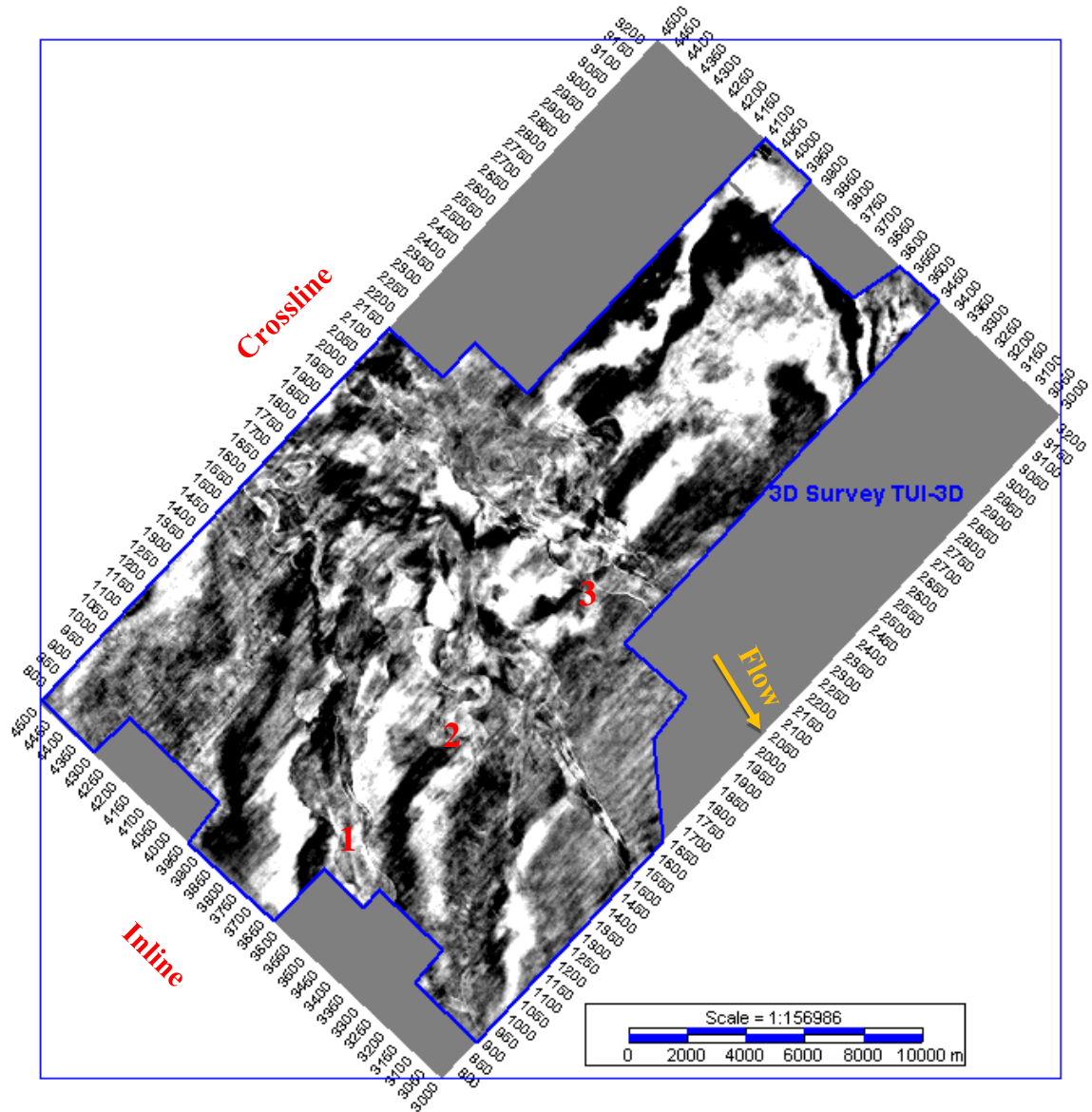


Figure 5.23. Time slice at 2.044 s showing three incised channels as indicated in Figure 5.21.

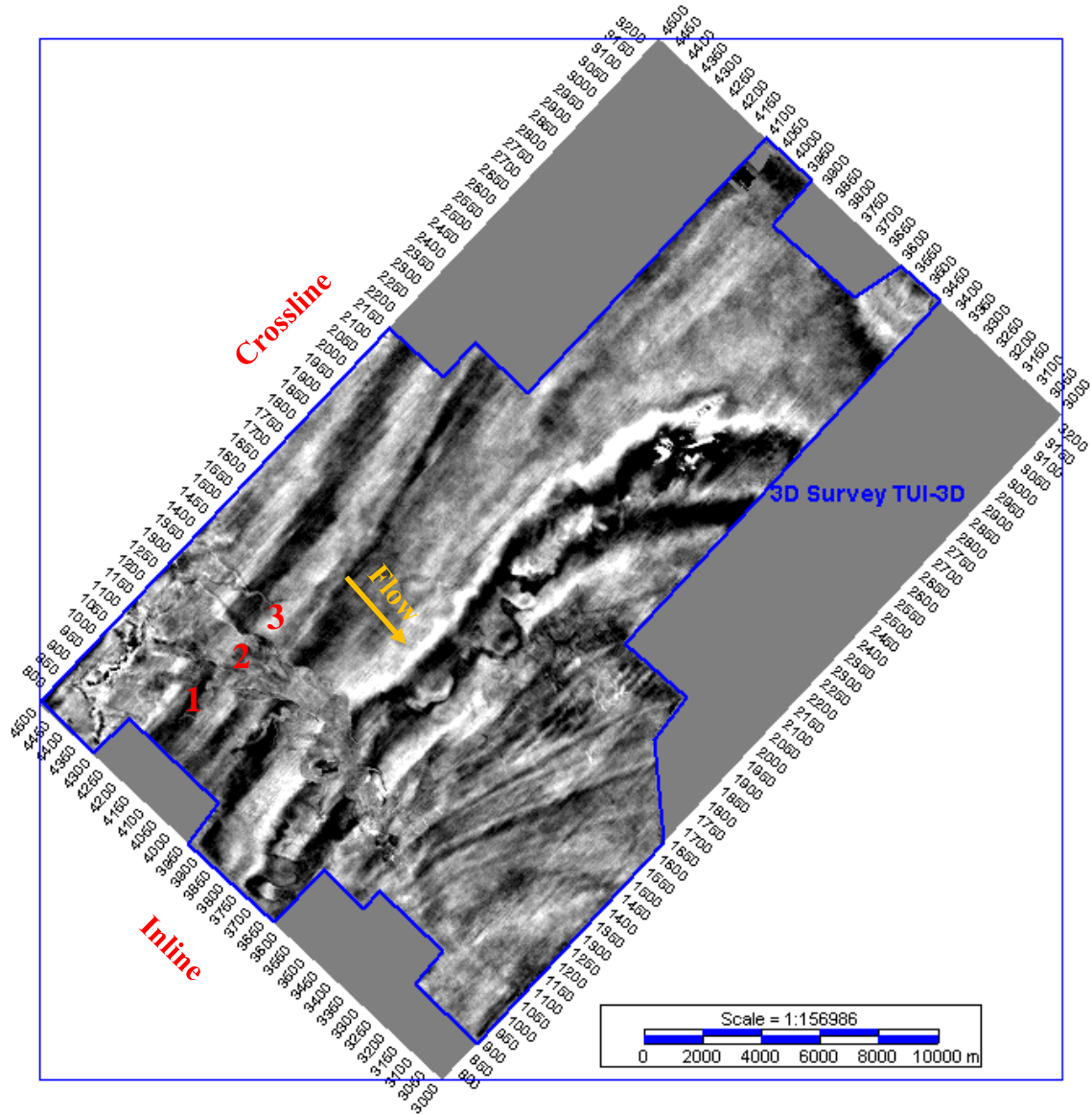


Figure 5.24. Time slice at 0.752 s illustrating incised channels as indicated in Figure 5.22.

6. WELL LOGGING CORRELATION AND PETROPHYSICAL ANALYSES

6.1. WELL-TO-WELL LOG CORRELATION

A well logging correlation helps to provide an understanding of the subsurface structure of the target formations in the study area. In this research, four wells, which are Kiwi-1, Amokura-1, Tui-1, and Taranui-1, were used to provide a correlation along 26,525 meters of the study area (Figure 6.1). Gamma ray (GR) and deep resistivity (RESD) logs were used to show the lithology, and formation tops were used to show the distribution of the target formations, which are Kaimiro “D” Sand, Farewell “E” Shale, Farewell “F” Sand, and North Cape. Additionally, lithology estimation was conducted by generating crossplots (Chapter 6.3). The correlation of four wells, the lithology of each formation and the location of the cross-section along the study area are shown in Figure 6.1. It was revealed that the North Cape Formation disappears, the Farewell “F” Sand becomes thinner, the Farewell “E” Shale becomes thicker, and the Kaimiro “D” Sand becomes thinner from SW to NE.

6.2. PETROPHYSICAL ANALYSES

A petrophysical analysis helps to provide an understanding of the reservoir characterization and its depositional environment. First, crossplots were generated so the lithology of each formation could be assessed. Then, the petrophysics module was used to generate curves such as effective porosity, permeability, volume of shale, and water saturation. Finally, zone attributes were calculated using these curves and are shown for the Kaimiro “D” Sand, Farewell “E” Shale, Farewell “F” Sand, and the Kapuni Group in Tables 6.1, 6.2, 6.3, and 6.4, respectively.

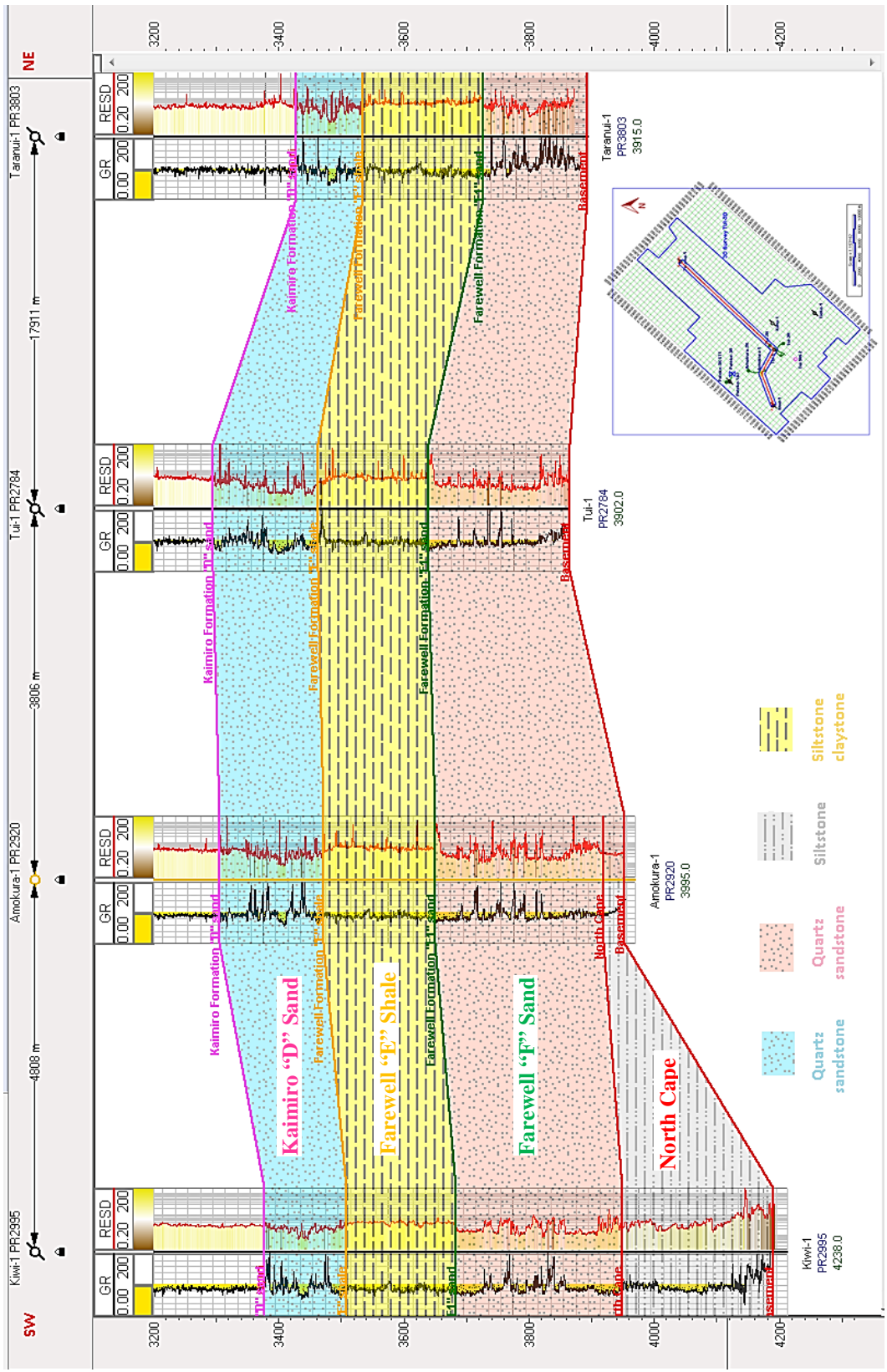


Figure 6.1. Well-to-well correlation showing the lithology and distribution of each target formation trough four wells.

After calculating reservoir properties for the Kapuni Group, the results indicate generally high porosity and permeability. In addition, Figures 6.2 and 6.3 show that there is high effective porosity and unmoved hydrocarbons for the Kapuni Group.

Table 6.1. Calculated petrophysical properties for the Kaimiro “D” Sand in the study area.

Well name	Gross (m)	Hpv (m)	Kh	Km (md)	Net (m)	Ngr	Pha	Phih	Swa
Amokura-1	166.00	30.39	110773	321.47	149.00	0.90	0.25	37.58	0.18
Kiwi-1	130.00	20.69	28076	56.68	116.80	0.90	0.21	24.44	0.15
Pateke-2	42.00	5.98	5611	30.06	37.60	0.90	0.19	7.23	0.16
Taranui-1	107.60	10.68	1956	0.56	92.60	0.86	0.13	11.89	0.09
Tui SW-2	178.40	20.76	5819	3.42	157.20	0.88	0.15	23.91	0.12
Tui-1	167.54	23.01	19207	15.52	148.80	0.89	0.18	27.18	0.14

6.2.1. Net/Gross Ratio (NGR). In the Net to Gross ratio, Gross indicates the thickness between two surfaces, which are top and bottom, and Net is the value (meters) that shows the thickness for the satisfied conditions of the producing zone (IHS, 2014). The Gross, Net, and Net-to-Gross ratio values for the Kaimiro “D” Sand, Farewell “E” Shale, Farewell “F” Sand, and Kapuni Group are shown in Tables 6.1, 6.2, 6.3, and 6.4, respectively.

Table 6.2. Calculated petrophysical properties for the Farewell “E” Shale in the study area.

Well name	Gross (m)	Hpv (m)	Kh	Km (md)	Net (m)	Ngr	Pha	Phih	Swa
Amokura-1	177.00	22.03	7352	10.07	155.60	0.88	0.17	26.35	0.15
Kiwi-1	176.00	19.22	2425	2.51	154.80	0.88	0.14	22.40	0.13
Pateke-2	214.00	23.71	3239	2.82	189.60	0.89	0.15	27.60	0.13
Taranui-1	191.40	15.01	381	0.10	166.00	0.87	0.10	16.58	0.08
Tui SW-2	166.90	15.00	7772	0.36	146.20	0.88	0.12	17.01	0.10
Tui-1	176.75	20.45	3535	4.42	158.60	0.90	0.15	23.86	0.13

Table 6.3. Calculated petrophysical properties for the Farewell “F” Sand in the study area.

Well name	Gross (m)	Hpv (m)	Kh	Km (md)	Net (m)	Ngr	Pha	Phih	Swa
Amokura-1	319	48.93	47143	54.47	284.00	0.89	0.21	58.61	0.16
Kahu-1	167	8.79	130.22	0.09	95.80	0.57	0.10	9.51	0.07
Kiwi-1	521	67.19	606704	10.50	459.20	0.88	0.17	78.33	0.13
Taranui-1	181.5	16.90	1788	2.06	129.60	0.71	0.15	19.03	0.10
Tui-1	240.25	33.08	12157	20.55	210.20	0.87	0.19	39.32	0.15

Table 6.4. Calculated petrophysical properties for the Kapuni Group in the study area.

Well name	Gross (m)	Hpv (m)	Kh	Km (md)	Net (m)	Ngr	Pha	Phih	Swa
Amokura-1	647.00	107.29	183088	88.36	580.80	0.90	0.22	126.66	0.15
Kahu-1	494.00	8.79	130.22	0.09	95.80	0.19	0.10	9.51	0.07
Kiwi-1	812.00	112.22	561901	17.30	723.60	0.89	0.18	130.29	0.13
Taranui-1	465.50	56.56	15049	7.26	392.40	0.84	0.16	63.29	0.10
Tui-1	569.54	80.35	49844	18.45	512.80	0.90	0.18	93.09	0.13

6.2.2. Porosity (ϕ). Porosity is a significant parameter because it measures the possible depository space for hydrocarbons. Effective porosity is a measure of the connected pore space. The porosity can be calculated using the following equation (Asquith & Gibson, 1982):

$$\phi_D = \frac{\rho_{matrix} - \rho_b}{\rho_{matrix} - \rho_{fluid}} \quad (4)$$

where ρ_{matrix} is the bulk density of the matrix, ρ_b is the formation's measured bulk density, ρ_{fluid} is fluid density, and ϕ_D is density porosity (fractional).

Effective porosity is calculated by using the following equation (Ajisafe, 2015):

$$\phi_{De} = \phi_D - V_{sh} \times \phi_{D_{sh}} \quad (5)$$

where ϕ_D is density porosity, ϕ_{Dsh} is density porosity in shale, V_{sh} is shale volume, and ϕ_{De} is effective density porosity.

In this research, the average porosity (Pha) and porosity meters (Phih), which is defined as average porosity times the Net, for the Kaimiro “D” Sand, Farewell “E” Shale, Farewell “F” Sand, and Kapuni group are shown in Tables 6.1, 6.2, 6.3, and 6.4, respectively. The effective porosity (PHIE) for Wells Amokura-1 and Taranui-1 is shown in Figures 6.2, and 6.3, respectively.

6.2.3. Water Saturation (Sw). Water saturation is the quantity of a rock’s pore space that is filled with water. It was calculated using the dual water method and the following equation (Best et al., 1978):

$$S_w = \left(\frac{R_w \times \frac{R_w}{\Phi_x^m \times (S_b \times R_w + (1-S_b) \times R_{w_h})}}{R_t} \right)^{\frac{1}{n}} \quad (6)$$

where a is the tortuosity exponent, m is the cementation exponent, n = saturation exponent, Φ is porosity, R_t is resistivity of the zone, S_b is bound-water saturation, R_w is water resistivity at formation temperature, and S_w is water saturation.

The dual water method separates the quantity of water into two parts. The first part is connected to the shale, and the second part is free in the pore volume. This method treats the two parts separately in terms of salinity of the water. It is usually good for shaly sands (Best et al., 1978).

The average saturation (S_{wa}) values for the Kaimiro “D” Sand, Farewell “E” Shale, Farewell “F” Sand, and Kapuni Group are shown in Tables 6.1, 6.2, 6.3, and 6.4, respectively.

6.2.4. Permeability (k). Permeability is defined as the ability of a liquid to transfer in a rock. In this research, the Wyllie-Rose (1950) permeability formula and the Morris-Biggs (1967) parameters for porosity, irreducible saturation exponents, and permeability constant were used by the petrophysics module of Kingdom Suite 2015. The following formula was used for permeability:

$$k = \frac{62500 \times \Phi_e^6}{S_{wi}^2} \quad (7)$$

where ϕ_e is effective porosity, S_{wi} is irreducible water saturation, and k is permeability (millidarcies).

Permeability meters (Kh), which is defined as the average permeability times the Net meters, and mean permeability (Km) for the Kaimiro “D” Sand, Farewell “E” Shale, Farewell “F” Sand, and Kapuni Group are shown in Tables 6.1, 6.2, 6.3, and 6.4, respectively.

6.2.5. Hydrocarbon Meters (HPV). Hydrocarbon meters is the porosity of the meters times the hydrocarbon saturation (IHS, 2014). It was calculated using the zone attribute module in Kingdom Suite 2015. The hydrocarbon meters values for the Kaimiro “D” Sand, Farewell “E” Shale, Farewell “F” Sand, and Kapuni Group are shown in Tables 6.1, 6.2, 6.3, and 6.4, respectively.

6.2.6. Volume of Shale (Vsh). Shale volume is a significant parameter in petrophysics, and it can be calculated using gamma ray logs because shale generally has higher gamma ray values than carbonate and sand. The first equation used for shale volume calculation is linear (Asquith & Kryqowski, 2004):

$$GRI = \frac{(Gr_{log} - Gr_{clean})}{(Gr_{shale} - Gr_{clean})} \quad (8)$$

$$Vsh = GRI \quad (9)$$

where Gr_{log} is the measured gamma ray values (API units), Gr_{clean} is the gamma ray value in a clean formation (API units), Gr_{shale} is the gamma ray value in 100% shale (API units), and Vsh is the formation's shale content (fractional). However, the relationship between GR and Vsh is not linear, so Steiber's (1970) formula was used in this research by Kingdom 2015:

$$Vsh = \frac{0.5 \times GRI}{1.5 - GRI} \quad (10)$$

The Shale volume (Vsh) for Wells Amokura-1 and Taranui-1 is shown in Figures 6.2, and 6.3, respectively.

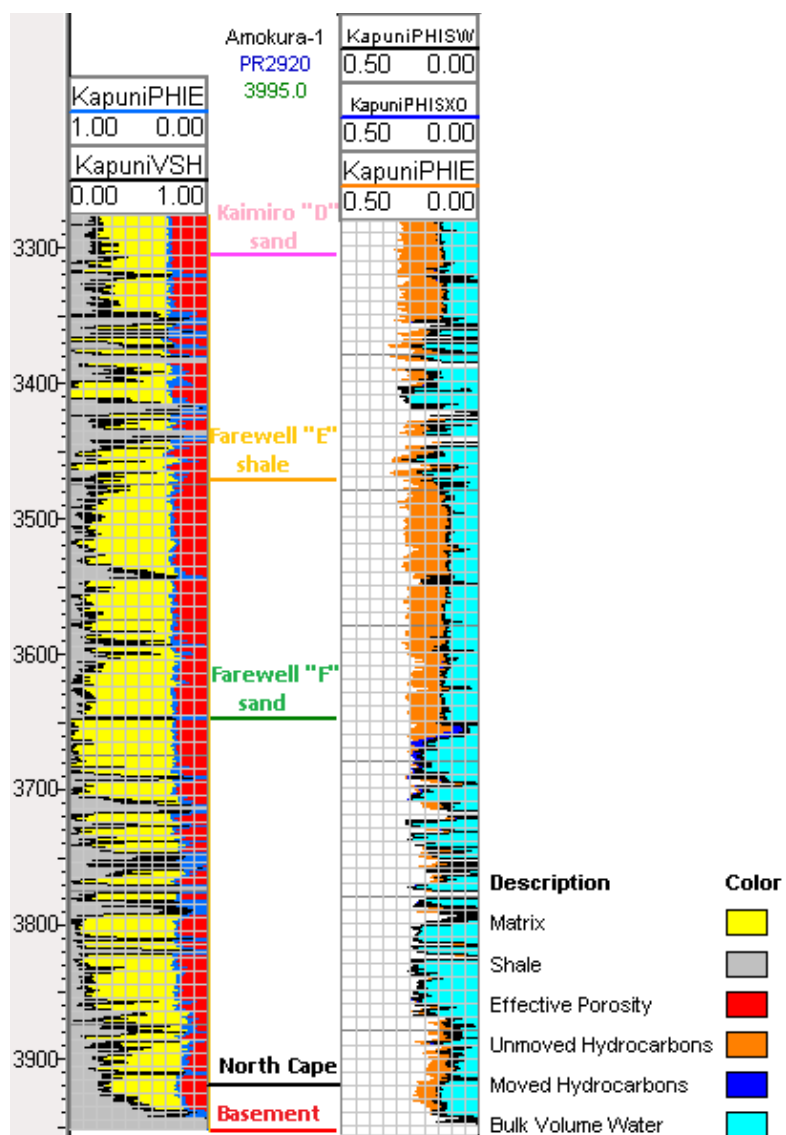


Figure 6.2. Volume of shale (VSH), effective porosity (PHIE), bulk volume water (PHISW), and bulk volume moved water (PHISXO) logs generated from petrophysical analysis for Well Amokura-1. They show good PHIE and unmoved hydrocarbons for the Kapuni Group, which consists of Kaimiro "D" Sand, Farewell "E" Shale, and Farewell "F" Sand. Additionally, the Farewell "F" Sand displays moved hydrocarbons.

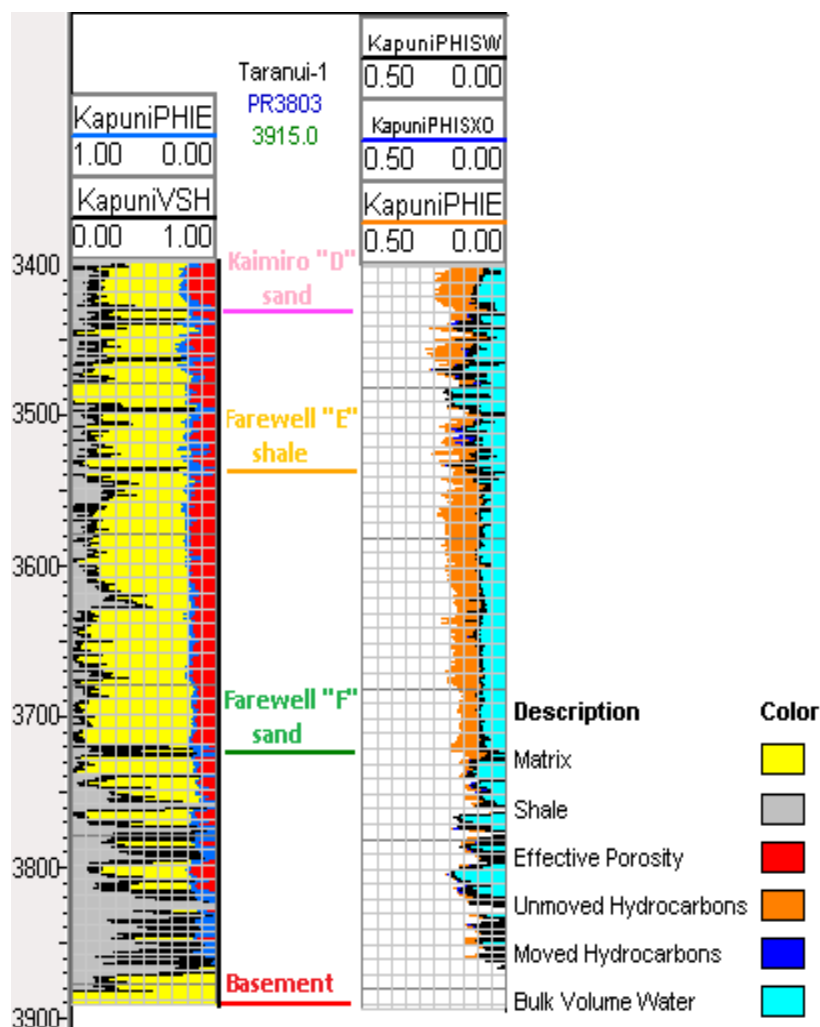


Figure 6.3. Volume of shale (VSH), effective porosity (PHIE), bulk volume water (PHISW), and bulk volume moved water (PHISXO) logs generated from petrophysical analysis for Well Taranui-1. They show good PHIE and unmoved hydrocarbons for the Kapuni Group, which consists of Kaimiro “D” Sand, Farewell “E” Shale, and Farewell “F” Sand.

6.3. CROSSPLOTS

Crossplots are very important in terms of determining the lithology. Density-neutron crossplot was generated using Kingdom Suite 2015. The density and neutron plot with the gamma ray log is good for identifying the lithology and porosity because the

neutron and density logs measure the quantities of hydrogen and electron density in a zone, respectively (Asquith & Krygowski, 2004). A high gamma ray also separates shale from other materials that have low radioactivity, so these three logs can be used for lithology. Density-neutron crossplots for the Kaimiro “D” Sand, Farewell “E” Shale, and Farewell “F” Sand are shown in Figures 6.4 to 6.6.

After analyzing the density-neutron crossplots, main lithology for the Kaimiro “D” Sand, Farewell “E” Shale, and Farewell “F” Sand were determined. Therefore, lithology for the Kaimiro “D” Sand is observed as sandstone, limestone, and siltstone, lithology for the Farewell “E” Shale is identified as mostly siltstone, and lithology for the Farewell “F” Sand is determined as sandstone, siltstone, and limestone.

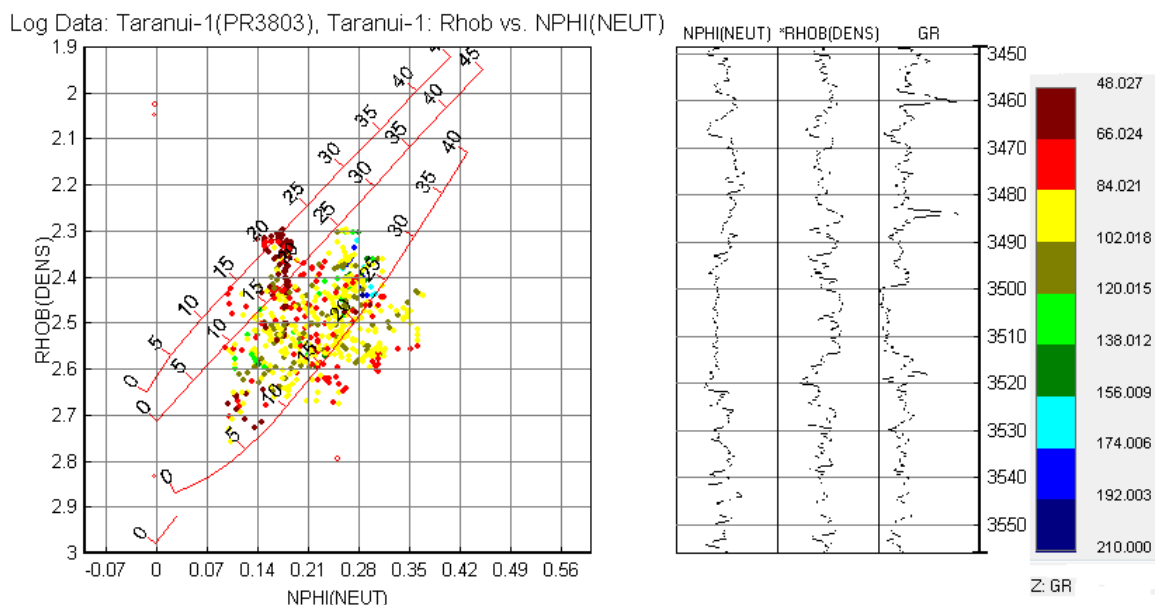


Figure 6.4. Density-neutron crossplot showing lithology of the Kaimiro “D” Sand in Well Taranui-1. The Kaimiro “D” Sand consists of sandstone, limestone, and siltstone. The color bar shows the gamma ray values.

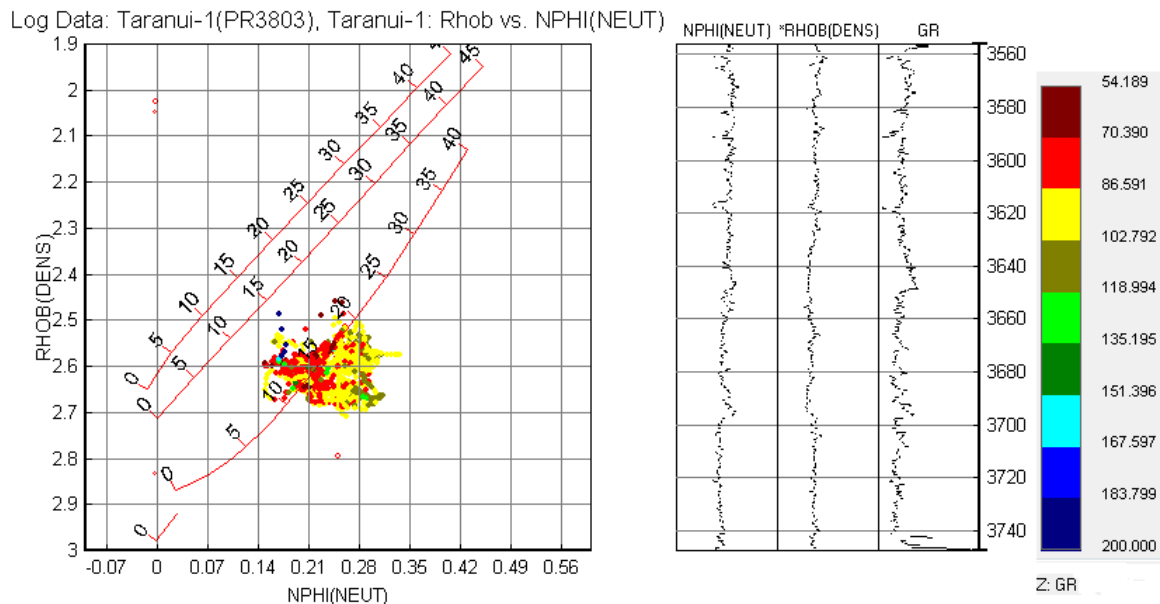


Figure 6.5. Density-neutron crossplot showing lithology of the Farewell “E” Shale in Well Taranui-1. The Farewell “E” Shale mostly consists of siltstone. The color bar shows the gamma ray values.

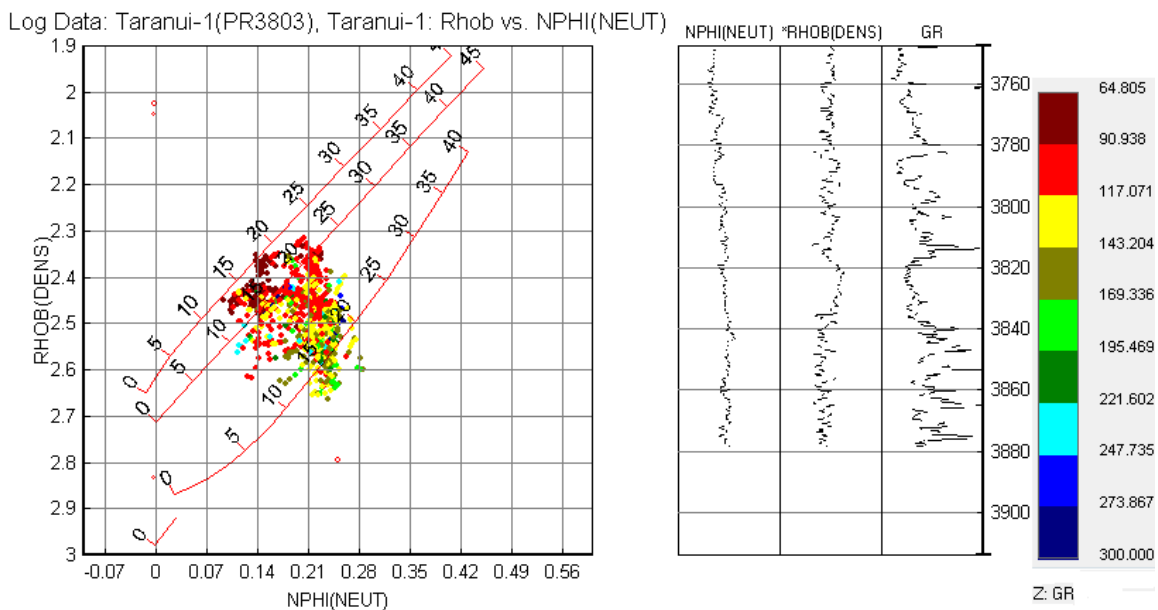


Figure 6.6. Density-neutron crossplot showing lithology of the Farewell “F” Sand in Well Taranui-1. The Farewell “F” Sand consists of sandstone, siltstone, and limestone. The color bar shows the gamma ray values.

7. CONCLUSIONS

The seismic data, well log, and well data gathered from the Tui-3D Field were examined in this research. Seismic structural and stratigraphic interpretations were conducted to understand the evolution of the target horizons. In addition, petrophysical analyses were applied to evaluate reservoir properties.

7.1. STRUCTURAL INTERPRETATION

Interpreted thirty-two minor faults in the Kapuni Group Horizons, which picked around Pateke, Amokura, and Tui oil reservoirs, might play a significant role in oil migration from the Farewell “F” Sand (reservoir) to the Kaimiro “D” Sand (possible reservoir), so picking faults for structural interpretation was a key part of the research.

In the study area, there is a proven reservoir, which is the Farewell “F” Sand. In order to find structural traps for hydrocarbon accumulations, valuable depth maps for the Farewell “F” Sand, and potential reservoir horizon, which is the Kaimiro “D” Sand, were generated. They revealed several anticlines and possible traps. In addition, the dipping of the target horizons were displayed resulting in a dipping toward the north.

7.2. STRATIGRAPHIC INTERPRETATION

Five different seismic facies, seismic reflection geometries for channels in the Moki “A” Sand Formation, and seismic reflection termination patterns were identified in the study area. Seismic stratigraphic interpretation helped to identify features such as channels, gullies, and lineaments.

Gullies were identified in the Giant Foresets Formation. Gullies are oriented toward the northwest-southeast, straight to low sinuous, up to 12 km, roughly 10 to 70 m deep, from 20 m to 500 m wide, U-shaped, and approximately parallel to each other.

The Kahu channel in the Farewell “F” Sand Formation were revealed. The Farewell “F” Sand Horizon onlaps to the basement and the Kahu channel might act as a trap where the Farewell “F” Sand and the Kahu channel coincide.

The time slices and vertical seismic sections suggested that channels, which are NW-SE oriented and high to moderate sinuous, were mostly deposited at different times in different areas within the Moki “A” Sandstone Formation.

Lineament features due to the presence of loose, coarse sand that formed in the shoreface and a canyon, which is straight to low sinuous, NW-SE oriented, roughly 2 km wide, 260 m deep, and 10 km long, were discovered in the shallower part of the area. Attributes such as chaos, local flatness, and sweetness were constructed, and they helped to better display these stratigraphic features either as time slices or horizon slices.

7.3. PETROPHYSICAL ANALYSES

Petrophysical analyses were applied to calculate the reservoir properties indicating high permeability, effective porosity, and unmoved hydrocarbons for the Kapuni Group Formations. Density-neutron crossplots showed the lithology for each formation. As a result, the Kaimiro “D” Sand mostly consists of sandstone, limestone, and siltstone, the Farewell “E” Shale mostly consists of siltstone, and the Farewell “F” Sand mostly consists of sandstone, siltstone, and limestone. In addition, a well-to-well

correlation indicated the disappearance of the North Cape Horizon (source rock). A seismic section showed that the horizon onlaps to the basement.

7.4. RECOMMENDATIONS

In the north of the study area, there is only one well drilled, which is Taranui-1. In order to better understand structure and stratigraphy of the north area, there should be more drilling in the future. By drilling more wells, the Kahu channel, which is a potential stratigraphic trap, can be observed if it continues over the area. The anticline indicated by the time structure map of the Farewell “F” Sand Horizon in the north of the study area (Figure 4.12) should be drilled for further investigation.

BIBLIOGRAPHY

- Ajisafe, Y.C. (2015), Petrophysical evaluation of reservoirs in 'y' prospect Niger delta, Ekiti state University, Faculty of Science, Department of Geology, Ado Ekiti, Nigeria, v. 62, p. 55-63.
- Asquith, G.B., and C.R. Charles (1982), Basic well log analysis for geologists, doi: 10.1306/Mth3425.
- Asquith, G., and D. Krygowski (2004), Basic well log analysis, second edition, *American Association of Petroleum Geologist and Society of Exploration Geophysics*, Methods in Exploration, p. 244.
- AWE (Australian Worldwide Exploration), Ltd. (2009), Australian Worldwide Exploration Presentation to PESA, *Petroleum Exploration Society of Australia*, p. 33.
- AWE, NZ. Pty. Ltd. (2010), Kahu-1 well completion report, Ministry of Economic Development New Zealand, Unpublished Petroleum Report, PR4272.
- AWE, NZ. Pty. Ltd. (2012), Tui SW-2 well completion report, Ministry of Economic Development New Zealand, Unpublished Petroleum Report, PR4271.
- Best, D.L., J.S. Gardner, and J.L. Dumanoir (1978), A computer processed wellsite log computation, Schlumberger Well Services, Houston, Texas. *SPWLA Nineteenth Annual Logging Symposium*.
- Boggs, S. (2006), Principles of sedimentology and stratigraphy (fourth edition), Pearson, Prentice Hall, Upper Saddle River, New Jersey.
- Bradshaw, J.D. (1989), Cretaceous geotectonic patterns in the New Zealand region, *Tectonics*, 8 (4), p. 803-820.

- Browne, G.H., and B.D. Field (1988), A review of Cretaceous – Cenozoic sedimentation and tectonics, East Coast, South Island, New Zealand, In James, D.P., & Leckie, D.A. (Editors), *Sequences, Stratigraphy, Sedimentology: Surface and Subsurface. Canadian Society of Petroleum Geologists, Memoir*, p. 15, 37-48.
- Bussell, M.R. (1994), Seismic interpretation of the Moki Formation on the Maui 3D survey, Taranaki Basin, *1994 New Zealand Petroleum Conference Proceedings*, Ministry of Commerce, p. 240–255.
- Engbers, P. (2002), Evaluation of Moki sands prospectivity in Maui PML, *2002 New Zealand Petroleum Conference Proceedings*, Ministry of Economic Development, p. 256–264.
- Funnell, R.H., V.M. Stagpoole, A. Nicol, S.D. Killops, A.G. Reyes, and D. Darby (2001), Migration of oil and gas into the Maui Field, Taranaki Basin, New Zealand, *Proceedings of the PESA Eastern Australasian Basins Symposium*, Melbourne, Australia.
- Hansen, R.J., and P.J.J. Kamp (2002), Evolution of the Giant Foresets Formation, northern Taranaki Basin, New Zealand, *2002 New Zealand Petroleum Conference Proceedings*, Ministry of Economic Development, p. 419–435.
- Hart, B.S. (2008), Channel detection in 3-D seismic data using sweetness, *AAPG Bulletin*, v. 92, no. 6, p. 733–742, doi:10.1306/02050807127.
- Higgs, K.E., E. Crouch, and M. Crundwell (2004), Biostratigraphic and petrographic study of the interval 3940m-TD, well Amokura-1, prepared for New Zealand Oversea Petroleum Limited, Confidential, Institute of Geological & Nuclear Sciences client report 2004/108, Project Number: 510W1100.
- Higgs, K.E., P.R. King, J.I. Raine, R. Sykes, G.H. Browne, E.M Crouch, and J.R. Baur (2012), Sequence stratigraphy and controls on reservoir sandstone distribution in an Eocene marginal marine-coastal plain fairway, Taranaki Basin, New Zealand, *Marine and Petroleum Geology*, 32(1): p.110-137.
- IHS, Global Inc. (2014), The Kingdom Software 2015 manual, 2d/3dPAK – EarthPAK.

- Killops, S.D., and R. Sykes (2003), Biomarker source and maturity evaluation of oil and bitumens from the Kapuni Group in Tui-1 well, Taranaki Basin, Institute of Geological and Nuclear Sciences client report, 2003/30 for NZ Overseas Petroleum Ltd (part of Tui-1 well completion report).
- King, P.R. (1990), Polyphase evolution of the Taranaki Basin, New Zealand, changes in sedimentary and structural style, in Ministry of Commerce, *1989 New Zealand Oil Exploration Conference Proceedings*, Petroleum and Geothermal Unit, Energy and Resources Division, Ministry of Commerce, p. 134-150.
- King, P.R., and G.P. Thrasher, (1996), Cretaceous-Cenozoic geology and petroleum systems of the Taranaki Basin, New Zealand, Lower Hutt: Institute of Geological & Nuclear Sciences, *Institute of Geological & Nuclear Sciences*, monograph 13, p. 243.
- King, P.R., and P.H. Robinson (1988), An overview of Taranaki Basin geology, New Zealand, *Energy Exploration and Exploitation*, 6 (3), p. 213-232.
- Knox, G.J. (1982), Taranaki Basin, structural style and tectonic setting, *New Zealand journal of geology and geophysics* 25, p. 125-140.
- Laird, M.G. (1981), The Late Mesozoic fragmentation of the New Zealand segment of Gondwana, in Cresswell, M.M., & Vella, P. (Editors) - Gondwana Five, *Proceedings of the Fifth International Gondwana Symposium, Wellington, New Zealand, Balkema, Rotterdam*, p. 311-318.
- Lock, R. (1985), The distribution, sedimentology and petroleum prospects of the Moki Formation, Taranaki Basin, New Zealand, PPL 38114, Wellington: Ministry of Economic Development, PR1150, p. 102, 4 enclosures.
- Matthews, E.R. (2002), Implications Of Neogene structural development on hydrocarbon prospectivity of the Tui–Maui Area, Offshore Taranaki, New Zealand, *2002 New Zealand Petroleum Conference Proceedings*, Ministry of Economic Development, p. 198–205.
- Matthews, E.R., R.P. Brand, R.J. Buchan, W.A. Jamieson, N.T. Jones, and K.L. Mills (1998), Exploration of the area West of the Maui Field, Offshore Taranaki Basin, *1998 NZ Petroleum Conference Proceedings*, p. 89-100.

Mills, K. (2000), Hochstetter-1 well completion report, Offshore Taranaki Basin, New Zealand, PEP 38460.

Morris, R.L., and W.P. Biggs (1967), Using log-derived values of water saturation and porosity, Trans, of SPWLA, *8th Annual Logging Symposium, Paper X*, p. 1-26.

Mortimer, N., A.J. Tulloch, and T.R. Ireland (1997), Basement geology of Taranaki and Wanganui Basins, New Zealand, *New Zealand Journal of Geology and Geophysics v. 40*, p. 223–236.

Muir, R.J., J.D. Bradshaw, S.D. Weaver, and M.G. Laird (2000), the influence of basement structure on the evolution of the Taranaki Basin, New Zealand, *Journal of the Geological Society*, London, v. 157, p. 1179-1185.

NZ (New Zealand) Oil & Gas - Tui Area Oil Fields (2016, January 21), Retrieved from NZ Oil & Gas Web site:
http://demo26.outwide.com/f37,4526/Tui_Oilfield_development_schematic.pdf.

NZOP (New Zealand Overseas Petroleum), Ltd. (2004), Pateke-2 well completion report, Ministry of Economic Development New Zealand, Unpublished Petroleum Report, PR2994.

NZP&M (New Zealand Petroleum & Minerals), (2013), New Zealand Petroleum Basins, p. 39.

NZP&M (New Zealand Petroleum & Minerals), (2014), New Zealand Petroleum Basins, Tui Area Oil Fields, 2014/2015 Revised Edition, p. 82.

Octanex, N.L. (2013), Matuku-1 well due to spud, Offshore Taranaki Basin, New Zealand, PEP 51906.

Our Projects | AWE Limited (2016, January 22), Retrieved from AWE Web site:
<http://www.awexplore.com/irm/content/tui-area-oil-project.aspx?RID=413>.

Palmer, J. (1985), Pre-Miocene lithostratigraphy of Taranaki Basin, New Zealand, *New Zealand journal of geology and geophysics*, 28(2), p. 197-216.

- Pilaar, W.F.H., and L.L. Wakefield (1978), Structural and stratigraphic evolution of the Taranaki Basin, offshore North Island, New Zealand, *APEA Journal*, v. 18, p. 93-101.
- Radovich, B.J., and R.B. Oliveros (1998), 3-D sequence interpretation of seismic instantaneous attributes from the Gorgon field: *The Leading Edge*, v. 17, p. 1286–1293.
- Pereira, L.A.G.R. (2009), Seismic attributes in hydrocarbon reservoirs characterization, *MSc. Thesis*, The Department of Geosciences of the University of Aveiro, Portugal.
- Roncaglia, L., M. Fohrmann, M. Milner, H.E.G. Morgans, and M.P. Crundwell (2013), Well log stratigraphy in the central and southern offshore area of the Taranaki Basin, New Zealand. *GNS Science Report*, 2013/27, p. 26.
- Soenandar, H.B. (1992), Seismic stratigraphy of the Giant Foresets Formation, Offshore North Taranaki– Western Platform, Ministry of Commerce (1992), *1991 New Zealand Oil Exploration Conference Proceedings*, p. 207–233.
- Steiber, S.J. (1970), Pulsed neutron capture log evaluation in the Louisiana Gulf Coast: *Society of Petroleum Engineers*, 45th Annual Meeting, paper SPE-2961.
- Strogen, D.P., K. Bland, J. Baur, and P. King (2012), Regional paleogeography and implications for petroleum prospectively, Taranaki Basin, New Zealand.
- Strogen, D.P., L. Roncaglia, and E.M. Crouch (2010), The Farewell Formation reservoir fairway: a study of Paleocene biostratigraphy, facies development and reservoir quality in the Taranaki Basin. p. 283 In: Hoskin, P., D. Hikuroa, J. Eccles (conveners) *GeoNZ 2010: geoscience, geothermal: abstract volume*: Auckland, 21-24 November 2010. Wellington: *Geoscience Society of New Zealand*, Geoscience Society of New Zealand miscellaneous publication 129A.
- Stroud, T., D Miller, and B. Leask / NZOP (2004), Amokura-1 well completion report, Ministry of Economic Development, New Zealand, Unpublished Petroleum Report, PR2920.

- Stroud, T., D. Miller, I. Fancher, S. Ward, and K. Mills / NZOP (2003), Tui-1 well completion report, Ministry of Economic Development New Zealand, Unpublished Petroleum Report, PR2784.
- Suggate, R.P. (1956), Puponga coalfield, *New Zealand journal of science and technology*, B, General section, 37(5), 539-559.
- Taner, M.T., and R.E. Sheriff (1977), Application of amplitude, frequency, and other attributes to stratigraphic and hydrocarbon exploration, in C. E. Payton, ed., *Seismic stratigraphy - Applications to hydrocarbon exploration: AAPG Memoir v. 26*, p. 301-327.
- Taylor, B., and G. D. Karner (1983), On the evolution of marginal basins, *Rev. Geophys. Space Phys.*, 21, 1727-1741.
- Vail, P.R. (1987), Seismic stratigraphy interpretation procedure, in Bally, A. W. (ed.), *Atlas of seismic stratigraphy: Am. Assoc. Petroleum Geology Studies in Geology 27*, v. 1, p. 1-10.
- Veritas DGC, Australia Pty. Ltd / New Zealand Overseas Petroleum Ltd (2003), Tui-3D seismic survey, Ministry of Economic Development New Zealand, Unpublished Petroleum Report, PR2830.
- Walley, A.M. (1991), New Zealand: notes to accompany Cretaceous -Cainozoic stratigraphic summary columns for the New Zealand region, *Paleogeography 33*, Canberra: Bureau of Mineral Resources and Petroleum Division of the Australian mineral Industries Research Association, *Phanerozoic History of Australia Project*, p. 42.
- Wyllie, M.R., and W.D. Rose (1950), Some theoretical considerations related to the quantitative evaluation of the physical characteristics of reservoir rock from electrical log data, *Petroleum Trans., AIME*, v. 189, p. 105-118.

VITA

Gorkem Yagci was born in Bartin, Turkey, in 1987. He received his B.S. degree in June 2011 from Istanbul University, in the Department of Geophysical Engineering, Istanbul, Turkey. He completed an internship in the Turkish Petroleum Company (TPAO) in Ankara, Turkey in 2010.

After graduating from Istanbul University, he was awarded a scholarship from TPAO to pursue his M.S. degree in seismic stratigraphy in the USA in 2011. He studied at Rice University in an intensive English program from August 2012 to August 2013 in Houston, Texas to obtain a sufficient TOEFL score for M.S. degree applications. He started his M.S. degree at Missouri University of Science and Technology in January 2014 in Rolla, Missouri. During his graduate studies, he worked on 3D seismic structural and stratigraphic interpretation of the Tui-3D Field in the Taranaki Basin, New Zealand. In May 2016, he received his Master of Science degree in geology and geophysics from the Missouri University of Science and Technology.